Studies on Genetic and Pharmacological Perturbations on Carbon and Energy Metabolism in *Toxoplasma gondii* and *Plasmodium falciparum*

Thesis Submitted to AcSIR
For the Award of the Degree of
DOCTOR OF PHILOSOPHY
In
BIOLOGICAL SCIENCES

By
Anurag
10BB12A26063

Under the guidance of
Dr. Dhanasekaran Shanmugam

BIOCHEMICAL SCIENCES DIVISION
CSIR-NATIONAL CHEMICAL LABORATORY
Pune-411008, INDIA
May 2018

DECLARATION

I, Anurag Shukla, hereby declare that the work incorporated in the thesis and entitled "Studies on Genetic and Pharmacological Perturbations on Carbon and Energy Metabolism in *Toxoplasma gondii* and *Plasmodium falciparum*" submitted for the award of the Degree of **Doctor of Philosophy in Biological Sciences** to the **Academy of Scientific & Innovative Research (AcSIR)**, New Delhi, has been carried out by me at Division of Biological Sciences, CSIR-National Chemical Laboratory, Pune-411008, India, under the supervision of Dr. Dhanasekaran Shanmugam. The work is original and has not been submitted as a part or full by me for any degree or diploma to this or any other university. I further declare that the material obtained from other resources has been duly acknowledged in this thesis.

Date: 22th May 2018

Anurag Shukla

(Enrollment No. 10BB12A26063)

सीएसआईआर - राष्ट्रीय रासायनिक प्रयोगशाला
(वैज्ञानिक तथा औद्योगिक अनुसंधान परिषद)
डॉ. होमी भाभा मार्ग, पुणे - 411 008, भारत
CSIR - NATIONAL CHEMICAL LABORATORY
(Council of Scientific & Industrial Research)
Dr. Homi Bhabha Road, Pune - 411 008, India

Certificate

This is to certify that the work incorporated in this Ph.D. thesis entitled **"Studies on Genetic and Pharmacological Perturbations on Carbon and Energy Metabolism in *Toxoplasma gondii* and *Plasmodium falciparum*"** submitted by Mr. Anurag Shukla to the Academy of Scientific and Innovative Research (AcSIR), New Delhi, India, is in fulfilment of the requirements for the award of the Degree of Philosophy and embodies original research work under my supervision and guidance. I further certify that this work has not been submitted to any other University or Institution in part or full for the award of any degree or diploma. Research material obtained from other sources has been duly acknowledged in the thesis. Any text, illustration, table, used in the thesis from other sources, have been duly cited and acknowledged.

(Student)

Mr. Anurag Shukla
Senior Research Fellow,
Biochemical Sciences Division,
CSIR-National Chemical Laboratory,
Dr. Homi Bhabha Road, Pashan,
Pune-411008

(Supervisor)

Dr. Dhanasekaran Shanmugam
Principal Scientist,
Biochemical Sciences Division,
CSIR-National Chemical Laboratory,
Dr. Homi Bhabha Road, Pashan,
Pune-411008

Communication Channels
NCL Level DID : 2590
NCL Board No. : +91-20-25902000
EPABX : +91-20-25893300
: +91-20-25893400
FAX
Director's Office : +91-20-25902601
COA's Office : +91-20-25902660
SPO's Office : +91-20-25902664
WEBSITE
www.ncl-india.org

Dedicated to my family and friends for their love and never ending support

Acknowledgements

As rightly said, journey is more beautiful than the destination, the voyage to research was made amazing with moments of success, failures, happiness, and learning, in the company, support and love of peers, friends, family and well-wishers. With the grace of almighty, I take this opportunity to express my sincerest gratitude and acknowledge their instrumental contribution in my Ph.D.

I would start it with the phrase from Sanskrit "Guruh bhramha, Guruh Vishnu, Guruh devo Maheshwara, Guruh sakshat Par Bramha, tasmay shree Guruve Namah". I consider myself fortunate to find my Guru, my mentor, ***Dr. Dhanasekaran Shanmugam****. I started my journey under his most capable but humble guidance in the field. He showed the right path, supported me on every step, taught me from minor details, to recognize my mistakes and corrected me. I am indebted and will always be for all his unending support and guidance. Most importantly to have patience both in research and in life with humbleness. I truly feel privileged to work in his guidance. Words will be insufficient to express my everlasting respect, gratitude and would ask more of your affection, and guidance. I most respectfully thank Dr. Geetha for her support, encouragement and Nithilan for his loving company.*

I take this opportunity to sincerely thank my Doctoral Advisory Committee (DAC) members Dr. Narendra Kadoo, Dr. Venkat Panchangnula and Dr. Mugdha Gadgil for their critical evaluation, continuous monitoring my progress, constructive and valuable inputs. I am obliged to Prof. J.K. Pal and Dr. Vasudevan Sheshadri for their valuable time in evaluating my progress, constructive inputs and facilitating my extensions.

I am obliged and extend my gratitude to Dr. H.V. Thulasiram for his extended support to letting me use his lab facility and equipment. I am also indebted to PMB group for facilitating the excess to their lab, equipment and support.

I would like to sincerely acknowledge the support and help I received from Dr. B. Shanthakumari and Dr. Mahesh J. Kulkarni for letting me use the HRMS facility and teaching me from basic to advance mass spectrometry. I would extend my thanks to Dr. Yashwant Kumar for his support in my initial learning phase of mass spectrometry and data analysis.

I am thankful to Dr. D. S. Reddy, and his lab members, Dr. Swati P. Joshi, Dr. Ashish Chinchansure, Dr. Subhash Padhey and Dr. Rajesh Chandramohandas for providing me opportunity to work with them and learn from diverse field of science.

I would take this opportunity to sincerely thank Dr. Amit Sharma with whom it was exciting and pleasure to work and discuss science and his lab members Dr. Jyoti Chhibber, and Varsha for the support and work we performed together successfully.

I am highly indebted and extend my gratitude to Dr. Suresh Gokhale, Dr. Santosh Jadhav, Mr. Sudhakar Babar and BAIF members for their support during my CSIR-800. It would have been extremely difficult without their hard work and constant support.

My Ph.D. endeavour started in the company of Dr. Prabhakar, Dr. Kritika, Dr. Pankaj, Dr. Swati, Dr. Dipesh, Avinash, Uttara, Nilofer, Arti, and Shiva without whom it would have been like blank pages of book at the first chapter itself. It would be unjust to say thank to such loving and caring seniors and friends. I request to continue your love and affection and best wishes forever.

I joined NCL as a stranger and within few days, I found friends who became like family in the form of Amol, Tejas, Anil, Subbu (Abhisek), Ameya, Ekta, Shakeel , Sudhakar and Prashant . Thank you buddies for always being there with me.

Words are not enough to thank my labmates, my friend, my colleague all together making an extended family in lab, Rahul, Meenakshi, Dr. Rupali, Parag, Sindhuri, Tejashri, Shweta, Sayyad Rohil, Milan Mathew, Dr. Khooshboo who were always there to listen, help, support, discuss and suggest. It would have been very difficult to achieve and reach to the goal. I heartily thank for all the moments we share, our ice cream parties, funny lab cleaning schedules and always standing together at the time of need. I am thankful to Neha, Gayatri and Anjali for their help and well wishes. Thank you for making the journey easier and happier.

Few people leave an impression, which becomes inseparable part of your journey, called life. Words are not enough to show my gratitude for my friend Dr. Uma. Thank you for your support, boosting confidence in testing time, sharing the best memories, everlasting friendship and affection.

I am indebted to all my friends from my childhood to Ph.D., Yuvraj, Piyush, Nandu, Ajay, Romanjeet, Swati, Ankita, Pooja, Madhu, Bhumika, Kishor, Abhilash, Soni Rakhi, DSN Raju, and Sudhakar who always stood by me, supported me and boosted my confidence to continue the journey.

"Family"…..the word itself contains the whole universe within it. Whoever and whatever I am today, is the love, support and upbringing and sacrifices of you all. My highest regards to my loving grandparents, beloved parents, my maternal uncle Arun Tripathi, Dr. Akhilesh Tripathi, my Sister Suman, brother Animesh, loved cousins Anu,

Ayush, Anmol, Abhinav, my loving nephew Dev and whole family. Thank you, Thank you for your blessing, constant support and unconditional love. It was your faith on me which pushed me beyond my limits to come this far and continuing my journey.

My sincerest thank to Head of Department, Biochemical Sciences Division, Dr. Ashok Giri, formar HODs Dr. Vidya Gupta, Dr. C.G. Suresh, for their support and lab facilities. I extend my gratitude and thanks to Director CSIR-National Chemical Laboratory for allowing me to carry out my research in this esteemed institute and providing the infrastructure facilities. I sincerely thank SAC office, CSIR-NCL for facilitating all the documentation and Academy of Scientific and Innovative Research (AcSIR), New Delhi for allowing me to submit my thesis for the award of Ph.D. degree. My sincerest thanks to Indian Council of Medical Research (ICMR), New Delhi, Govt. of India for the Ph.D. fellowship.

Last but the most importantly, I thank the God for all the strength and courage he has bestowed upon me in every phase of my life.

Thank You…..

Anurag Shukla

Contents

List of Figures & Tables

List of Tables

List of Abbreviations

Δ*hk*	Hexokinase knockout
Δ*pepck*	PEPCK knockout
µM	Micro molar
2DG	2-Deoxyglucose
3GP	3-Phosphoglycerate
ATP	Adenosine triphosphate
Atq	Atovaquone
BCKDH	Branched chain ketoacid dehydrogenase
BP	Base pair
Cas	CRISPR associated systems
cDNA	Complementary deoxyribonucleic acid
Clad	Cladosporine
CLQ	Chloroquine
CMCM	Complete malaria culture media
CoA	Coenzyme A
CRISPR	Clustered Regularly Interspaced Short Palindromic Repeats
Cytb	Cytochrome b
DAPI	4',6-diamidino-2-phenyllindole
DHFR-TS	Dihydrofolate reductase thymidylate synthase
DHO	Dihydroorotate
DHOD	Duhydroorotate dehydrogenase
DIC	Differential interference contrast
DMEM	Dulbacco's Modified Eagle Medium

DMSO	Dimethyl sulfoxide
dNTP	Deoxyribonucleic acid
EDTA	Ethylendiamine tetraacetate
ETC	Electrone transport chain
FBP	Fructose 1,6-bisphosphate
G3P	Glycerol-3-phosphate
G6P	Glucose-6-phosphate
gDNA	Genomic deoxyribonucleic acid
GFP	Green fluorescent protein
Glc	Glucose
Gln	Glutamine
gt1	Glucose transporter 1
HA	Hemagglutinin
HF	Halofuginone
HFF	Human foreskin fibroblast
hk	Hexokinase
HRMS	High resolution mass spectrometer
h	Hour(s)
hxgprt	Hypoxanthin-xanthine-guanine phosphoribosyltransferase
iRBCs	infected RBCs
KO	Knockout
KRS	Lysyl-tRNA synthetase
LW	Lawson
mM	Milli molar

MMV	Medicines for Malaria Venture, Geneva
MRD	Multi drug resistance
MS	Mass spectrometry
NADH	Nicotinamide adenine dinucleotide
nM	Nano molar
OPLS-DA	Orthogonal-partial least square-discriminate analysis
PBS	Phosphate buffered saline
PCA	Principle component analysis
PCR	Polymerase chain reaction
PDH	Pyruvate dehydrogenase
PEP	Phosphoenolpyruvate
PEPC	Phosphoenolpyruvate carboxylase
PEPCK	Phosphoenolpyruvate carboxykinase
Pf	*Plasmodium falciparum*
PFA	Paraformaldehyde
*Pf*CRT	*Plasmodium falciparum* chloroquine resistant transporter
Pfcytb^{mut}	*Plasmodium falciparum* cytochrome b mutant
PLS-DA	Partial least square-discriminate analysis
PRS	Prolyl-tRNA synthetase
Pru	Prugniaud
PV	Parasitophorpous vacuole
PVM	Parasitophorpous vacuole membrane
Pyr	Pyrimethamine
qRT-PCR	Quantitative reverse-transcription PCR

RBCs	Red blood cells
RNA	Ribonucleic acid
RP	Reverse phase
rpm	Rotations per minute
RPMI	Roswell Park Memorial Institute Media
sOPLS-DA	Sparse-orthogonal-partial least square-discriminate analysis
TCA	Tricarboxylic acid
Tg	*Toxoplasm gondii*
Ub	Ubiquinone
UMP	Uracil monophosphate
UPLC	Ultra-performance liquid chromatography
UPRT	Uracil phosphoribosyl transferase
VIP	Variable important for projections
wt	Wild type

Abstract

The causative agents for malaria and toxoplasmosis in humans are the apicomplexan parasites *Plasmodium falciparum* and *Toxoplasma gondii*. These infectious diseases are a huge health and economic burden, especially in poor countries. Understanding the nutritional needs, metabolic capabilities, and response to anti-parasitic molecules are key aspects for developing new therapeutic intervention against these diseases. In the first part of this study, the focus was on applying mass spectrometry based metabolomics in combination with genetics, pharmacology and biochemical techniques to comprehensively dissect central carbon and energy metabolism in *T. gondii*. In the second part of this study, the focus is on characterizing atovaquone resistance in *P. falciparum*, studying the effect on mtETC efficiency due to mutations in *Pfcytb*, and identification of novel atovaquone like compounds targeting *Pfcytb* enzyme. In addition, we have used untargeted metabolomics to capture inhibitor specific metabolic response in *P. falciparum*, to understand primary and secondary effects of the treatment, and to pursue mode of action and target identification studies.

Toxoplasma gondii is a promiscuous parasite and serves as a model organism for studies and apicomplexan parasite biology and drug discovery. The ability of *T. gondii* to adapt to different environmental conditions, by modulating various cellular processes, including cellular metabolism, makes it one of the most successful pathogen. Previous studies have shown that glucose is a dispensable nutrient in the presence of glutamine as an alternate source of carbon during asexual development. To further confirm the dispensability of glycolysis and its effect on virulence and tissue cyst formation by the parasite, we generated a hexokinase gene null mutant *(*Δ*hk*) in two strains of *T. gondii*; RH (Type-1; virulent and cannot form tissue cyst in mice) and Prugniad (Type-2; moderately virulent and can form tissue cyst in mice). The knockout parasite showed

minor growth defect in comparison to wild type parasites in the presence of glutamine. Interestingly, in the absence of glutamine, the parasite die not die, but continued to grow with a severe fitness defect. This growth defect could not be compensated with non-essential amino acid (NEAA) or acetate. RH Δ*hk* mutants remained virulent in mice while Prugniad Δ*hk* mutants were compromised in virulence. Prugniad Δ*hk* mutants were capable of differentiating into bradyzoites *in vitro*, but were unable to form mature tissue cysts in mice.

^{13}C-labeled metabolic flux analysis revealed that in the absence of glucose, glutamine is utilized as a major carbon source and metabolic intermediates of glycolysis and pentose phosphate pathway incorporated ^{13}C derived from glutamine, thus providing evidence that gluconeogenesis is operational. To further validate the essentiality of gluconeogenesis for asexual stages of the parasite, we generated mutant parasites lacking a functional phosphoenolpyruvate carboxykinase (PEPCK) gene in RH strain background. PEPCK was found to be conditionally essential; dispensable in presence of glucose but essential in glucose depleted media. Our study highlights the metabolic flexibility in *T. gondii*, which confers the ability to either use glucose or glutamine as the sole nutrient for asexual propagation. These studies also revealed that the parasite is capable of obtaining bulk cellular ATP efficiently from either substrate level phosphorylation *via* glycolysis or from mitochondrial oxidative phosphorylation.

P. falciparum and *T. gondii* can perform *de novo* biosynthesis of pyrimidine nucleotides, which can be blocked by atovaquone, a potent and lethal inhibitor of mtETC complex III protein CYTb. *P. falciparum* readily develops resistance to atovaquone by mutating the *Pfcytb* gene to abolish atovaquone binding. We generated atovaquone resistant *P. falciparum* parasites to study the effect of *Pfcytb* gene mutation on pyrimidine biosynthesis and mtETC. Several clonal lines of *Pfcytb* mutants were tested, and one of

them, with >1000 fold decreased sensitivity to atovaquone, was selected for further studies. We mapped mutation as a P177L change in the *Pfcytb* gene. Further biochemical and metabolic studies showed that the mutant parasites have intact pyrimidine biosynthesis and mtETC despite the mutation in *Pfcytb* gene. We then identified novel atovaquone like molecules with similar nano molar potency against both wild type and *Pfcytb* mutant *P. falciparum*. Thus, our study validates mtETC, particularly *Pfcytb*, as an important target for development of novel antimalarial drugs.

Untargeted metabolomics is a useful approach for studying drug MOA. In fact, this has already been used for characterizing a variety of antimalarial molecules, including some frontline antimalarial drugs such as chloroquine and pyrimethamine. In this study, we have characterized the early (4 h) and late (8 h) metabolic response to two potent *P. falciparum* aminoacyl tRNA synthetase inhibitors; cladosporine and halofuginone. These two compounds showed distinct metabolic effects in comparison to the antimalarial drugs chloroquine and pyrimethamine. Interestingly, although both cladosporine and halofuginone act by inhibiting protein sythesis in *P. falciparum*, we found that their metabolic response was very different. Our findings will be helpful in further characterizing the effects of these two novel antimalarial compounds.

Publications

1. **Anurag Shukla**, Kellen L. Olszewski, Manuel Llinas, Leah M. Rommereim, Barbara A. Fox, David J. Bzik, Dong Xia, Jonathan Wastling, Daniel Beiting, David S. Roos# and Dhanasekaran Shanmugam#; Dynamics of metabolism, proliferation and differentiation in Toxoplasma gondii mutants deficient in glycolysis and gluconeogenesis (https://doi.org/10.1016/j.ijpara.2018.05.013).

2. Gowtham Subramanian, Meenakshi A Belekar, **Anurag Shukla**, Jie Xin Tong, Ameya Sinha, Trang TT Chu, Akshay S. Kulkarni, Peter R Preiser, D. Srinivasa Reddy, Kevin SW Tan, Dhanasekaran Shanmugam and Rajesh Chandramohanadas; Targeted phenotypic screening in Plasmodium falciparum and Toxoplasma gondii reveals novel modes of action for MMV Malaria Box molecules; (mSphere. Jan 2018, 17;3(1).

3. Paresh Athawale, Gorakhnath Jachak, **Anurag Shukla**, Dhanasekaran Shanmugam, Srinivasa D. Reddy; Efforts to Access the Potent Anti-trypanosomal Marine Natural Product Janadolide: Synthesis of Des-tert-butyl Janadolide and its Biological Evaluation; ACS Omega 2018, 3, 2283-2289

4. Ashish A. Chinchansure, Manisha Arkile, **Anurag Shukla**, Dhanasekaran Shanmugam, Dhiman Sarkar, Swati P. Joshi; Leucas mollissima, a Source of Bio-active Compounds with Antimalarial and Antimycobacterium Activities; 2015, Planta Med Lett 2015; 2: e35–e38

5. **Anurag Shukla**, Thejashri B. Hingamire, Akshay S. Kulkarni, Rahul Singere, Subhash Padhye, D. Srinivasa Reddy, Dhanasekaran Shanmugam; Bioactivity and metabolic effects of napthoquinone based analog series on wild type and atovaquone resistant Plasmodium falciparum (To be communicated).

6. **Patent:** Dumbala Srinivasa Reddy, Dhanasekaran Shanmugam, Remya Ramesh, **Anurag Shukla**, and Meenakshi Anil Belekar. A Pharmaceutical composition for preventing and treating malaria and toxoplasmosis. PCT/IN2017/050067 (WO) & 201611005767 (IN).

Chapter 1: Introduction

A brief introduction on the biology of apicomplexan parasites Toxoplasma gondii and Plasmodium falciparum and highlight unique aspects of their cellular metabolism. Antiparasitic drugs and parasite resistance will also be discussed.

1. Introduction

Since ancient times, humans have been afflicted with infectious diseases and have been constantly fighting to survive their scourge. From time to time, there have been many episodes of infectious disease epidemics, which have resulted in many instance of almost wiping out the human population from infected areas [Dobson *et al*., 1996]. Humans succumb to infectious agents ranging from bacteria, virus and eukaryotic species. The infrakingdom *Alveolata*, comprises of many important parasitic protists which together impose a huge infectious disease burden on human and animals. *Alveolata* comprises of unicellular eukaryotic organism with at least five divergent groups; *Apicomplexa*, *Ciliata*, *Dinoflagellata*, *Chromerida* and *Colpodellidae*. These five groups are completely different in their tropism and niche. The characteristic feature, a flattened vesicles like structure beneath the plasma membrane (cortical alveoli) gives the name *Alveolata* to this very successful omnipresent organisms [Gould *et al*., 2008a]. The ciliates which have evolutionary lost the plastid organelle are free living predators of small bacteria and protist, while dinoflagellates include free livings algae of oceans, fresh water bodies, are adopted to both photosynthetic (autotrophic) and heterotrophic (predators or parasitic) life style. Chromarids are the photosynthetic subclade of alveolate protozoans. The genus is repreented by species *Chromeria velia* and *Vitrella brassicaformis* [Moore *et al*., 2008]. The genus Colpodella are free living small flagellated protists. They mainly feed on to other smaller free-living protist by penetrating their cell membrane and consuming prey's cytoplasm [Simpson *et al*., 1996].The *Apicomplexans* are group of exclusively obligate parasitic organisms with different levels of physical interaction with host [Fig 1.1]. These parasites can be epicellular or intracellular in their localization within the host, from whom they acquire nutrients to varying degrees in order to survive [Danne *et al*., 2013; Bartosova-Sojkova *et al*., 2015].

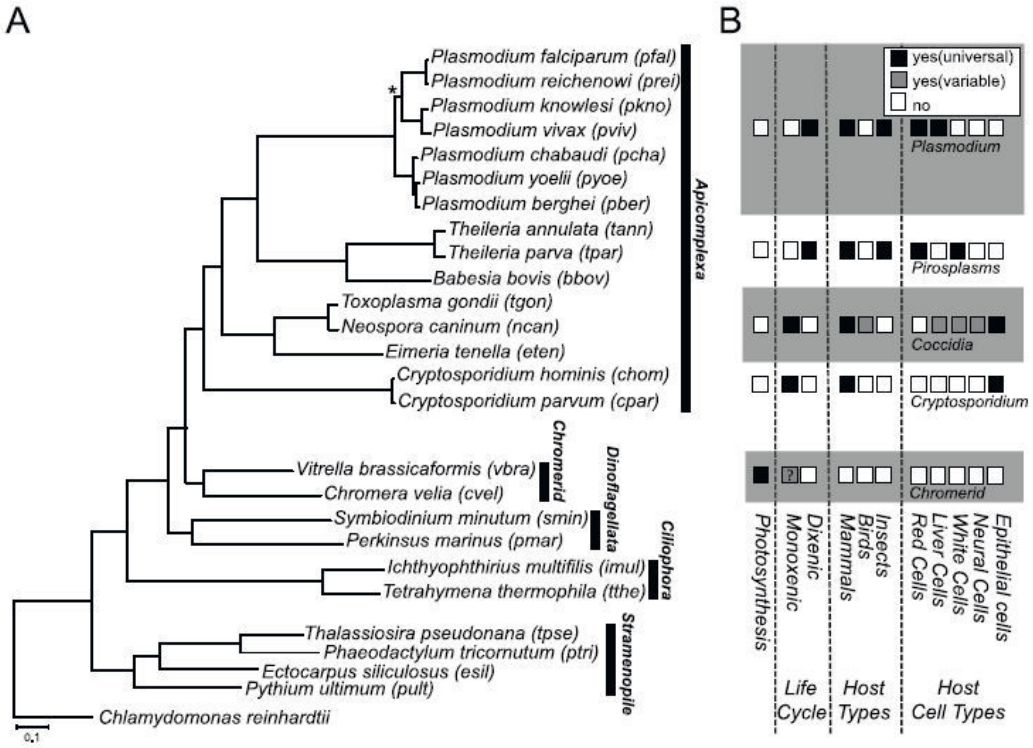

***Figure 1.1 Schematic for classification of Phylum Alveolata and Apicomplexa*:** *Reproduced from Woo et al., 2015*; *Figure illustrates the evolutionary relationship and life style strategies of apicomplexan parasites with respect to other major alveolate clades. (A) 26 Alveolate species and 5 out group species were used to construct this maximum likelihood tree based on concatenated sequence alignment of 101 genes which are present as 1:1 orthologs in all species. (B) Different niches and life style strategies of apicomplexan parasites and chromerids.*

The phylum *Apicomplexa* is estimated to include > 6000 parasitic species, many of them obligate intracellular parasites of diverse host species with complex lifestyles. These parasites have evolved to infect hosts ranging from arthropods to higher mammals including humans. It is believed that, there is at least one apicomplexan parasite for each invertebrate and vertebrate organism [Seeber *et al*., 2007]. These parasite group includes some of the most notorious human and animal pathogens genus, such as *Plasmodium*,

Toxoplasma, Babesia, Thileria, Cryptosporodia, Eimeria, and *Neospora*. Infections due to these parasites are known to cause heavy human and livestock loss worldwide, annually.

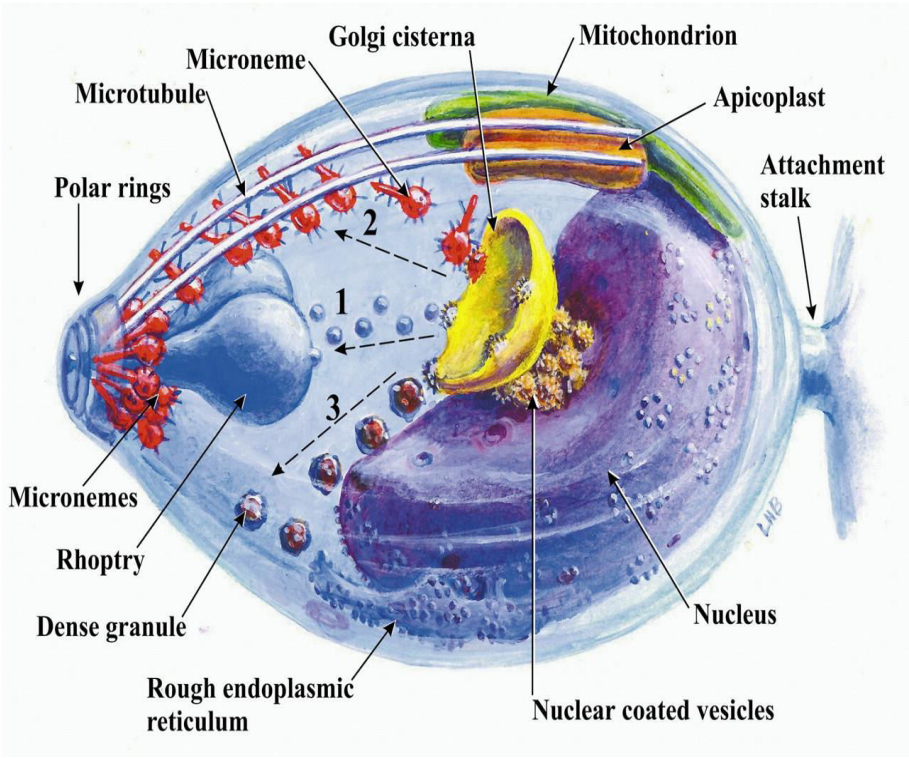

Figure 1.2 Representation of the morphological structures of apicomplexan parasites; *Adopted from Bannister et al., 2003; Schematic shows the typical apicomplexan cellular structures. Presence of apical organelles "Polar ring, micronemes, rhoptry, dense granules", and other organelles, including a single mitochondrion and apicoplast is depicted.*

Apicomplexan parasites have conserved cellular morphology and cellular structure for their invasive stages. The clade defining apical organelles consisting of rhoptries, micronemes and the conoid structure, help in host cell invasion. Intracellular microtubular structure under the inner membrane complex supports the cellular morphology [Striepen *et al*, 2007]. All apicomplexan parasites possess a single golgi stack, a secondary endosymbiont organelle called apicoplast, a mitochondrion, and a nucleus surrounded by

endoplasmic reticulum. Except in *Cryptosporidium* species where the mitrochondrion is significantly degenerated and has become a mitosome, all other apicomplexan parasites harbour a single mitochondrion in close proximity to the apicoplast [Fig 1.2]. They also possess unique secretory organelle called as the dense granules which transport and facilitate secretion of proteins into the PV.

Only few apicomplexan parasites have been studied extensively because of technical limitation in isolation them from the host and growing them *in vitro*, and their amenability for genetic manipulation. The two most intensively studied human parasites from this group are etiological agents of malaria and toxoplasmosis, *Plasmodium sp.* and *Toxoplasma gondii* respectively. While other apicomplexan parasites, such as the tick transmitted *Babesia sp.* (responsible for babesiosis or haemolytic anaemia), and *Cryptosporidium sp.* (responsible for gastroenteritis with diarrhoea), predominantly infect cattle, they can also infect humans opportunistically [Checkley *et al*, 2015; Vannier *et al*, 2012]. The other agriculture related important parasite genus from this group are *Theileria*, *Neospora*, *Sarcocystis* and *Eimeria*, and together these cause significant economic burden and losses worldwide.

Plasmodium falciparum, the deadliest among human malaria parasites responsible for ~ 500,000 deaths annually [WHO 2016], was first discovered by Charles Laveran in 1880. Most of the fatality happens in young children in sub-Saharan Africa. Other milder forms of malaria are caused by four different species of *Plasmodium*; *P. vivax*, *P. ovale*, *P. malariae* and *P. knowlesi* [Kantele *et al*., 2011]. *Toxoplasma gondii*, first observed by Charles Nicolle and Louis Manceaux in 1908 from a rodent named “Gundi”, is named after its arc like morphology [Dubey *et al*, 2008]. This promiscuous parasite is so versatile in its infection that it has the ability to infect all nucleated cells from warm blooded animals. It is estimated that ~30% of the world’s human population is chronically

infected with this parasite, with reports on seropositivity reaching upto 43% of the population in some countries like France [Berger *et al*., 2009]. The infection is usually controlled and asymptomatic in immunocompetent individuals, however chronically infected people harbour the cyst form of the parasite within tissues of organs such as the brain. It is a significant threat to the life of immunocompromised individuals such as those with AIDS, organ transplant or undergoing cancer treatment [Halonen *et al.*, 2013].

Clinical treatment for toxoplasmosis is solely dependent on only two drugs at present, pyrimethamine and sulfadiazine. But only acute infections, where the parasites grows and proliferates rapidly as tachyzoites, are affected by these drugs. Thus, chronic infection due to slow growing tissue cyst forms of the parasites cannot be cured by these drugs. This leaves the patients infected for lifelong. The emergence and increased spread of drug resistance parasites for available drugs is a significant threat to our efforts to control and eliminate these diseases. Thus, there is an urgent need to identify novel antiparasitic drugs for clinical management of this important group of parasites.

1.1 Description of two model apicomplexan parasites

All apicomplexan parasites follow complex life cycle. They have distinct sexual and asexual stages within different definitive and intermediate hosts. Asexual stages propagate within intermediate host by rapid replication, and differentiate into either transmission competent stages, or lapsing into dormancy. Most of the apicomplexan parasites survival and further transmission *via* asexual stages depends on the successful establishment of a replicative niche in their respective host cells. The formation of non-fusogenic parasitophorous vacuole (PV) surrounded by parasitophorous vacuolar membrane (PVM), following host cell invasion, helps the parasite to survive in hostile host environment. This event is followed by asexual replication and egression from the

host cells by rupturing the host cell membrane, a process which ensures the continual of the infection cycle. The life cycles of *T. gondii* and *P. falciparum* parasites are discussed in detail below.

1.2 *T. gondii* life cycle

Any warm blooded animal can serve as a host for asexual stage of *T. gondii* parasites while the sexual stage is restricted to its definitive host, which can be any naïve felid. During the asexual cycle in the intermediate hosts, the parasite alters between two developmental stages, the fast growing tachyzoite and the slow growing bradyzoites. The tachyzoites are characteristic to the acute infection, while the presence of bradyzoite tissue cysts indicate chronic infection. These parasites can virtually infect any nucleated cell and replicate several rounds within each infected cell. Depending on the strain, each round of cell division can take between 6 to 10 hours, and typically the parasites egress out of an infected host cell after 5 to 6 rounds of cell division. *In vivo*, parasites are known to infect dendritic cells and macrophages after egressing out of intestinal epithelium, which helps in their dissemination to various tissues in the body through blood including penetrating the blood-placental and blood-brain barriers, to infect the foetus or the brain tissue [Hunter *et al*., 2012]. The fast replication of the parasites with destruction of host cells triggers strong immune response which induces the *T. gondii* differentiation into slow-growing bradyzoites which from the tissue cysts [Dubey *et al.,* 1998]. To evade the immune clearance, bradyzoites form tissue cyst in the central nervous system and striated muscles. The thick walled cysts encapsulate thousands of bradyzoites, which functions as physical barrier for evading any host immune system attack and prevent access to clinical drugs used to treat acute infection [Hunter *et al*., 2012].

In chronically infected individuals, *T. gondii* can persist for the life span of the host as tissue cysts [Fig 1.3]. Bradyzoites are capable of re-differentiating back to tachyzoites and causes relapse of infection in immunocompromised individuals. The sexual stages are initiated in the naïve felines when they consume infected meat containing bradyzoite cysts. The parasites infect the feline intestinal epithelium, where they differentiate into morphologically distinct schizont stages followed by the formation of merozoites. These merozoites after few rounds of replication differentiate into macro and micro gametes, which after conjugation produces diploid unsporulated oocysts [Pittman *et al*., 2015]. These oocysts are protected with impermeable thick walls to survive and tolerate harsh environmental conditions, and are shed *via* faeces into the environment, upto 20 million/day for upto two weeks following infection [Dumetre *et al*., 2013].

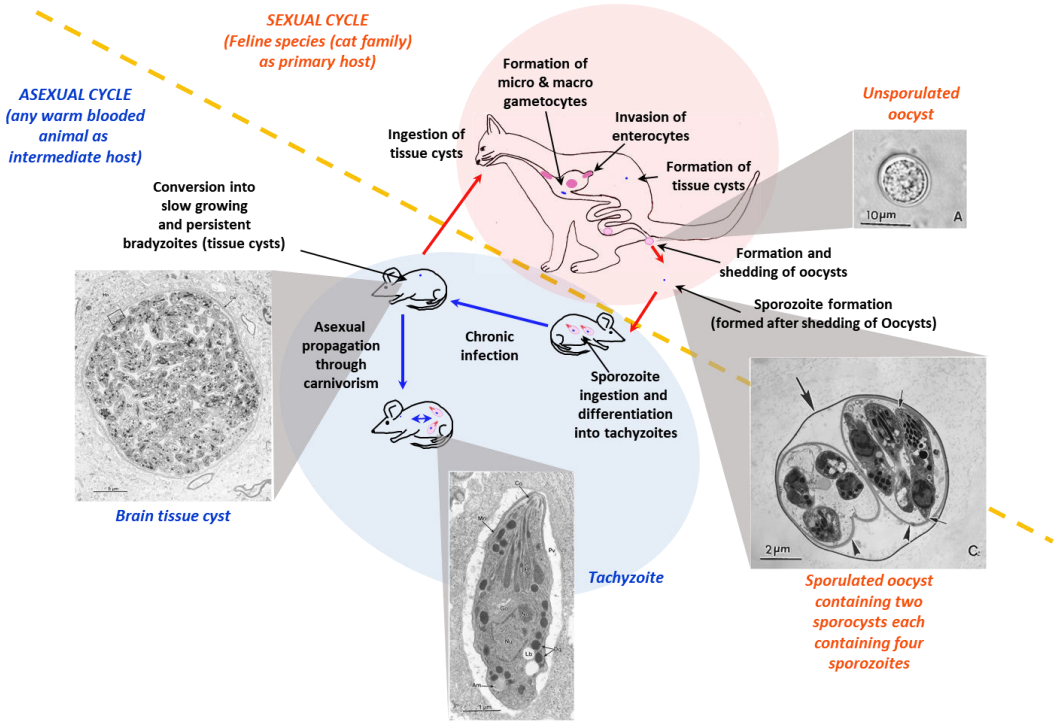

Figure 1.3; Life cycle of T. gondii; *Figure scource, DS Lab, CSIR-NCL, Pune; Electron micrograph reproduced from Dubey et al., 1998; Figure illustrates the complete life cycle of Toxoplasma gondii. Sexual cycle occurs in the intestinal epithelium of feline species (Cats), and unsporulated oocysts are shed into the environment. The haploid sporozoites initiate the asexual cycle upon entering the secondary host, where*

they differentiate into fast replicating tachyzoites. The parasite continues to replicate as tachyzoites until challenged by the host immune system, when they differentiate into bradyzoites and persist as latent cysts in host brain or muscle tissues, during chronic infection.

These oocyst undergo meiosis and mitosis to produce eight mature infectious haploid oocyst wall encapsulated sporozoites, which can remain infectious for many years in the environment. The oocysts are transmitted to humans by contaminated water and undercooked meat, which once ingested initiate new infection in epithelium of the small intestine of the host after rupturing of the cyst by digestive enzymes and release of the sporozoites [Fig 1.3][Pitmann *et al*., 2015].

1.3 *P. falciparum* life cycle

The life cycle of human malaria parasite *P. falciparum* alternates between the mosquito vector, which helps in transmitting the parasite and where the sexual developmental phases occur, and the human host, where the the asexual development and propagation occurs. Many other vertebrate host are known to harbour various different species of *Plasmodium*, which are typically resitricted in host range [Huff *et al*., 1947; Boddey *et al*., 2013; Menard *et al*., 2013]. The asexual stage infection starts with the injection of *Plasmodium* sporozoites into the blood stream, from the saliva of infected mosquitos during blood meals. Few of these sporozoites reach the liver, and infect, differentiate and proliferate within suitable hepatocytes over the course of 7-14 days. During this replicative phase, millions of merozoites are formed, and the heavily infected hepatocytes rupture to release the sporozoites into blood stream, where they infect the red blood cells. Within the RBCs, the parasites undergo a periodic developmental cycle that occurs over a period of 48 h and progresses through the formation of ring, trophozoite and schizont stage parasites. Finally the mature parasites and egress out of the infected RBC

as merozoites. The repeated lysis and reinfection of fresh RBCs continues, leading to acute infection and symptoms of malaria [Gueirard *et al.,* 2010; Boddey *et al*., 2013]. Freshly formed merozoites invade new RBCs and continue the intraerythrocytic cycle of asexual replication. A few parasites sporadically differentiate into male and female gametocytes. When these gametocytes enter the mosquito, they give rise to micro and macro-gametes respectively to continue the sexual cycle of development in the mosquito gut epithelium [Kuehn *et al*., 2010].

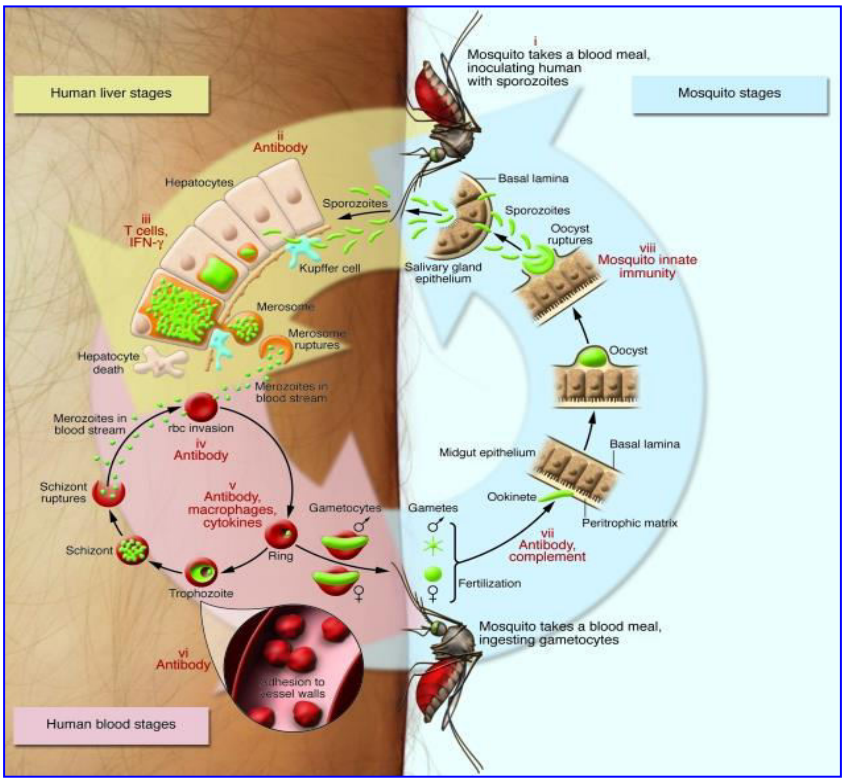

Figure 1.4 life cycle of Plasmodiumm falciparum*; Reproduced from Greenwood et al., 2008. The figures depicts both the asexual (left half) and sexual (right half) development of the parasite. The red cell stages can be continuously cultured in the laboratory.*

In mosquito, the female gametocyte which differentiates into macro-gametes is fertilized by exflagillated motile micro-gametes to produce motile zygotes. The zygote differentiate into an ookinet, which then develops into sessile oocysts after traversing the

mosquito mid-gut wall. Within the oocytes thousands of sporozoites are formed which are released in mosquito body cavity upon rupture. The sporozoites travel to the salivary glands, then to salivary duct, from where they are transmitted to human host during a bite. This then initiates a new infection and asexual propagation within the susceptible host [Fig. 1.4] [Kuehn *et al*., 2010; Boddey *et al*., 2013; Menard *et al*., 2013].

1.4 Metabolic capabilities of apicomplexan parasites

Owing to their diversity in life cycle and host preference, apicomplexan parasites appear to have evolved various survival strategies, including in metabolic streamlining, and understanding this is important for combating these parasites. The availability of complete genome sequence for many these parasites has facilitated the prediction of complete metabolic repertoires using comparative genomics techniques [Katinka *et al*. 2001; Gardner *et al*. 2002; Abrahamsen *et al*. 2004; Xu *et al*. 2004; Woo et al., 2015]. However, experimentally validating the functionality of metabolic landscape is important to understand the plasticity and adaptability of parasites metabolism for successful completion of life cycle in different stages and host, vector or environment. Understanding of differential or specific metabolic need of the parasites is the first step towards identifying a valid target for any future therapeutic intervention.

1.5 Modulation in metabolism at different life stages of the parasite

The parasites metabolism has been fascinatingly evolved under the influence of host. It is integral part of parasite's metabolic evolution to subvert the host defence at the same time optimally minimizing the energy consumption on anabolism and scavenge the required nutrients. The requirements of nutrients for motile, invading or fast replicating parasites are significantly high. The small organic molecules availability in host facilitate

generation of energy or as a building block for macro-molecule has helped the parasites to abandon some core metabolism otherwise present in eukaryotic cells and have been driving force behind the evolution of obligate in contrast to opportunistic parasitism [Borza *et al*., 2005]. The metabolism of the parasites are influenced by their environmental niches. Many of the apicomplexan parasites replicate within more than one niche; while some other (e.g. *T. gondii*) survives in open environment within stress-resistant cysts. Digenetic parasites like *Plasmodium* are transmitted between mammalian hosts to mosquito vectors. This adaptability requires sensing the environmental niches in which metabolism again play a very important role. Threshold concentration of many metabolites are trigger for many morphological changes and leads to commitment to stage differentiation [Lujan *et al.*, 1996; Billker *et al*., 1998; Engstler *et al*., 2004]. Parasites need to adapt their metabolism during different life cycle stages to sync with altered growth conditions and nutrient availability in their respective niches. The mosquito gut epithelium environment is completely different to human hepatocytes and these both are metabolically different to red blood cells (RBCs). Thus forcing *Plasmodium* parasites to modulate their metabolism accordingly in sexual and asexual stages accordingly. Similarly, *T. gondii* have fast growing tachyzoites, cysts forming bradyzoites and oocysts in their life cycle, all needing to adjust their metabolism according to the respective environments and nutrient availability.

It is fascinating as well important to understand the underlying mechanism of this plasticity in metabolic capacity which is characteristic of successful parasitism. Residing in nutrient rich niches, a large number of transporters are expressed to ensure the fulfilment the requirements. Nearly 2.5 % of total genomic sequence of *P. falciparum* codes for transporters or channels [Martin *et al*., 2009]. When we study the genome data of *P. falciparum* and *T. gondii*, complete set of Tricarboxylic acid cycle (TCA) genes are

present and expressed but the stage specific functional importance and contribution of oxidative phosphorylation in total cellular energy production is not well defined [Vercesi *et al*., 1998; Uyemura *et al*., 2004]. Many TCA cycle enzymes like succinyl-CoA synthase in *T. gondii* was disrupted, but had minimal (30%) growth rate defect, which could be restored by supplying exogenous succinate [Fleige *et al*., 2008] in asexual tachyzoite stages. Many of the glycolytic enzymes were duplicated in the genome of T. gondii and are targeted to the apicoplast, where they might have role to play in production of ATP for fulfilling the organelle's own need [Flegie *et al*., 2007] while the source for malarial parasites apicoplast energy is still not well defined.

In malarial parasites intraerythrocytic stages, for very long time, incomplete anaerobic oxidation of glucose in glycolysis was considered to be the sole source of energy [Roth *et al*., 1988]. Recent transcriptional, proteomics and metabolomics analysis reinvestigated the pathway and highlighted three different clusters of malarial parasites isolated from patients. First cluster showed similar to anaerobic conditions by inducing the expression of glycolytic, amino acid and nitrogen metabolism genes typical to *in-vitro* culture. The other cluster showed induced expression of gees associated with genes of TCA cycle, fatty acid metabolism and metabolism and uptake of glycerol. This finding reflects the condition of glucose starvation, pointing towards the metabolic switch from anaerobic to mitochondrial metabolism [Daily *et al*., 2007; Polonais *et al*., 2010].

Differential metabolic need and operability of TCA cycle in asexual and sexual stages of the malarial parasites were further proven by proteomic studies and metabolomics studies where TCA cycle intermediates like citrate, malate, succinate, α-ketoglutarate derived were detected signifying the function of mitochondrial metabolism [Lasonder *et al*., 2008, Olszewski *et al*., 2009]. Still the function of mitochondria in asexual stages were found to be dispensable as observed in the study where 6 out of 10 (α-ketoglutarate

dehydrogenase subunit E1, succinyl-CoA synthetase α subunit, succinate dehydrogenase flavoprotein subunit, Citrate synthase, aconitase and isocitrate dehydrogenase) genes of TCA cycle were successfully knocked out without affecting the asexual stages but were found to be non-viable into sexual stages specially late gametocytes development were halted in aconitase knockout lines, whereas α-ketoglutarate dehydrogenase mutant were defective in oocyst development [Ke *et al*., 2015].

1.6 Evolutionary streamlining of organelle metabolism

As is the case for eukaryotic organisms, apicomplexan parasites compartmentalize their metabolism between cytoplasm and different organelles. Energy generating anaerobic glucose catabolism by glycolysis is cytoplasmic, which is not an energy efficient pathway [Vander Heiden *et al*., 2009], but all apicomplexan parasites depend on it for obtaining carbon and energy [Lockwood *et al*., 1991; Edwards *et al*., 1992; Yarlett *et al*., 1996; Muller *et al*., 2001]. The complete oxidation of glucose is achieved *via* the TCA cycle, which is localized to the mitochondrion. Many prior studies have established the importance of mitochondrial metabolism for the survival of *P. falciparum* and *T. gondii* [Seeber et al., 2008], especially in those stages where parasites may not have access to free glucose. For example, protein expression profile and subcellular targeting studies reveal that the ookinete stages of *P. falciparum* have higher expression of mitochondrial respiratory enzymes, when they traverse the glucose depleted region of the mosquito gut epithelium.

Morphological studies support this findings with well-developed cristae in the mitochondrion during this stage, in comparison to the asexual stages [Sinden *et al*., 1978]. In addition to TCA cycle and oxidative phosphorylation, the mitochondrion also houses pathways associated with pyrimidine biosynthesis, haem biosynthesis, iron-sulphur

cluster biogenesis and metabolism of amino acid [Seeber *et al*., 2014] [Fig. 5]. Increased dependence of the parasite on mitochondrial metabolism during the sexual stages suggests that the parasite either requires a more efficient energy production mechanism in addition to glycolysis or they are utilizing carbon and energy sources other than glucose to support the physiological activities *via* the mitochondrial oxidative metabolic pathways [Hall *et al*., 2005]. Aplicomplexan parasites appear to have lost their peroxisomes, which normally host pathways for β-oxidation of fatty acids [Ding *et al*., 2000; Katinka *et al*., 2001; Gardner *et al*., 2002; Abrahamsen *et al*., 2004; Xu *et al*., 2004] thus leaving these parasites with limited capability to metabolize lipids and use fatty acids as a source of energy [Katinka *et al*., 2001; Das *et al*., 2002].

The other very unique feature of the apicomplexan parasites is the presence of a 35kb circular DNA possessing, self-replicating, non-photosynthetic organelle surrounded with four membranes, which was identified as relic of plastid [Kohler *et al*., 1997], and called as the apicoplast. This organelle was acquired by an ancestral apicomplexan *via* secondary endosymbiont event, probably involving a red alga [Waller *et al*., 2000]. It is now well documented that the organelle is essential for parasite development [Fichera & Roos 1997; McConkey *et al*., 1997], and possess anabolic pathways for fatty acid and isoprene biosynthesis [Waller *et al*., 1998; Jomma *et al*., 1999; Foth *et al*., 2003]. The essentiality of 2-deoxy-D-xylulose-5-phosphate (DXP) synthase and DXP reductoisomerase in *P. falciparum*, both involved in synthesis of isoprene pyrophosphate (IPP) and localized to apicoplast, indicates the importance of this organelle and was probably facilitated by the loss of cytoplasmic mevolonate pathways [Jomaa *et al*., 1999; Smit *et al*., 2000; Ginger *et al*., 2005] This organelle also contains the metabolic pathways for phospholipids biosynthesis, a second iron-sulphur cluster and part of haem biosysnthesis [Seeber *et al*. 2014].

Thus, both the endosymbiotic organelles, apicoplast and mitochondrion, house metabolic functions important to apicomplexan parasites, and contribute to different extent for the parasites adaptation to various host niches. The repertoire of metabolic pathways has been tailored to satisfy the unique metabolic needs of each parasites [Danne *et at*., 2013; Janouskovec *et al*., 2015; Polonais et al., 2010; Seeber *et al*., 2008; Sheiner *et al*., 2013]. There is growing evidence that both organelles have evolved collaborative metabolic relationship and may be functionally interconnected [Hopkins *et al*., 1999, Waller *et al*., 2000; Leister *et al*., 2005] [Fig. 1.5].

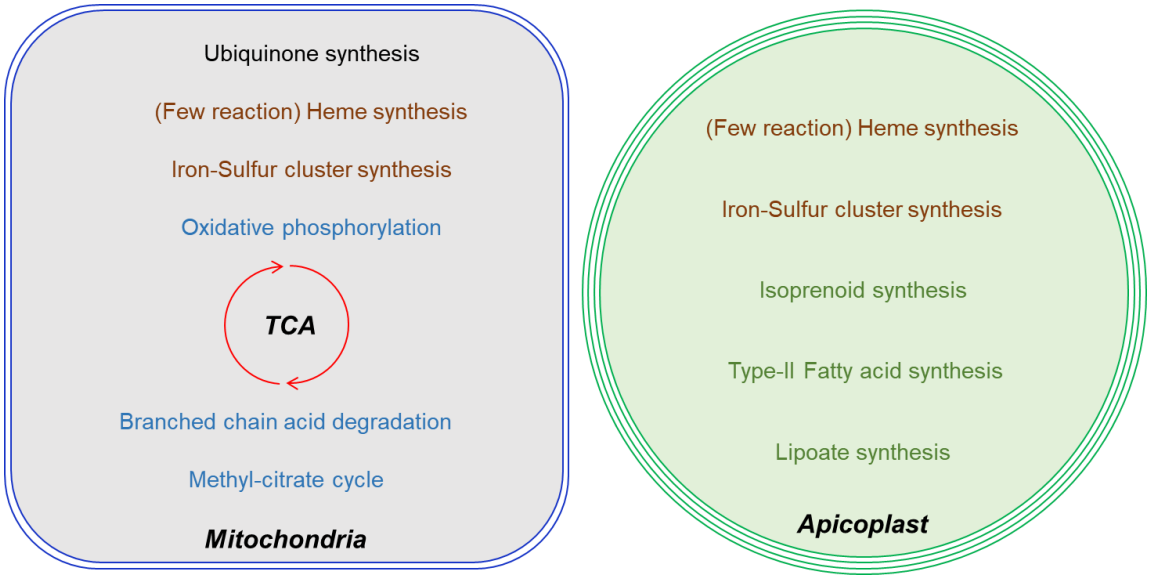

Figure 1.5 Major metabolic pathways associated with mitochondrion and apicoplast of apicomplexan parasites.

Most apicomplexan parasites have a high rate of replication during asexual proliferation and thus demand higher rate of lipid biosynthesis to meet the synthesis of parasite endomembrane structures and increasing size of parasitophorous vacuole to accommodate the increasing number of parasites [Charron *et al*., 2002]. In *T. gondii* and *P. falciparum*, part of fatty acid (FA) requirements are fulfilled by scavenging from the host and serum, eventhough they possess the capacity of *de novo* synthesis. All apicoplast

bearing parasites also possess the type-II proteobacterial like FAS II pathway which is localized to this organelle and possess the complete set of enzymes as discrete units, is used for *de novo* synthesis of FAs [Mazumdar *et al*., 2007]. In addition, an ER associated Type-I FAS enzyme, composed of a single polypeptide of ~1 MDa is present in few of these parasites, including in *T. gondii*. Thus, the unique and essential organellar metabolic functions make these valid targets for developing pharmaceutical intervention to treat parasitic infections [Lim *et al*., 2010].

1.7 Metabolic functions are prominent targets for anti-parasitic therapeutics

The unique aspects of apicomplexan metabolism which enable the parasites to adapt to different host niches during the various developmental stages remain largely under studied. The possible role of a metabolic switche that can trigger stage conversion in these parasites is something that remains unexplored. These parasites have evolved to maximally utilize available nutrients from the host environment, while at the same time escaping the host mediated immune response. Increased understanding of the unique features of metabolic functions in apicomplexan parasites has facilitated the identification of novel anti-parasitic drug targets. At present many of the clinical drugs used against malaria or toxoplasmosis are targeting specifically the essential metabolic function in the parasites. Haem detoxification by haemozoin formation is a prominent drug target in malaria parasite food vacuole, and is targeted by 4-amino quinolone class of drugs like chloroquine (CQ), amodiaquine (AQ) and piparaquine (PPQ). In both *T. gondii* and *P. falciparum* sulphadoxin (SDX), pyrimethamine (PYR) and cycloguanil (CYC) target the folate biosynthesis pathway. Inhibition of cytochrome bc1 complex in mitochondrial electron transport chain is inhibited by naphthoquinone class of drugs, such as atovaquone (ATQ) [Fig 1.6] [Blasco *et al*., 2017].

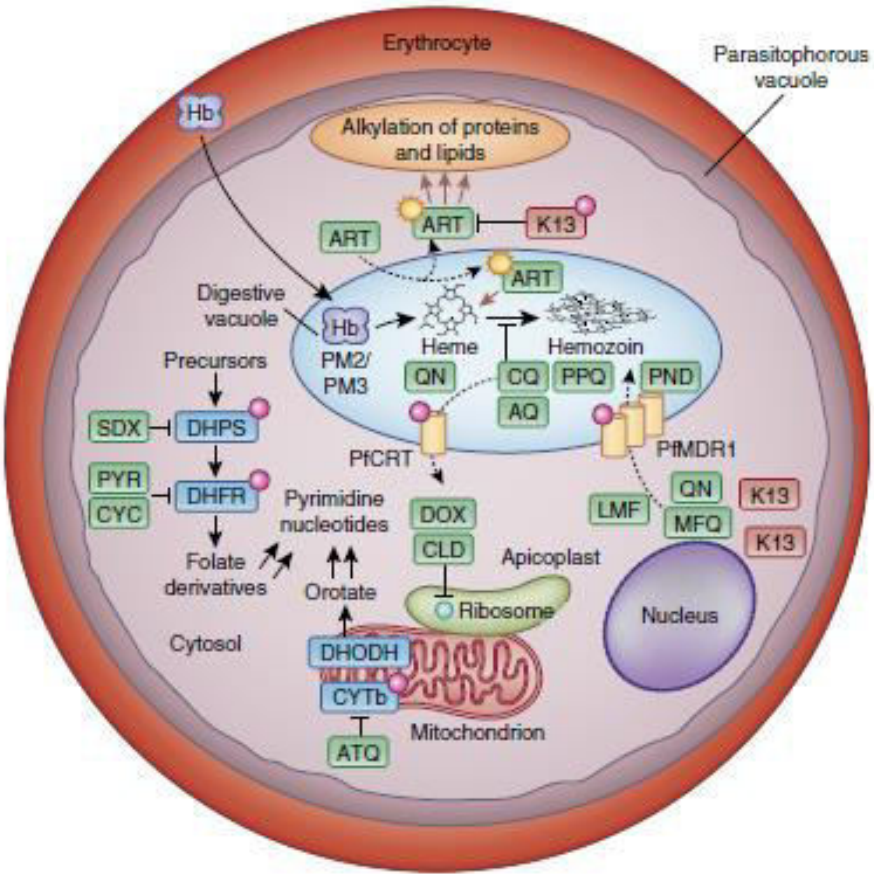

Figure 1.6 Schematic for drugs and their targets in Plasmodium falciparum; *Reproduced from Blasco et al., 2017; SDX, Sulphodoxine; PYR, Pyrimethamine; CYC, Cycloguanil; DHPS, dihydrooperate synthase; DHFR, dihydrofolate reductase; CQ, Chloroquine; ATQ, Atovaquone; CYTb, Cytochrome b; DHODH, Dihydroorotate dehydrogenase; AQ, Amodiaquine; PPQ, Piparaquine.*

These are a few examples were, essential metabolic functions in the parasite have been targeted successfully. However, there is scope for developing more novel drug molecules that target many other unique metabolic functions in the parasite with higher potency, higher specificity, less toxicity, and most importantly with less chance for developing drug resistance. Therefore, there is a need to study and identify novel metabolic target and develop therapeutic molecules to treat and reduce the growing concern of drug resistant parasites.

1.8 Studying parasite metabolism using global and targeted approaches

To expand our understanding of apicomplexan parasite metabolic capabilities, host response, and development of drug resistance, classical approaches using cell biology, genetics, and biochemical techniques have been pursued. These classical techniques have the limitation of not being able to provide a global picture of metabolism in apicomplexan parasites. Additionally, in biochemical assay relative large sample material, such as cellular fractions or enzyme preparations are needed, which is a big drawback, given the technical issue associated with scale up of parasite cultures. In fact, even in well studied parasites such as *P. falciparum* and *T. gondii*, only certain life cycle stages are accessible to biochemical studies. Here, using more advanced techniques, such as genomics, proteomics and metabolomics, can help in capturing the global profile of parasite metabolic capability and their functional validation. The use of these techniques to study parasite metabolism is discussed in detail below.

1.8.1 Genomics and transcriptomics

Recent advances in sequencing technology and comparative genomics using bioinformatics, has revolutionized the field of parasitology, and has helped in generating and understanding global metabolic networks from related organism, even for those that cannot be grown in the lab. Genome level metabolic network reconstruction (GENREs) technique, which creates mathematical metabolic reactions framework for an organism, emphasising relationships between genes, proteins, and metabolic reactions, and predicts the theoretical effect of knocking out of any gene in the related system, has been reported [Reed *et al*., 2003; Durot *et al*., 2009; Dunphy *et al*., 2018].

Parasitic disease	Recomonded drug	Resistance Reported
Malaria	Chloroquine	1957
	Quinine	1910
	Pyrimethamine/Sulphadoxine	1967
	Primaquine	
	Mefloquine	1982
	Halofantrine	
	Tetracycline	
	Doxycycline	
	Proguanil	1949
	Artemether	
	Artesunate	2011
	Artemisinin	2008
	Atovaquone	1997
	Pipraquine	1989
	ASSP	2011
	AL (Artemether + lumefantrine)	
	PA (Artesunate + pyronaridine)	
	DHA-PPQ (dihydroartemisinin + piperaquine)	2000
	ASMQ (Artesunate + mefloquine)	2002
	Amodiaquine	1971
Toxoplasmosis	Pyrimethamine	
	Sulfadiazine	
	Calcium folinate	

Table 1.1 WHO approved drugs against Protozoan parasites and year of resistance reported. *Data compiled from WHO report 1995 and Blasco et al., 2017.*

The availability of complete genome sequence of apicomplexan parasites of the genus *Plasmodium*, *Toxoplasma*, *Theileria*, and *Cryptosporodium*, and other related free living organism, such as *Chromera velia* has made it possible to map metabolic functions, and study their requirement for the parasite from a biological and evolutionary perspective [Gardner *et al*., 2002, Kissinger *et al*., 2003, Gardner *et al*., 2005, Abrahamsen *et al*., 2004, Woo et al., 2015]. This has spurred in-depth studies on global metabolic networks in many apicomplexan parasites. For example; *P. falciparum's* metabolic network was

reconstructed by Carey et al., 2017, Feng et al., 2014 and Tewari et al., 2017, while Song et al., 2013, has generated the *T. gondii* network [Fig. 1.7].

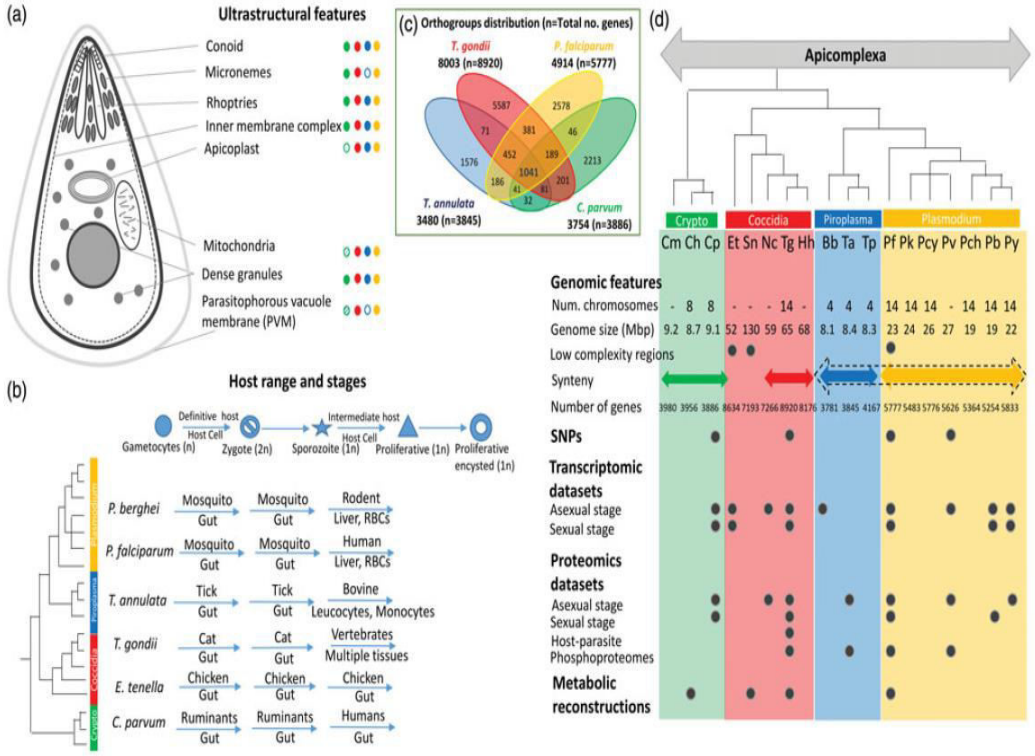

Figure 1.7 Comparative genomics studies of apicomplexan parasites; *Adapted from Swapna et al., 2017*; *(A) common ultrastructure features; (B) Comparison of apicomplexan parasite host and tissues specificity according to their life stages; (C) Shared orthologs between T. gondii, P. falciparum, T. annulata and C. parvam; (D) Comparison of genome size and number of annotated genes and gene features, availability of various genome scale functional datasets, including SNP analysis, transcriptomics and proteomics data sets, and global metabolic network predicted from genomic data, for various apicomplexan parasites.*

The whole genome data and reconstructed metabolic network data have together helped understand metabolic functions in concerned organisms and in related organisms. Though genomics is a powerful technique which provides comprehensive information about all possible metabolic and cellular functions, on the basis of the conserved genes and their predicted functions, biochemical evidences are always needed to validate these

functions which is a tedious, on a global scale. Thus genomic studies need to be complemented with other global experimental approaches to validate any finding or proposed function.

1.8.2 Genetics and Biochemical Assays

The classical way of assigning function to a gene is done using either forward or reverse genetic approaches. In forward genetics, the gene(s) linked to a phenotype is mapped by genetic or genomic approaches, while in reverse genetics a gene is first mutate to find out the associate phenotype and function. Sometimes, gene knockdown or overexpression is carried out to find out the function. Genetic and biochemical assays are the gold standard techniques classically to validate the function of any gene or protein in particular organisms. In case of apicomplexan parasites, which are amenable to genetic manipulation in the laboratory, these techniques has been successfully employed Wang et al., 2016. Generation of ΔKu80 knockout strains in *T. gondii* has made gene knockout studies much easier by preventing unintended non-homologous recombination from happening [Fox *et al*., 2009]. Development of selection markers like uracil phosphoribosyltransferase (UPRT) [Donald *et al*., 1995], hypoxanthine guanine phosphoribosyltransferase (HXGPRT) [Donald *et al*., 1996], dihydrofolate reductase (DHFR) [Donald *et al*., 1993], chloramphenicol acyltransferase (CAT) [Kim et al., 1993] has greatly facilitated the development of various genetic manipulation techniques and studies [Huynth *et al*., 2009]. Many gene with metabolic (example, knockout of the major glucose transporter GT1 [Martin *et al*., 2009] and the glycolytic enzymes aldolase [Shen *et al*., 2014] and fructose bisphosphate-1 [Martin *et al*., 2015]) and non-metabolic functions have been achieved in *T. gondii* by these approaches, helping to validate their function and essentiality for the parasites life cycle. In *Plasmodium sp*., genome editing

techniques such as zinc-finger nuclease [Ma *et al*., 2015; Suarej *et al*., 2017], and homology based recombination modification [Fox *et al*., 2009] have been implemented to study the function of gene of interest.

Though these techniques are handy, comprehensive and widely used, they are used to one gene at a time and sometimes can be technically challenging. Thus, a major bottleneck of these techniques is that they are not very useful for genome-scale studies. The newly introduced CRISPR-Cas9 [Sidik *et al*., 2014; Shen *et al*., 2014] mediated genome editing, is now fast becoming the method of choice for different gene manipulation studies, in single gene and genomic scale studies. However, in addition to these genetic approaches, biochemical studies are needed, especially at the global level, to accelerate new discoveries on parasite metabolism.

1.8.3 Metabolomics as a tool for generating global metabolic profiles

There is now increased need to generate global profile of metabolic intermediates and end products, as well as other small molecules, from biological samples, and this is being addressed by the technique of metabolomics. Metabolomics is a newer addition to the other 'omics' approaches such as genomics, transcriptomics and proteomics. Metabolomics can be defined as the study of chemicals in Biosystems [Salinas *et al*., 2014]. The two major approaches in metabolomics are targeted (i.e, analyzing only one or a small number of specific chemical entities) and untargeted (i.e, complete profiling of total metabolite content) analysis of small molecules and their biochemical relations in a given biological system of interest [Kafsack *et al*., 2010; Jones *et al*., 2012]. Metabolomics deals with end products of biochemical process specific to cells, tissues, bodily fluid, organs or whole organism which can be experimentally analysed. It can be used to validate predicted metabolic functions inferred from genome data, and investigate

exposure to external chemicals like drugs, toxins, contaminants or other chemicals and their effects [Jones *et al*., 2012]. Metabolomics applications have also revolutionized the field of parasitology and have been extensively used to improve our understanding of metabolic capabilities in apicomplexan parasites, primarily *T. gondii* and *P. falciparum.* From the technology side, metabolomics is carried out either by Nucleic Magnetic Resonance (NMR) or mass spectrometry (MS), both of which can capture the chemical makeup of biological samples, while having their advantages and disadvantages.

In NMR metabolomics, both solid and liquid state analysis has been successfully used for metabolic profiling from spectral analysis of body fluids (urine, serum, plasma, metabolic extracts) followed by statistical analysis using multivariate methods like PCA (Principle component analysis) and OPLSDA (Orthogonal Partial Least Square-Discriminant Analysis) to identify either changes in levels of metabolites or even identify unique metabolites [Lindon *et al*., 2001; Lindon *et al*., 2006; Sengupta *et al*., 2011]. The strategy of NMR based metabolomics has also been implemented in identification of novel biomarkers for disease conditions [Robertson *et al*., 2007; Brindle *et al*., 2007]. With respect to malaria, parasites in culture have been used to study the changes in metabolic profile during the course of intraerythrocytic development of the parasite [Teng *et al*., 2009]. Using NMR, host-pathogen interaction studies in case of malaria infection were carried out in urine samples of human and rodent samples [Basant *et al*., 2010; Li *et al*., 2008; Kochar *et al*., 2009; Lauridsen *et al*., 2007; Sengupta *et al*., 2010; Sengupta *et al*., 2011]. Though the NMR offers exact quantification and identification of metabolites, lower sensitivity and requirement of large amount of samples are big challenges in performing metabolomics experiments. Having access to a good NMR facility can also be a significant challenge for performing these experiments.

Global metabolomics got a boost with the advent of MS based profiling of small molecules. MS coupled with either liquid (LC-MS) or gas (GC-MS) chromatographic platform is a very robust technique which can separate, detect and identify thousands of biologically important small molecules of molecular weight < 1000 Da in a single run, with very small quantity of complex biological sample. Nowadays, both LC-MS and GC-MS techniques are being used extensively for studying parasite metabolism and discerning essential functions in different life cycle stages and host parasite interaction [Lakshmanan *et al*., 2011; Wang *et al*., 2013].

MS based metabolomics is being combined with stable isotope labelling techniques have greatly enhanced our ability to track the kinetics of various metabolic pathways in apicomplexan parasites and their adaptation to different environmental conditions [Kafsack *et al*., 2010; Lakshmanan *et al*., 2011; Salinas *et al*., 2014]. Such studies have helped in dissecting central carbon metabolism, such as glycolysis and TCA cycle, in both *Plasmodium* and *T. gondii* [Cobbold *et al*., 2013; Ke *et al*., 2015; MacRae *et al*., 2012; MacRae *et al*., 2013; Storm *et al*., 2014]. For example, such studies have revealed that the TCA cycle is fuelled by either glucose glutamine derived carbon in both parasites. Pyruvate, the end product of glycolysis, was found to be converted to acetyl-CoA by the non-canonical mitochondrial branched chain ketoacid dehydrogenase (BCKDH), and enter TCA cycle in both *T. gondii* and *P. berghei* [Oppenheim *et al*., 2014]. Anaplerotic conversion of phosphoenolpyruvate (PEP) to oxaloacetate is another mechanism for entry of glucose derived carbon into TCA cycle [MacRae *et al*., 2012; Nitzsche *et al*., 2016]. Unexpected findings, like the GABA shunt mediated conversion of glutamine to GABA, which acts as a temporary energy source in extracellular parasites by feeding into the TCA cycle and supporting their survival and host cell invasion in absence of glucose or glutamine for short periods, have been made using LC-MS metabolomics

[MacRae *et al*., 2012]. Combined with genetics and biochemical assays, MS based metabolomics has significantly helped in dissecting the apicomplexan metabolism. It provides a powerful hands on tool to study the effect of gene functions and nutrient requirements at systems level. MS based metabolomics has also been used to study the global metabolic perturbations caused by novel antiparasitic inhibitors, thus providing a way to study their mode of action for many anti-malarial compounds [Creeck *et al*., 2016; Llinas *et al*., 2016]. Thus, from the above discussed examples, it is clear that MS based metabolic studies has greatly facilitated in-depth studies to pinpoint the plasticity in nutrient metabolism in apicompelxan parasites, and helping to identify new targets for chemotherapeutic interventions.

1.9 Scope of the thesis

Parasitic infection cause thousands of deaths worldwide annually. It is also responsible for heavy monetary loss and productive time loss, thus inflicting a great economic burden. Nearly 200 million people get infected with *Plasmodium* annually [WHO malaria report, 2016] and nearly every 3rd person carries the *T. gondii* infection asymptomatically which can overtake the immune system at any time. Thus, studying parasite life cycle stage specific nutrient requirements and identifying essential metabolic needs of the parasite, will help in developing effective treatment options in future. In this study, I have used the two model apicomplexan parasites *P. falciparum* and *T. gondii* to dissect their metabolic capabilities by using genetics, biochemistry and MS based metabolomics. The specific aims and objectives of the thesis are listed below.

Aim 1. *Dissecting the essentiality of glycolysis and gluconeogenesis during asexual growth and differentiation of T. gondii.*

Aim 2. *Identifying atovaquone drug analogs, validating their conserved Cytb mediated mode of action by MS metabolomics and evaluating their efficacy against atovaquone resistant parasites.*

Aim 3. *Profiling drug specific metabolite pertubations in P. falciparum to study their mode of action using untargeted LC-MS metabolomics.*

The research work carried out to address these various objectives is elaborated in the following chapters.

1.10 References:

Abrahamsen, MS. *et al*. (2004). "Complete genome sequence of the apicomplexan, Cryptosporidium parvum." Science 304(5669): 441-445.

Allman EL. *et al*. (2016). Metabolomic Profiling of the Malaria Box Reveals Antimalarial Target Pathways; Antimicrobial Agents and Chemotherapy, 60, 6635-6649.

Bartosova-Sojkova, P., Oppenheim, R.D., Soldati-Favre, D., and Lukes, J. (2015). Epicellular Apicomplexans: Parasites "On the Way In". PLoS pathogens 11, e1005080.

Basant A, Rege M, Sharma S, Sonawat HM (2010). Alterations in urine, serum and brain metabolomic profiles exhibit sexual dimorphism during malaria disease progression. Malar J, 9:110.

Berger F., Goulet V., Le Strat Y., Desenclos JC. (2009). Toxoplasmosis among pregnant women in France: Risk factors and change of prevalence between 1995 and 2003. Rev Epidemiol Sante Publique; 57(4): 241-8.

Billker, O. *et al*. (1998). Identification of xanthurenic acid as the putative inducer of malaria development in the mosquito. Nature 392, 289–292.

Blasco B., Leroy D., Fidock DA., (2017). Antimalarial drug resistance: linking Plasmodium falciparum parasite biology to the clinic. Nature Medicine 23, 917-928.

Boddey, J.A., and Cowman, A.F. (2013). Plasmodium nesting: remaking the erythrocyte from the inside out. Annual review of microbiology 67, 243-269.

Borza, T., Popescu, C. E. & Lee, R. W. (2005). Multiple metabolic roles for the nonphotosynthetic plastid of the green alga Prototheca wickerhamii. Eukaryot. Cell 4, 253–261.

Brindle JT. *et al*. (2002). Rapid and noninvasive diagnosis of the presence and severity of coronary heart disease using 1H-NMR-based metabonomics. Nat Med, 8:1439-1445.

Charron, A.J., and Sibley, L.D. (2002). Host cells: mobilizable lipid resources for the intracellular parasite Toxoplasma gondii. J Cell Sci 115: 3049–3059.

Checkley, W. *et al*. (2015). A review of the global burden, novel diagnostics, therapeutics, and vaccine targets for cryptosporidium. Lancet Infect Dis 15, 85-94.

Cobbold, SA. *et al*. (2013). Kinetic flux profiling elucidates two independent acetyl-CoA biosynthetic pathways in Plasmodium falciparum. The Journal of biological chemistry 288, 36338-36350.

Creek Dj. *et al*. (2016). Metabolomics-Based Screening of the Malaria Box Reveals both Novel and Established Mechanisms of Action; Antimicrobial Agents and Chemotherapy, 60, 6650-6663.

Daily JP. *et al*. (2007). Distinct physiological states of Plasmodium falciparum in malaria-infected patients. Nature 450, 1091-1095.

Danne JC. *et al.* (2013). Alveolate mitochondrial metabolic evolution: dinoflagellates force reassessment of the role of parasitism as a driver of change in apicomplexans. Mol Biol Evol 30: 123– 139.

Danne, JC. *et al*. (2012). Alveolate mitochondrial metabolic evolution: dinoflagellates force reassessment of the role of parasitism as a driver of change in apicomplexans. Mol Biol Evol 30: 123–139.

Das, S. *et al*. (2002). Lipid metabolism in mucousdwelling amitochondriate protozoa. Int. J. Parasitol. 32, 655–675.

Ding, M., Clayton, C. & Soldati, D. (2000). Toxoplasma gondii catalase: are there peroxisomes in toxoplasma? J. Cell Sci. 113, 2409–2419.

Dobson AP., Carper ER. (1996). Infectious Diseases and Human Population History. BioScience, 42;2, 115-126.

Donald R.G., Carter D., Ullman B., Roos D.S., (1996). Insertional tagging, cloning, and expression of the Toxoplasma gondii hypoxanthine-xanthine-guanine phosphoribosyltransferase gene. Use as a selectable marker for stable transformation. J Biol Chem. 14;271 (24):14010-9.

Donald R.G., Roos D.S., (1993). Stable molecular transformation of Toxoplasma gondii: a selectable dihydrofolate reductase-thymidylate synthase marker based on drug-resistance mutations in malaria. Proc Natl Acad Sci U S A. 15;90 (24):11703-7.

Donald R.G., Roos D.S., (1995). Insertional mutagenesis and marker rescue in a protozoan parasite: cloning of the uracil phosphoribosyltransferase locus from Toxoplasma gondii. Proc Natl Acad Sci U S A. 6;92 (12):5749-53.

Dubey, J. P., Lindsay, D. S., and Speer, C. A. (1998). Structures of Toxoplasma gondii tachyzoites, bradyzoites, and sporozoites and biology and development of tissue cysts. Clinical microbiology reviews 11, 267-299

Dubey, J.P. (2008). The history of Toxoplasma gondii--the first 100 years. The Journal of eukaryotic microbiology 55, 467-475.

Dumetre, A. *et al*. (2013). Mechanics of the Toxoplasma gondii oocyst wall. Proceedings of the National Academy of Sciences of the United States of America 110, 11535-11540.

Dunphy LJ, Papin JA, (2018). Biomedical applications of genome-scale metabolic network reconstructions of human pathogens; Current Opinion in Biotechnology, 51:70–79.

Durot M, Bourguignon P-Y, Schachter V (2009). Genome-scale models of bacterial metabolism: reconstruction and applications. FEMS Microbiol Rev, 33:164-190.

Edwards, M. R., Schofield, P. J., O'Sullivan,W. J. & Costello, M. (1992). Arginine metabolism during culture of Giardia intestinalis. Mol. Biochem. Parasitol. 53, 97–103.

Engstler, M. & Boshart, M. (2004). Cold shock and regulation of surface protein trafficking convey sensitization to inducers of stage differentiation in Trypanosoma brucei. Genes Dev. 18, 2798–2811.

Fichera, M. E. & Roos, D. S. (1997). A plastid organelle as a drug target in apicomplexan parasites. Nature 390, 407–409.

Fleige T, Pfaff N, Gross U, BohneW (2008). Localisation of gluconeogenesis and tricarboxylic acid (TCA)-cycle enzymes and first functional analysis of the TCA cycle in Toxoplasma gondii. International Journal for Parasitology. pp. 1121–1132.

Fleige, T. *et al*. (2007). Carbohydrate metabolism in the Toxoplasma gondii apicoplast: localization of three glycolytic isoenzymes, the single pyruvate dehydrogenase complex, and a plastid phosphate translocator. Eukaryot Cell 6: 984–996.

Foth, BJ. *et al*. (2003). Dissecting apicoplast targeting in the malaria parasite Plasmodium falciparum. Science 299, 705–708.

Fox BA. e*t al*. (2009). Efficient gene replacements in Toxoplasma gondii strains deficient for nonhomologous end joining. Eukaryot Cell. 8(4):520-9.

Gardner, MJ. *et al*. (2002). Genome sequence of the human malaria parasite Plasmodium falciparum; Nature, 419:498–511.

Ginger, ML. *et al*. (1999). Elucidation of carbon sources used for the biosynthesis of fatty acids and sterols in the trypanosomatid Leishmania mexicana. Biochem. J. 342, 397–405.

Gould, SB. *et al*. (2008a). Alveolins, a new family of cortical proteins that define the protist infrakingdom Alveolata. Molecular biology and evolution 25, 1219-1230.

Gueirard, P. *et al*. (2010). Development of the malaria parasite in the skin of the mammalian host. Proc Natl Acad Sci U S A 107: 18640-18645.

Hall, N. *et al*. (2005). A comprehensive survey of the Plasmodium life cycle by genomic, transcriptomic, and proteomic analyses. Science 307, 82–86.

Halonen, S.K., and Weiss, L.M. (2013). Toxoplasmosis. Handb Clin Neurol 114, 125-145.

Hangjun Ke *et al*. (2015). Genetic Investigation of Tricarboxylic Acid Metabolism during the Plasmodium falciparum Life Cycle; Cell Reports 11, 164–174.

Hopkins, J. *et al* (1999). The plastid in Plasmodium falciparum asexual blood stages: a three-dimensional ultrastructural analysis. Protist 150, 283-295.

Huff, CG. (1947). Life Cylce of Malarial Parasites. Annu. Rev. Microbiol. 1: 43-60.

Hunter, CA., and Sibley, LD. (2012). Modulation of innate immunity by Toxoplasma gondii virulence effectors. Nat Rev Micro 10, 766-778

Huynh, MH., Carruthers, VB., (2009). Tagging of endogenous genes in a Toxoplasma gondii strain lacking Ku80. Eukaryot. Cell 8, 530–539.

Jomaa, H. *et al*. (1999). Inhibitors of the nonmevalonate pathway of isoprenoid biosynthesis as antimalarial drugs. Science 285, 1573–1576.

Jones DP., Park Y, Ziegler TR (2012). Nutritional metabolomics: progress in addressing complexity in diet and health. Annu Rev Nutr 32: 183-202.

Kafsack BFC, Llinás M (2010). Eating at the table of another: metabolomics of host-parasite interactions. Cell Host Microbe 7: 90-99.

Kantele, A., and Jokiranta, T.S. (2011). Review of cases with the emerging fifth human malaria parasite, Plasmodium knowlesi. Clin Infect Dis 52, 1356-1362.

Katinka MD. e*t al*. (2001). Genome sequence and gene compaction of the eukaryote parasite Encephalitozoon cuniculi. Nature, 414, 450–453.

Kim K., Soldati D., Boothroyd J.C., (1993). Gene replacement in Toxoplasma gondii with chloramphenicol acetyltransferase as selectable marker. Science. 5;262(5135):911-4.

Kochar DK. e*t al*. (2009). Severe Plasmodium vivax malaria: a report on serial cases from Bikaner in Northwestern India. Am J Trop Med Hyg, 80:194-198.

Kohler, S. *et al*. (1997). A plastid of probable green algal origin in Apicomplexan parasites. Science 275, 1485–1489.

Kuehn, A., and Pradel, G. (2010). The coming-out of malaria gametocytes. J Biomed Biotechnol 2010, 976827.

Lakshmanan V, Rhee KY, Wang W, Yu Y, Khafizov K, et al. (2012); Metabolomic analysis of patient plasma yields evidence of plant-like a-linolenic acid metabolism in Plasmodium falciparum. J Infect Dis 206: 238–248.

Lauridsen M, Hansen SH, Jaroszewski JW, Cornett C (2007). Human urine as test material in 1H NMR-based metabonomics: recommendations for sample preparation and storage. Anal Chem, 79:1181-1186.

Leister, D. (2005); Genomics-based dissection of the cross-talk of chloroplasts with the nucleus and mitochondria in Arabidopsis. Gene 354, 110-116.

Li JV. e*t al*. (2008). Global metabolic responses of NMRI mice to an experimental Plasmodium berghei infection. J Prot Res, 7:3948-3956.

Lim L, McFadden GI., (2010). The evolution, metabolism and functions of the apicoplast. Philos Trans R Soc Lond B Biol Sci. Mar 12;365(1541):749-63.

Lindon J, Holmes E, Nicholson J (2006). Metabonomics techniques and applications to pharmaceutical research & development. Pharma Res, 23:1075-88.

Lindon JC, Holmes E, Nicholson JK (2001). Pattern recognition methods and applications in biomedical magnetic resonance. Prog NMR Spec, 39:1-40.

Lockwood, BC. & Coombs, GH. (1991). Amino acids catabolism in anaerobic protists. In Biochemical protozoology (ed. G. H. Coombs & M. J. North), London; Taylor & Francis. pp. 113–122.

Lujan, HD. *et al*. (1996). Cholesterol starvation induces differentiation of the intestinal parasite Giardia lamblia. Proc. Natl Acad. Sci. USA 93, 7628–7633.

Ma, D., Liu, F., (2015); Genome editing and its applications in model organisms. Genomics Proteomics Bioinformatics 13, 336–344.

MacRae, JI. *et al*. (2013). Mitochondrial metabolism of sexual and asexual blood stages of the malaria parasite Plasmodium falciparum. BMC biology 11, 67.

MacRae, JI. *et al*. (2012). Mitochondrial metabolism of glucose and glutamine is required for intracellular growth of Toxoplasma gondii. Cell host & microbe 12, 682-692.

Martin, R.E., Ginsburg, H., and Kirk, K. (2009). Membrane transport proteins of the malaria parasite. Molecular microbiology 74, 519-528.

Mazumdar, J., and Striepen, B. (2007). Make it or take it: fatty acid metabolism of apicomplexan parasites. Eukaryot Cell 6: 1727–1735.

McConkey, GA. e*t al*. (1997). Inhibition of Plasmodium falciparum protein synthesis. Targeting the plastid-like organelle with thiostrepton. J. Biol. Chem. 272, 2046–2049.

Menard, R. *et al*. (2013). Looking under the skin: the first steps in malarial infection and immunity. Nature reviews Microbiology 11, 701-712.

Moore RB. *et al*. (2008). "A photosynthetic alveolate closely related to apicomplexan parasites". Nature. 451 (7181): 959–963.

Muller, M. *et al*. (2001). Presence of prokaryotic and eukaryotic species in all subgroups of the PP(i)-dependent group II phosphofructokinase protein family. J. Bacteriol. 183, 6714–6716.

Nitzsche, R. *et al*. (2016). Metabolic Cooperation of Glucose and Glutamine Is Essential for the Lytic Cycle of Obligate Intracellular Parasite Toxoplasma gondii. J Biol Chem 291:126-41.

Olszewski KL. *et al*. (2009); Host parasite interaction revealed by Plasmodium falciparum Metabolomics. Cel Host Microb, 5:191-199.

Oppenheim, RD. *et al*. (2014). BCKDH: the missing link in apicomplexan mitochondrial metabolism is required for full virulence of Toxoplasma gondii and Plasmodium berghei. PLoS Pathog 10:e1004263.

Pittman, KJ., and Knoll, LJ. (2015). Long-Term Relationships: the Complicated Interplay between the Host and the Developmental Stages of Toxoplasma gondii during Acute and Chronic Infections. Microbiology and molecular biology reviews: MMBR 79, 387-401.

Polonais, V., and Soldati-Favre, D. (2010). Versatility in the acquisition of energy and carbon sources by the Apicomplexa. Biology of the cell / under the auspices of the European Cell Biology Organization 102, 435-445.

Reed JL, Vo TD, Schilling CH, Palsson BO: (2003). An expanded genome-scale model of Escherichia coli K-12 (iJR904 GSM/GPR). Genome Biol, 4:R54.

Robertson DG, Reily MD, Cantor GH, John CL, Jeremy KN, Elaine H (2007); Metabonomics in preclinical pharmaceutical discovery and development. The Handbook of Metabonomics and Metabolomics Amsterdam: Elsevier Science B.V; 241-277.

Roth, E.F., Jr., Calvin, M.C., Max-Audit, I., Rosa, J., and Rosa, R. (1988). The enzymes of the glycolytic pathway in erythrocytes infected with Plasmodium falciparum malaria parasites. Blood 72: 1922-1925.

Salinas JL., Kissinger JC., Jones DP., Galinski MR., (2014). Metabolomics in the fight against malaria; Mem Inst Oswaldo Cruz, Rio de Janeiro, Vol. 109(5): 589-597.

Seeber F., Limenitakis J., Soldati-Favre D., (2008). Apicomplexan mitochondrial metabolism: a story of gains, losses and retentions. Trends Parasitol; 24(10):468-78.

Seeber, F., Feagin, J.E., and Parsons, M. (2014). Chapter 9 - The Apicoplast and Mitochondrion of Toxoplasma gondii. In Toxoplasma Gondii (Second Edition), L.M. Weiss, and K. Kim, eds. (Boston: Academic Press), pp. 297-350.

Seeber, F., Limenitakis, J., and Soldati-Favre, D. (2008). Apicomplexan mitochondrial metabolism: a story of gains, losses and retentions. Trends Parasitol 24: 468–478.

Seeber, F., Steinfelder, S., (2007). Diversity, nomenclature, and taxonomy of protists. Syst. Biol. 56 (4), 684–689.

Sengupta A. *et al*. (2010). A urine 1H NMR based metabonomic approach to understand the host metabolic response towards plasmodium vivax infection. IFFF, 172-176.

Sengupta A. *et al*. (2011). Global host metabolic response to Plasmodium vivax infection: a 1H NMR based urinary metabonomic study; Malaria Journal, 10:384.

Sheiner, L. *et al*. (2013). The metabolic roles of the endosymbiotic organelles of Toxoplasma and Plasmodium spp. Current opinion in microbiology 16, 452-458.

Shen, B. *et al*. (2014). Efficient gene disruption in diverse strains of Toxoplasma gondii using CRISPR/CAS9. MBio 5:e01114-14.

Shen, B., Sibley, LD., (2014). Toxoplasma aldolase is required for metabolism but dispensable for host-cell invasion. Proc Natl Acad Sci U S A 111:3567-72.

Sidik, SM. e*t al*. (2014). Efficient genome engineering of Toxoplasma gondii using CRISPR/Cas9. PLoS One 9:e100450.

Simpson AGB., Patterson DJ., (1996). "Ultrastructure and identification of the predatory flagellate Colpodella pugnax Cienkowski (Apicomplexa) with a description of Colpodella turpis n. sp. and a review of the genus". Systematic Parasitology. 33 (3): 187–198.

Sinden, R. E. (1978). In Rodent malaria (ed. R. Killick-Kendrick & W. Peters), London:Academic Press. Cell biology. pp. 85–168.

Smit, A. & Mushegian, A. (2000). Biosynthesis of isoprenoids via mevalonate in Archaea: the lost pathway. Genome Res. 10, 1468–1484.

Storm, J. *et al*. (2014). Phosphoenolpyruvate carboxylase identified as a key enzyme in erythrocytic Plasmodium falciparum carbon metabolism. PLoS pathogens 10, e1003876.

Striepen, B. *et al*. (2007). Building the perfect parasite: cell division in apicomplexa. PLoS Pathog 3: e78.

Suarez CE. e*t al*. (2017). Advances in the application of genetic manipulation methods to apicomplexan parasites International Journal for Parasitology 47, 701–710.

Teng R. *et al*. (2009). Metabolite profiling of the intraerythrocytic malaria parasite Plasmodium falciparum. NMR Biomed, 22:292-302.

Uyemura SA. *et al*. (2004). Oxidative phosphorylation rotenone-insensitive malate- and NADH-quinone oxidoreductase in Plasmodium yoelii mitochondria in situ. The Journal of biological chemistry 227, 385-393

Vander Heiden MG. *et al*. (2009). Understanding the Warburg effect: the metabolic requirements of cell proliferation. Science. 22;324 (5930):1029-33

Vannier, E., and Krause, P.J. (2012). Human babesiosis. N Engl J Med 366, 2397-2407.

Vercesi, AE. *et al*. (1998). Respiration and oxidative phosphorylation in the apicomplexan parasite Toxoplasma gondii. The Journal of biological chemistry 273, 31040-31047.

Waller, RF. *et al*. (1998). Nuclear-encoded proteins target to the plastid in Toxoplasma gondii and Plasmodium falciparum. Proc. Natl Acad. Sci. USA 95, 12 352–12 357.

Waller, RF. e*t al*. (2000). Protein trafficking to the plastid of Plasmodium falciparum is via the secretory pathway. EMBO J. 19, 1794–1802.

Wang JL. e*t al*. (2016); The Past, Present, and Future of Genetic Manipulation in Toxoplasma gondii. Trends Parasitol. l;32 (7):542-553.

Wang Q. *et al*. (2010). Acetylation of metabolic enzymes coordinates carbon source utilization and metabolic flux. Science 327: 1004–1007.

WHO Report 2016

Woo, YH. *et al*. (2015). Chromerid genomes reveal the evolutionary path from photosynthetic algae to obligate intracellular parasites. Elife. 4:e06974.

Xu, P. et al. (2004). The genome of Cryptosporidium hominis. Nature 431, 1107–1112.

Yarlett, N. *et al*. (1996). The contribution of the arginine dihydrolase pathway to energy metabolism by Trichomonas vaginalis. Mol. Biochem. Parasitol. 78, 117–125.

Chapter 2

Studies on nutrient metabolism and essentiality of hexokinase and phosphoenolpyruvate carboxykinase enzymes in T. gondii

2.1 Introduction:

Apicomplexan species are remarkably diverse in their cellular metabolism, often harbouring a reduced set of pathways in comparison to their hosts or even related free-living protists [Woo, *et al*., 2015]. As a consequence, these parasites resort to scavenging a variety of essential nutrients and metabolites from the host [Polonais and Soldati-Favre, 2010]. Glucose is the preferred nutrient for *Toxoplasma gondii* and its assimilation via glycolysis supports optimal growth of the parasite. In addition, certain glycolytic enzymes are also located in the apicoplast [Fleige *et al*., 2008], a secondary endosymbiotic plastid organelle [McFadden *et al*., 1996; Köhler *et al*., 1997], where they are involved in the inter-conversion of triose-phosphate intermediates to provide precursors for biosynthesis of fatty acids (acetyl-CoA) and isoprene units (pyruvate and glyceraldehyde 3-phosphate) [Roos *et al*., 2002; Seeber *et al*., 2003; Ralph *et al*., 2004; Seeber *et al*., 2010]. Moreover, the pyruvate dehydrogenase enzyme, which converts the glycolytic end product pyruvate to acetyl-CoA, is located only in the apicoplast and hence may have no role in mitochondrial acetyl CoA production [Foth *et al*., 2005; Crawford *et al*., 2006]. Instead, the branched chain keto-acid dehydrogenase (BCKDH) enzyme was shown to facilitate the synthesis of acetyl-CoA in the mitochondrion of *Toxoplasma* and *Plasmodium* [Oppenheim *et al*., 2014].

It is also likely that pyruvate is converted to oxaloacetate by pyruvate carboxylase enzyme in the mitochondrion [MacRae *et al*., 2012], although the expression of this enzyme in tachyzoite stage parasites appears to be very low [Nitzsche *et al*., 2017]. The flux of carbon from glycolysis into the Krebs cycle has been demonstrated previously in T. gondii by metabolic labeling studies, in both extracellular and intracellular tachyzoite stage parasites [MacRae *et al*., 2012]. Glycolysis is also the major source of cellular ATP in *T. gondii*. Biochemical studies in *T. gondii* indicate that bulk ATP production can be

accounted for by glycolysis, rather than by mitochondrial oxidative phosphorylation [Al-Anouti *et al*., 2004; Lin *et al*., 2011; Saliba and Kirk, 2001].

Despite the importance of glucose as a key nutrient, tachyzoite stage mutant parasites lacking the major glucose transporter (*Tg*gt1) were viable [Blume *et al*., 2009]. Glutamine was found to be necessary for growth and motility of Δ*gt1* mutant parasites, and metabolic labeling studies revealed an active gluconeogenic pathway *via* which carbon derived from glutaminolysis was channelled to replenish glycolytic intermediates [Nitzsche *et al*., 2016]. The non-essentiality of glycolysis was further confirmed by the finding that the glycolytic enzyme aldolase is dispensable in tachyzoite stage *T. gondii* [Shen and Sibley, 2014]. In the absence of robust glycolysis, as is the case in Δ*gt1* mutants, glutamine is the key nutrient supporting the survival of the parasite [Nitzsche *et al*., 2016; MacRae *et al*., 2012]. Glutaminolysis contributes carbon flux to the Krebs cycle, and helps replenish glycolytic intermediates via gluconeogenesis, thereby facilitating the growth and replication of Δ*gt1* parasites. This finding was further supported by the fact that phosphoenolpyruvate carboxykinase (Δ*pepck1*) enzyme, which catalyzes the first step in glyconeogenesis is essential for survival of *T. gondii* in the absence of glycolysis [Nitzsche *et al*., 2017].

However, the role of glycolysis during asexual stage conversion and tissue cysts formation in animal hosts has not been studied yet. Bradyzoite stage parasites are characterized by the presence of intracellular amylopectin granules, and the cyst wall they form contains lectin binding polysaccharides [Dubey *et al*., 1998]. It is likely that these complex polysaccharides are derived primarily from the carbon backbones of glycolytic intermediates. In *T. gondii*, two isoforms of the enzyme lactate dehydrogenase, which facilitates glycolytic flux by regulating pyruvate and NAD^+ levels, were found to be essential for establishing chronic infection in mice [Abdelbaset *et al*., 2017]. In this study,

we have investigated the essentiality of the glycolytic enzyme hexokinase for the growth, replication and asexual differentiation of tachyzoite stage parasites. Hexokinase knockout parasites (Δ*hk*; glycolytic mutant) exhibit a moderate fitness defect in vitro and decreased virulence in mice. Although Δ*hk* parasites were capable of differentiating into bradyzoites in vitro, they were severely compromised in mature tissue cyst formation in vivo. Isotope resolved metabolic labeling studies with $U^{13}C$-glucose and $U^{13}C$-$U^{15}N$-glutamine were performed to track the metabolic changes in Δ*hk*, and validate glutaminolysis as the major pathway for carbon and energy acquisition in these parasites. The importance of gluconeogenesis for parasite survival in the absence of glycolysis was confirmed using phosphoenolpyruvate carboxykinase mutant parasites (Δ*pepck1*) deficient in gluconeogenesis. Further, our studies also confirm that, *T. gondii* tachyzoites are capable of maintaining cellular ATP homeostasis by *via* either glycolysis or mitochondrial oxidative phosphorylation.

2.2 Methodology

*** Ethical Statement: All the research work has been carried out with the approval from Institutional Biosafety Committee (IBSC) and Institutional Ethics Committee.**

2.2.1 Molecular genetic methods

Parasite genomic DNA and total RNA were isolated using respective kits from Qiagen. Genomic DNA was amplified using either Herculase II Fusion (Stratagene), GoTaq (Promega) thermo stable DNA polymerases, or LA Taq polymerase (Takara). The hexokinase gene (*Tghk*) knock out construct contained 1082 kb and 1126 kb flanking sequences upstream and downstream of the gene loci (TGME49_265450; ~5.3 Kb) interspaced by the canonical *T. gondii* HXGPRT selection cassette [Donald *et al*., 1996]. Δ*hxgprt*Δ*ku80* parental strains of RH and Prugniaud *T. gondii* were transfected with PCR

amplified *Tghk* gene knockout cassette, followed by selection in the presence of mycophenolic acid and cloning stable lines of mutant parasites using limiting dilution method. *Tghk* gene deletion was confirmed by PCR amplification of genomic DNA isolated from mutant parasites. The sequences of primers used in this study are listed in [**Table 2.1**]. Δ*hk* mutants were complemented using the PSBLV72 cosmid (obtained from David Sibley lab, Washington University), which includes the entire wild type hexokinase gene loci in the middle of a ~25 Kb piece of *T. gondii* chromosome IX. The constitutively expressing copy of PEPCK gene (*Tgpepck1*; TgME49_289650) was ablated *via* genome editing using the CRISPR/Cas9 system [Sander and Joung, 2014]. The CRISPR guide RNA was engineered to target the Cas9 endonuclease to exon I of *Tgpepck1*. The Cas9 endonuclease and the guide RNA were expressed from a plasmid previously optimized for expression in *T. gondii* [Shen *et al*., 2014; Sidik *et al*., 2014]. Along with this plasmid, a PCR fragment containing the human *dhfr* gene cassette conferring pyrimethamine resistance, flanked by 40 bp of homologous region spanning the Cas9 cut site, was used to repair the Cas9 cut site resulting in targeted disruption of *Tgpepck1*. A clonal line of Δ*Tgpepck1* parasite was isolated by limiting dilution method, under pyrimethamine selection.

RH Δ*Tgpepck1* parasites were complemented with a plasmid constitutively expressing the *Tgpepck1-HA* cDNA under the β-tubulin promoter. The cDNA was cloned in-frame to a HA epitope tag encoding sequence located in the 3' end of the gene, to facilitate visualizing the expression and localization of *TgPEPCK-HA* in the complemented strain RH Δ*pepck1*$^{+Tgpepck1\text{-}HA}$. HFF monolayers grown on glass coverslips were infected with RH Δ*pepck1*$^{+Tgpepck1\text{-}HA}$ parasites and maintained in optimal growth conditions for 24 hours, before fixing with 4% paraformaldehyde and proceeding for immunostaining with anti-HA rabbit antibodies (Invitrogen) and donkey anti-rabbit secondary antibodies

coupled to Alexafluor594 (Molecular Probes). Clonal lines of the complemented strain were isolated by using glucose deprivation as negative selection against Δ*pepck1* parasites.

Primer Name	Primer Sequence (5'->3' orientation)	Remarks
HEXF1	cagcagacagtcgtatcatgccgt	Forward primer for amplifying 1082 bp 5' flanking sequence of *Tghk* gene
HEXR1	cgccatcgcctgcttaccgga	Reverse primer for amplifying 1082 bp 5' flanking sequence of *Tghk* gene
HEXF2	catcagacgccgggaagagca	Forward primer for amplifying 1126 bp 3' flanking sequence of *Tghk* gene
HEXR2	acgactatcaggcagacgagcac	Reverse primer for amplifying 1126 bp 3' flanking sequence of *Tghk* gene
HEX-KO-F	ccttcttgcacgagtgtcatgcaaccagacg	Forward primer for verfication of *Tghk* gene disruption from genomic DNA
HEX-KO-R	gtgtgcgcatcccgtcagtctgtaattcc	Reverse primer for verfication of *Tghk* gene disruption from genomic DNA
PEPCK1-Cr-F	gtcagctccgtggaagttcggttttagagct agaaatagc	Forward primer for making *Tgpepck* guide RNA construct
PEPCK1-Cr-R	aacttgacatccccatttac	Reverse primer for making *Tgpepck* guide RNA construct
PEPCK1-Cr-dhfr-F	gaaacctgtggcttacatatcgctgaag tgaggcatacatcgccaggctgtaaatc ccg	Forward primer for donor DNA fragment amplification to facilitate repair of the Cas9 cut site in *Tgpepck* gene loci
PEPCK1-Cr-dhfr-R	gacgacgaattgcctctgagcatcgga agattttcggttccctgcaagtgcataga agg	Reverse primer for donor DNA fragment amplification to facilitate repair of the Cas9 cut sitein *Tgpepck* gene loci
pkoF	cctcaacaaggaacgcatcaagg	Forward primer for verfication of *Tgpepck* gene disruption from genomic DNA
pkoR	ttctgaccgagcgagagaattgg	Reverse primer for verfication of *Tgpepck* gene disruption from genomic DNA
PEPCK1-cDNA-1835-F	gtcagctccgtggaagttcg	Forward primer for *Tgpepck* cDNA (1835bp fragment) amplification
PEPCK1-cDNA-1079-F	gccagacctccgtcgccatg	Forward primer for *Tgpepck* cDNA (1079bp fragment) amplification
PEPCK1-cDNA-F	atgaattatacaatgcacttgtctcgc	Forward primer for full length *Tgpepck* cDNA (2031 bp without stop codon)
PEPCK1-cDNA-R	gtggctgctggtccggttttt	Reverse primer for all *Tgpepck* cDNA fragments

Table 2.1: **List of primers used in this study and their intended purpose.**

2.2.2 Parasite strains and specific growth conditions

All experiments reported in this study were done with either RH (Type I) or Prugniaud (Pru; Type II) strains of *T. gondii*. The parasite strains used in this study are listed below and the abbreviations used to denote them are indicated within parentheses:

RH wild type (RH *wt*)

RH Δ*TghxgprtΔTgku80* (*RH Δku80*) [Rommereim *et al*., 2013; Fox *et al*., 2009]

RH Δ*TghxgprtΔTgku80ΔTghk*$^{+Tghxgprt}$ (RH Δ*hk*)

RH Δ*TghxgprtΔTgku80ΔTghk*$^{+Tghxgprt+Tghk}$ (RH Δ*hk*$^{+Tghk}$)

Pru Δ*TghxgprtΔTgku80* (Pru Δ*ku80*) [Fox *et al*., 2011]

Pru Δ*TghxgprtΔTgku80ΔTghk*$^{+Tghxgprt}$ (Pru Δ*hk*)

RH Δ*Tgpepck1* (RH Δ*pepck1*)

RH Δ*Tgpepck1*$^{+Tgpepck1-HA}$ (RH Δ*pepck1*$^{+Tgpepck1-HA}$)

Human foreskin fibroblasts (HFF) were used as host cells for parasite infection in all experiments and routine maintenance of tachyzoite stage parasites in the laboratory was done as previously reported [Roos *et al*., 1994]. Minimum essential medium (MEM; Invitrogen) containing 5.5 mM glucose and 4 mM glutamine, in addition to salts, vitamins and essential amino acids, was used as complete medium for optimal growth of parasites. Nutrient deprivation experiments were carried out in culture medium with similar composition but lacking either glucose or glutamine. For this, Dulbecco's modified eagle medium (DMEM; Invitrogen) containing 4 mM glutamine and no glucose or MEM containing 5.5 mM glucose and no glutamine were used respectively. These two mediums included other components such as salts, vitamins, and essential amino acids in similar proportions that found in the complete medium, and serum was not added to any of the media used for growth assays.

Two-week old confluent HFF monolayers were used for parasite growth assays, and both host cells and parasites were washed in respective starvation mediums before setting up the infection. The viability of confluent HFF monolayers is not affect by the starvation conditions over the course of assaying parasite growth rate (typically 2 -3 days) as determined by Almar Blue cell viability assays. When required, nonessential amino acids (100x MEM-NEAA; Invitrogen) were added to the culture medium to a final 1x

concentration. Sodium acetate, sodium pyruvate, sodium succinate dibasic hexahydrate, sodium propionate, glycerol, 2-deoxyglucose and azaserine (all purchased from Sigma) were used in specific growth experiments at concentrations given in the relevant sections.

2.2.3 Intracellular replication rate assays

Intracellular tachyzoites growing in complete medium were freshly released and washed in the medium of choice before being used to infect HFF monolayers in the presence of complete or minimal medium. 3 – 5 hours after infection, the monolayers were washed with appropriate media to remove un-invaded parasites. Then, parasite replication rates were determined from vacuole size as previously reported. Briefly, the vacuole size (log_2 of parasite count per vacuole) is estimated for at least hundred random vacuoles in each replicate, at various times (typically with a gap of 6 or 12 hours) over a period of 2 – 3 days depending on the strain of the parasite. The average vacuole size at each time point is used to determine the replication rate and the doubling time indicates the time taken for the parasite to divide once. The formulae used for calculating the number of doublings is (Σ((number of parasites in vacuole)number of vacuoles))/total number of vacuoles. Typically, 100 vacuoles were counted per replicate sample from a T25 flask infected with ~10^5 parasites, at 6 or 12 hour time intervals starting from the time of infection.

2.2.4 Plaque forming assays

To assess long term growth of *T. gondii* tachyzoites under differing growth conditions, we carried out plaque forming assays. Either 200 or 50 freshly lysed tachyzoites were inoculated into T25 culture flask or 6 well culture plates, respectively. Following infection with parasites, the HFF monolayers were incubated undisturbed in

optimal growth conditions (or in nutrient deprived condition) for 8-10 days before visualizing the plaques formed due to monolayer disruption by the parasites. The monolayers where fixed with ice-cold methanol (100%) and stained with crystal violet dye as previously reported [Ufermann *et al*., 2016]. Plaque counts from in each flask/well were obtained by manual inspection.

2.2.5 Virulence and differentiation studies in mice

Pru Δ*ku80* and Pru Δ*hk* tachyzoites were used to assess the essentiality of glycolysis for virulence (in acutely infected) and tissue cyst formation (in chronically infected) in C57BL/6 mice. Acute infection was initiated by injecting mice intraperitoneally with either low ($2x10^5$) or high ($2x10^6$) parasite dose and virulence was assessed based on percent survival of mice, with daily monitoring until 100% mortality was reached in the control group of mice infected with Pru Δ*ku80* parasites. Chronic infection in mice was initiated by injecting ~200 tachyzoites intraperitoneally and the cyst burden in animal brain was assessed 3 and 5 weeks post infection as previously reported [Dubey, 1997; Ferguson and Hutchinson, 1987; Bohne *et al*., 1998].

2.2.6 *In vitro* asexual differentiation of *T. gondii* and bradyzoite cyst wall staining

In vitro stage conversion studies were done essentially as previously described using the CO_2 starvation protocol [Knoll and Boothroyd, 1998]. Pru Δ*ku80* and Pru Δ*hk* tachyzoites were allowed to infect two-week old confluent HFF monolayers grown on glass coverslips in 6 well plates. Immediately after parasite inoculation, the plates were placed in a 37°C incubator maintaining CO_2 at atmospheric levels (>0.04%) and the infected monolayers were washed 3 - 5 hours post infection to remove un-invaded parasites. The monolayers were then continuously maintained in low CO_2 condition for

one week following which the infected monolayers were fixed and stained to visualize bradyzoite cyst wall polysaccharides. 2% formaldehyde (Polysciences) in phosphate buffered saline (PBS) was used to fix the monolayer for 10 minutes following which it was washed in PBS twice and permeablized using PBS containing triton X-100 (Sigma). The monolayers were then blocked for 30 minutes in PBS containing 5% fetal bovine serum and stained with 0.1 mg/ml TRITC labeled dolichos biflorus lectin (Sigma) in blocking solution. Coverslips were mounted on glass slides using Fluoromount-G (SouthernBiotech) and imaged using an Olympus IX70 inverted microscope equipped with a mercury vapor lamp, appropriate barrier/emission filters (DeltaVision), and a Photometrics CoolSNAP high-resolution digital CCD camera.

2.2.7 Metabolic labeling, metabolite extraction, and LC-MS profiling

DMEM minus glucose media supplemented with $U^{13}C$ glucose (5.5 mM) and MEM minus glutamine media supplemented with $U^{13}C$-$U^{13}N$ glutamine (4 mM) were used as culture mediums for metabolic labeling studies using RH *wt*, RH Δku80, RH Δ*hk*, and RH Δ*pepck1* parasites. Freshly isolated extracellular (host cell free) tachyzoites stage parasites were washed once in complete medium and resuspended in either ^{13}C labeled glucose or glutamine (Cambridge Isotope Laboratories, Inc.) containing medium at a density of 10^8 parasites per milliliter. Labeling was allowed to proceed over a time period of 5, 10, 15, 30, 60 and 120 minutes in 1 ml culture suspension. At each time point, metabolites were extracted from replicate parasite samples using a modified version of a previously reported protocol [Olszewski *et al*., 2009]. Briefly, host cell-free parasites were collected by centrifugation at 3000 rpm for 5 minutes at 4° C, the supernatant was removed, and the cell pellet immediately resuspended in 200 µl of ice cold 80% acetonitrile (Chem-Impex; JT Bakers) in water and incubated in ice for 15 minutes with

intermittent vortexing. The supernatant was then collected after centrifuging at 13,000 rpm for 5 minutes and the pellet was further extracted twice with 100 µls of the same solvent using ultrasound in a sonicating iced water bath for 15 minutes. All the extracts were pooled (total 400 µls) and stored in -80°C until further processing for liquid chromatography coupled mass spectrometry (LC-MS) analysis.

The acetonitrile:water extracts from parasites were dried under nitrogen flow and resuspended in 200 µls of water:methanol (97:3) containing 10 mM tributylamine and 15 mM acetic acid. This solvent was also used as buffer A and methanol as buffer B for liquid chromatography using a Synergy Hydro-RP column (Phenomenex) with a bed volume of 100 mm x 2 mm and particle size of 2.5 µ. For some samples, an alternate method, using a Thermo Accucore C18 column with a bed volume of 150 mm x 2.1 mm and 2.6 µ particle size, was used. A solvent system composed of water buffered with 0.1 % formic acid (buffer A) and acetonitrile (buffer B), was used on a 20 minute gradient run with a flow rate of 200 µl/min as follows- hold at 10% acetonitrile for 30 seconds and gradually ramp up to 15%, 20%, 50%, 60% and 90% acetonitrile by 3, 6, 10, 12, 13 minutes, hold at 90% acetonitrile till 15 minutes, ramp down to 10% acetonitrile by 15.5 minutes and hold till 20 minutes. LC-MS analysis was done using an Exactive Orbitrap mass spectrometer, coupled to an Accela U-HPLC (Thermo Fisher Scientific) and HTC PAL autosampler (CTC Analytics AG). The mass spectrometer was run in negative mode, scanning a mass-charge ratio (m/z) range of 85-1000. All other parameters used for LC-MS instrumentation in this study were similar to published protocols [Lu *et al*., 2010; Melamud *et al*., 2010].

2.2.8 LC-MS data processing and analysis

The RAW file output from the mass spectrometer was converted from the profile mode into centroid mode using the ReAdW or Proteowizard program [Chambers *et al*., 2012] and further analyzed using the MAVEN [Clasquin *et al*., 2012] program. Data from replicate samples for each time point was aligned within MAVEN and ion chromatograms were extracted for each compound to within 10 PPM window of the expected m/z value. Peaks were detected from these ion chromatograms and their quality was ascertained using default settings available in MAVEN. Metabolites were identified by matching the retention times as well as the m/z values to >99% pure commercial standards for which in-house calibration was done. Grouped peaks from replicate samples for all time points were matched to the expected retention time of standards, and the peaks with a quality score of at least 0.5 was handpicked for metabolites of interest. In addition to the $^{12}C/^{14}N$ containing parent compounds, $^{13}C/^{15}N$ labeled isotopomers for each metabolite were also selected by accounting for the expected shift in m/z values. Peak height was used as a measure of metabolite abundance and incase of ^{13}C labeled compounds, we also accounted for the natural distribution of the isotope as calculated by the Qual Browser included in the Xcalibur software suite (Thermo Fisher scientific) and corrected the final signal output accordingly. The relative abundance of unlabelled and ^{13}C labeled isotopomers of each metabolite was calculated for all samples over the experimental time course. Signals obtained from blank runs were used for noise correction and only peaks with a signal intensity of at least 1000 counts (approximate instrument limit for quantitation) were considered. Since we expected the signal levels of metabolites to change across the experimental time points (especially for isotopically labeled forms), we only considered those metabolites that had a signal count of at least

1000 or more in at least one time point. ^{13}C labeled isotopomers of metabolites are plotted only if they represent 10% or more of the total metabolite pool in at least one time point. Although we could reliably detect between 50 - 100 different metabolic intermediates from the different samples (in addition to hundreds of other unknown mass features), only a few key intermediates of glycolysis, pentose phosphate pathway and the Krebs cycle are presented, as these are relevant to the studies performed here. The raw and processed data from metabolomics studies has been deposited in the metabolomics workbench repository under the study ID ST000817.

2.2.9 Measuring total cellular ATP content in *T. gondii*

ATP was measured in extracellular tachyzoite stage parasites suspended in complete media or media lacking glucose or glutamine. Freshly isolated tachyzoites from infected monolayers were separated from host cell debris, collected by centrifugation (3000 rpm for 5 minutes at 25°C) and washed once in the medium of choice before being resuspended in the same medium at a density of $2x10^6$ parasites per milliliter. 50 µls of this suspension (10^5 parasites) was added to individual wells in a white opaque 96 well plate pre-seeded with 50 µls of appropriate culture medium. In experiments using atovaquone, the pre-seeded medium contained 2, 20 or 200 nM of the drug or 1% DMSO only as control. To assess the effect of nutrient deprivation on ATP synthesis, a time course experiment was carried out in which parasites incubated in different media were sampled for total cellular ATP content at 0.5, 1, 2, 3, 9 and 15 hours. For assessing atovaquone effect on ATP synthesis in conjugation with nutrient starvation, ATP content was measured in parasites at a fixed time point of 2 hours after exposure to atovaquone. ATP content in *T. gondii* was measured using the firefly luciferase activity based ATPlite assay kit (Perkin Elmer). The luciferase activity is directly proportional to the free ATP

available from the parasite cell to drive the light emitting reaction. The luminescence read outs where measured using the Analyst HT system (LjL Biosystems) and accompanying CriterionHost software (Molecular Devices).

2.3 Results

2.3.1 Measuring growth kinetics of RH *wt* parasites under nutrient deprivation

In agreement with previous reports [Blume *et al*., 2009; Nitzsche *et al*., 2016], we found that *T. gondii* tachyzoites were capable of continuously propagating in the absence of glucose in culture medium. Three flasks were set-up for 1st vacuole growth: one with complete medium and two with media lacking glucose. After 45 hours of growth, tachyzoites were harvested and inoculated into another set of three flasks for 2nd vacuole growth: two with complete medium and one with media lacking glucose. Number of parasites per vacuole was estimated during 2nd vacuole growth also. Glucose deprived tachyzoite stage parasites exhibit only a moderate fitness defect (doubling time ~9 hours) in comparison to growth in the presence of 5.5 mM glucose (doubling time ~7 hours) [Fig. 2.1A]. Glutamine (4 mM) alone as a carbon source was sufficient to supported parasite growth in the absence of glucose, and the addition of other carbon sources such as pyruvate, acetate, succinate, glycerol and propionate (5 mM each), did not help in restoring optimal growth of the parasite.

Interestingly, continuous culturing of tachyzoite stage parasites in the absence of glucose did not result in progressive loss or gain of parasite fitness. In fact, glucose-deprived parasites were capable of immediately resuming optimal growth, without any lag, when again provided with glucose [Fig. 2.1B]. These observations highlight the ability of tachyzoite stage *T. gondii* to adapt their growth in response to nutrient availability. We also noted that nutrient stress imposed by continuous cultivation of *T.*

gondii tachyzoites in the absence of glucose did not lead to asexual stage conversion or induction of bradyzoite specific markers.

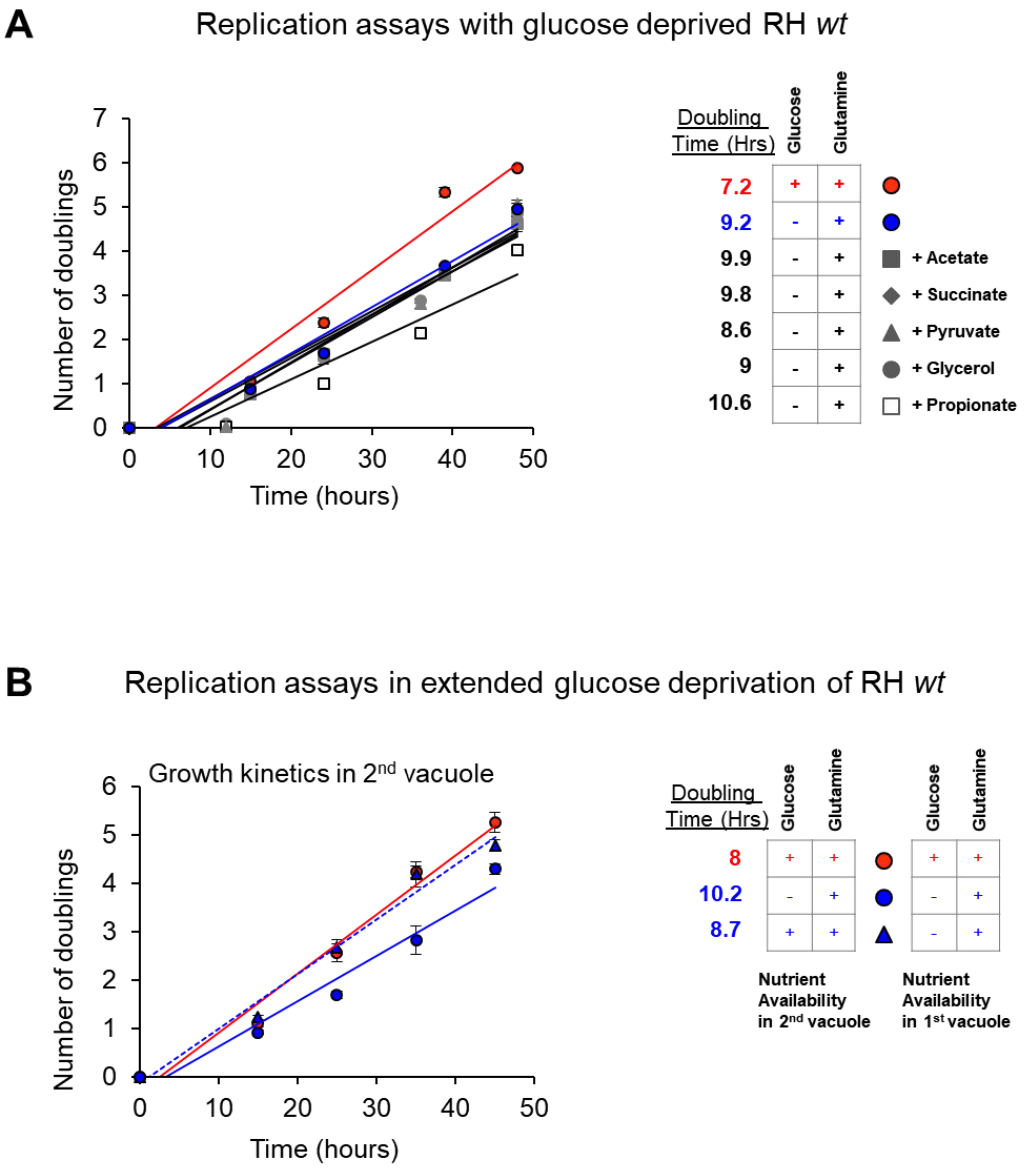

Figure 2.1 Replication rate kinetics of wild type RH parasites in the presence (red) and absence of glucose (blue). *A, shows the growth kinetics of RH wt parasites. The linear fit shown in solid red denotes the optimal growth of parasites in complete culture medium, with a doubling time of ~7.2 hours. In the absence of glucose (solid blue fit), a slight but consistent growth defect is observed, with a doubling time of ~9.2 hours. glucose minus medium containing 4 mM glutamine is supplemented with 5 mM each of acetate, succinate, pyruvate, glycerol and propionate, to check their effect on parasite growth. In addition to glutamine, the presence of other metabolites as potential carbon source did not help the parasites overcome*

the fitness defect imposed by glucose deprivation. B, depicts the growth kinetics of RH wt parasites in the second vacuole following glucose deprivation in the first vacuole. The solid red fit indicates growth of parasite in complete medium in the first and second vacuoles. The solid blue fit indicates continued growth of parasite in medium lacking glucose in the first and second vacuoles. The dashed blue fit indicates growth of parasite in complete medium in second vacuole following glucose deprivation during growth in the first vacuole. The results indicate that T. gondii tachyzoites are capable of altering their growth in response to glucose availability, and short-term glucose deprivation does not result in extended fitness defect.

2.3.2 The glycolytic enzyme hexokinase are not essential for *T. gondii* tachyzoites

Since *T. gondii* tachyzoites are capable of scavenging a variety of metabolites from host cells, it is likely that when deprived of external glucose, they can acquire host-derived glucose. This was observed in the earlier work, where residual glycolytic activity is detectable in Δ*gt1* mutants parasites [Nitzsche *et al*., 2016]. To further validate the essentiality of glucose and its metabolism via glycolysis in *T. gondii*, we proceeded to knockout the single copy hexokinase gene (*Tghk*; TGME49_265450), which catalyses the first step in glycolysis. In the absence of hexokinase, the parasites cannot metabolize glucose even if it is available. We generated *Tghk* gene knock-out parasites in both RH and Pru strains of *T. gondii* (from the respective Δ*ku80* parental strains) via homologous recombination mediated gene replacement, in which part of the *Tghk* gene locus was replaced by the *Tghxgprt* selection cassette. The absence of *Tghk* gene was confirmed by genomic PCRs (in RH & Pru; data not shown) and by DNA microarray analysis (in RH only) using the Affymetrix Toxoarray [Bahl *et al*., 2010] [Fig. 2.2A]. Obtaining Δ*hk* mutants in two different strains of *T. gondii* further confirmed that glucose and glycolysis are not essential for survival of tachyzoite stage parasites.

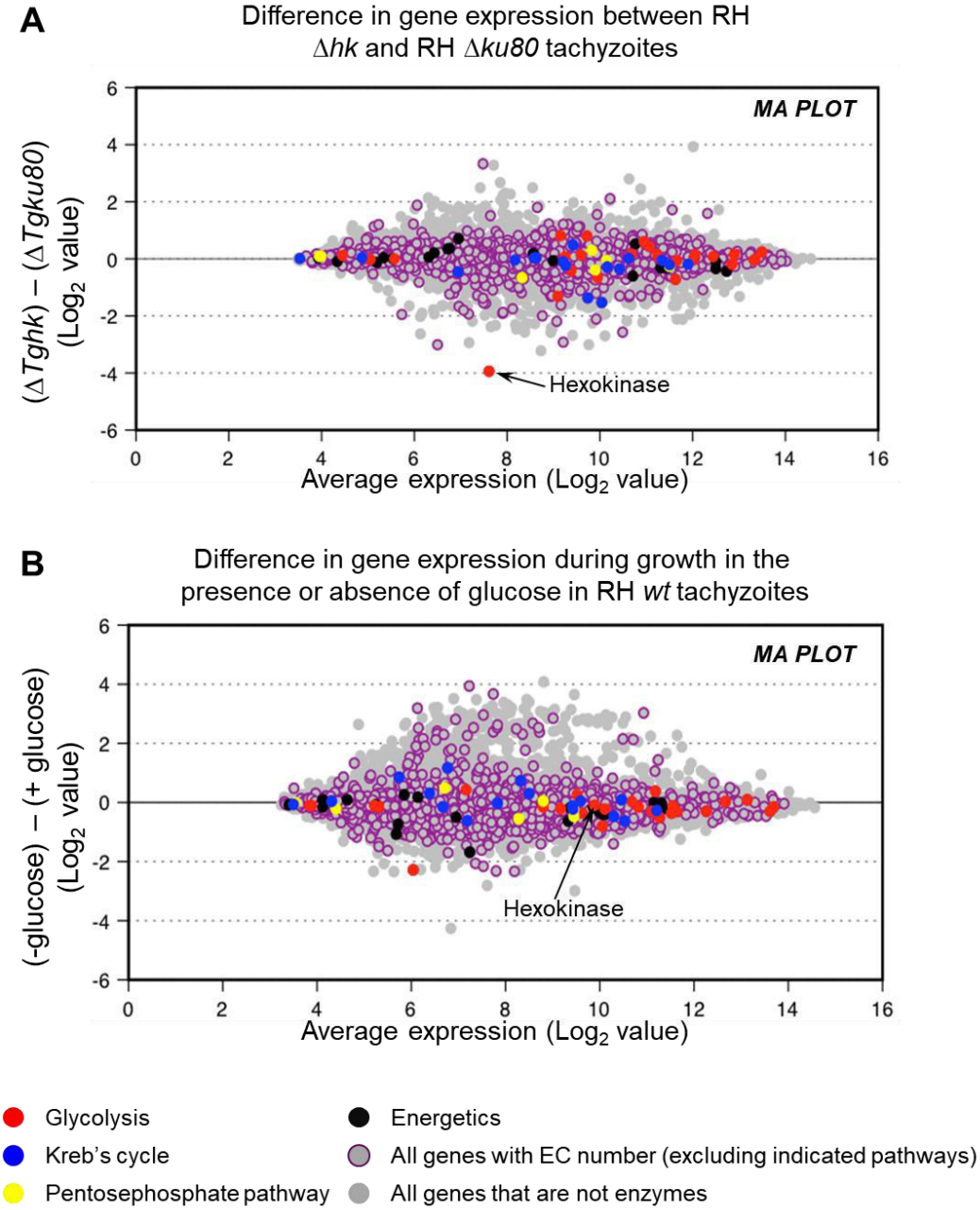

Figure 2.2 MA plots of Affymetrix Toxoarray expression profiling datasets. *Gene expression profiling was conducted for RH Δku80 and RH Δhk parasites grown in complete media (A), and for RH wt parasites grown in the presence and absence of glucose for 48 hours (B). Arrow indicates the hexokinase gene. Gene encoding enzymes from various metabolic pathways are color-coded.*

Interestingly, from the microarray based differential gene expression anlysis of RH wild type and Δ*hk* mutant parasites, we found that almost none of the genes that encode enzymes of central carbon metabolism were found to be altered in their expression in the mutant [Fig. 2.2A]. This was true even when wild type parasites were starved for glucose, and their gene expression was compared to parasites growing in optimal conditions [Fig. 2B].

2.3.3 Pharmacological validation of Δ*Tghk* parasites using 2-deoxyglucose as a metabolic probe

T. gondii encodes all enzymes necessary for reverse synthesis of glycolytic intermediates via gluconeogenesis [ToxoDB.org] and this pathway is important for metabolic adaptation during glucose deprivation (in RH *wt*) or when the parasites are not capable of oxidizing glucose (in RH Δ*hk*). In fact, there was no detectable difference in replication rate kinetics of RH Δ*hk* parasites in the presence (doubling time ~8.9 hours) or absence (doubling time ~9.1 hours) of glucose [Fig. 2.3A]. For functional validation of hexokinase gene knockout, we used 2-deoxyglucose (2DG) as a metabolic probe.

2DG is a structural analog of glucose that can be transported into cells via the glucose transporter and is converted by hexokinase into 2-deoxyglucose-6-phosphate (2DG-6P), an anti-metabolite which inhibits glucose-6-phosphate dependent enzymes [Barban, 1962]. The EC_{50} for 2DG-mediated parasite killing was ~500 µM. 5mM 2DG treatment completely inhibited RH *wt* parasite growth resulting in their death, but only in the absence of glucose [Fig. 2.3B, 2.4A]. 1 mM glucose was capable of completely reversing the growth inhibitory effects of 2 mM 2DG [Fig. 2.4B]. These results are consistent with the fact that glucose is the preferred substrate over 2DG, for both the glucose transporter

and hexokinase enzyme. Therefore, there is probably only a minimal accumulation of 2DG-6P within the parasite in the presence of glucose.

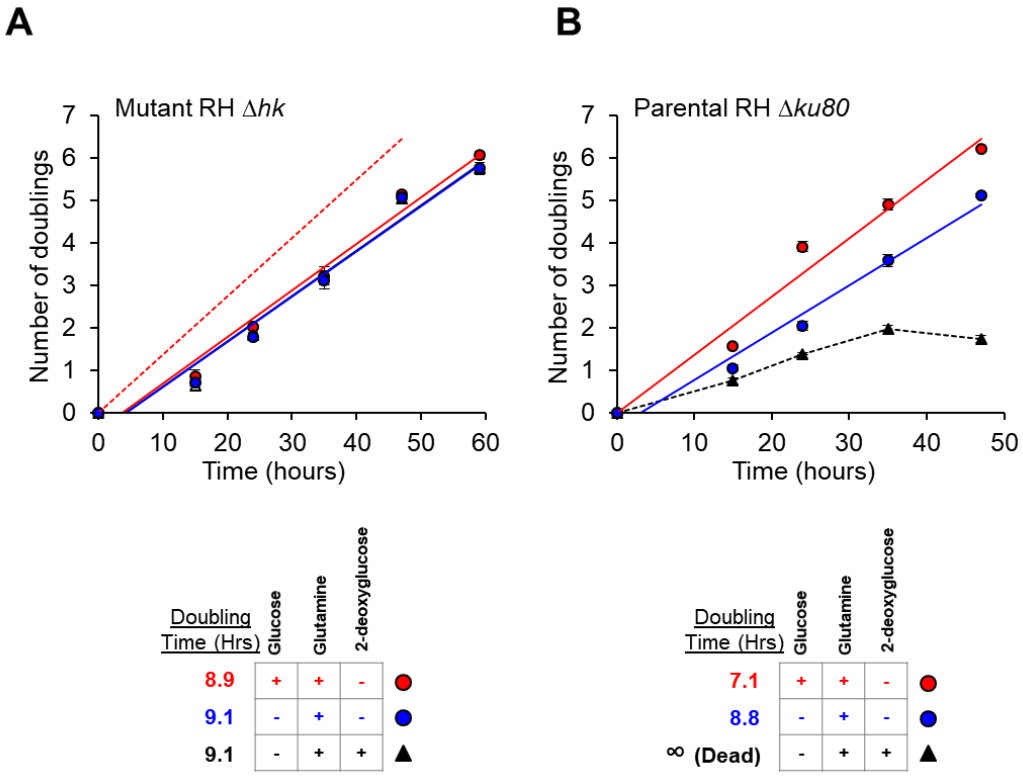

Figure 2.3 Replication studies with RH Δhk and RH Δku80 parasites. *Replication kinetics of RH Δhk (A) and RH Δku80 (B) tachyzoite stage parasites in the presence and absence of glucose and 2-deoxyglucose. The red dashed line in A indicates the replication rate of parental strain in optimal growth conditions. The black dashed line in B indicates that parasites stop replicating and die when treated with 2-deoxyglucose concomitant with glucose deprivation.*

In contrast, the growth of RH Δ*hk* parasites (doubling time ~9.1 hours) was not affected by 5 mM 2DG, even in the absence of glucose [Fig. 2.3A], thus functionally validating the hexokinase knockout. However, RH Δ*hk* parasites complemented with a functional hexokinase gene (RH Δhk^{+Tghk}) were susceptible to growth inhibition by 5 mM2DG in the absence of glucose [Fig. 2.5].

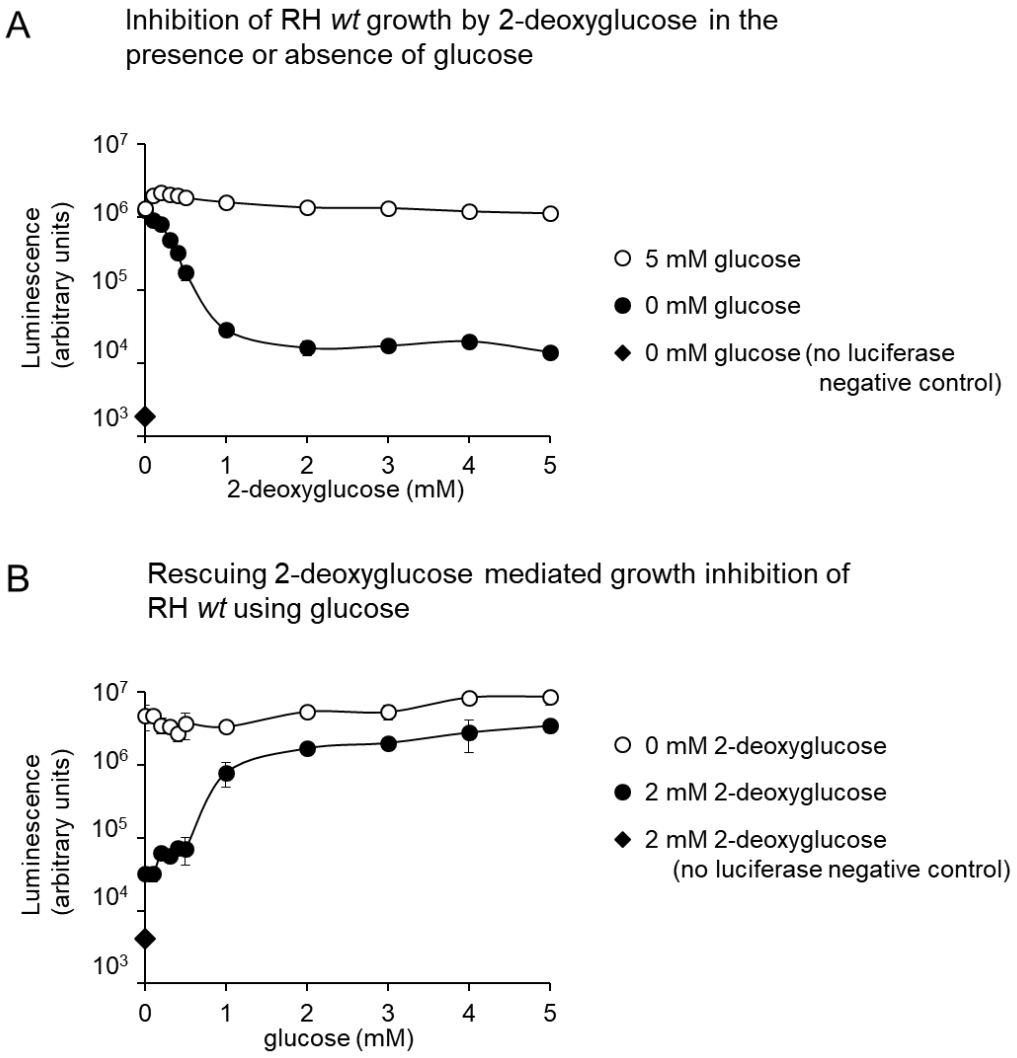

Figure 2.4 Effect of 2-deoxyglucose (2DG), on the growth of wild type RH parasites. *Transgenic parasites expressing the firefly luciferase gene were used to find the concentration of 2DG at which parasite growth is completely inhibited (A), and the concentration of glucose needed to reverse the growth inhibiting effect of 2 mM 2DG (B).*

It should also be noted here that, any 2DG-6P produced inside the host cell (by host hexokinase activity) is not inhibitory to parasite growth. This supports the notion that phosphorylated metabolites, such as intermediates of glycolysis, are not capable of transiting from the host cells into parasites.

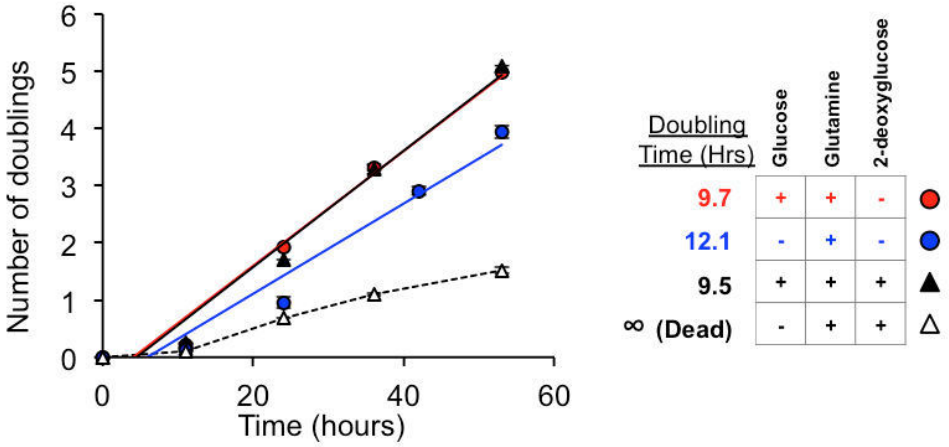

Figure 2.5: Replication rate assays with TgΔhk mutants complemented with a functional Tghk gene. *The data depicted in red and blue indicated the parasite growth observed in the complete and minus glucose medium respectively. The dashed line indicates the Tghk complemented strain dying after exposure to 2DG.*

2.3.4 *In vivo* virulence and differentiation studies with Δ*hk* parasites

Since glucose is physiologically the most abundant nutrient in the host, it is readily available for the parasite. In studies with Δ*gt1* parasites, it was found that the in vivo virulence of the mutant parasite is not compromised [Blume *et al*., 2009]. In accordance with this, we found that the parasite burden achieved following acute intra-peritoneal infection of mice with 200 RH Δ*hk* tachyzoites, was comparable to that seen with RH *wt* parasites. However, since our interest was to study importance of glycolysis for asexual differentiation in vivo, further experiments were conducted with Pru Δ*hk* parasites. We first monitored virulence following acute infection with either the parental Pru or mutant Pru Δ*hk* tachyzoites, each in two different doses of $2x10^5$ (low) and $2x10^6$ (high) parasites. In the low dose group [Fig. 2.6A], 3 out of 4 mice infected with parental Pru parasites succumbed to infection before day 10, while the 4th mouse died at day 40. However, none of the mice infected with low dose of Pru Δ*hk* parasites succumbed to

infection till day 40. In the high dose group, all mice infected with either the *wt* or Δ*hk* parasites strains died before day 10 [Fig. 2.6A].

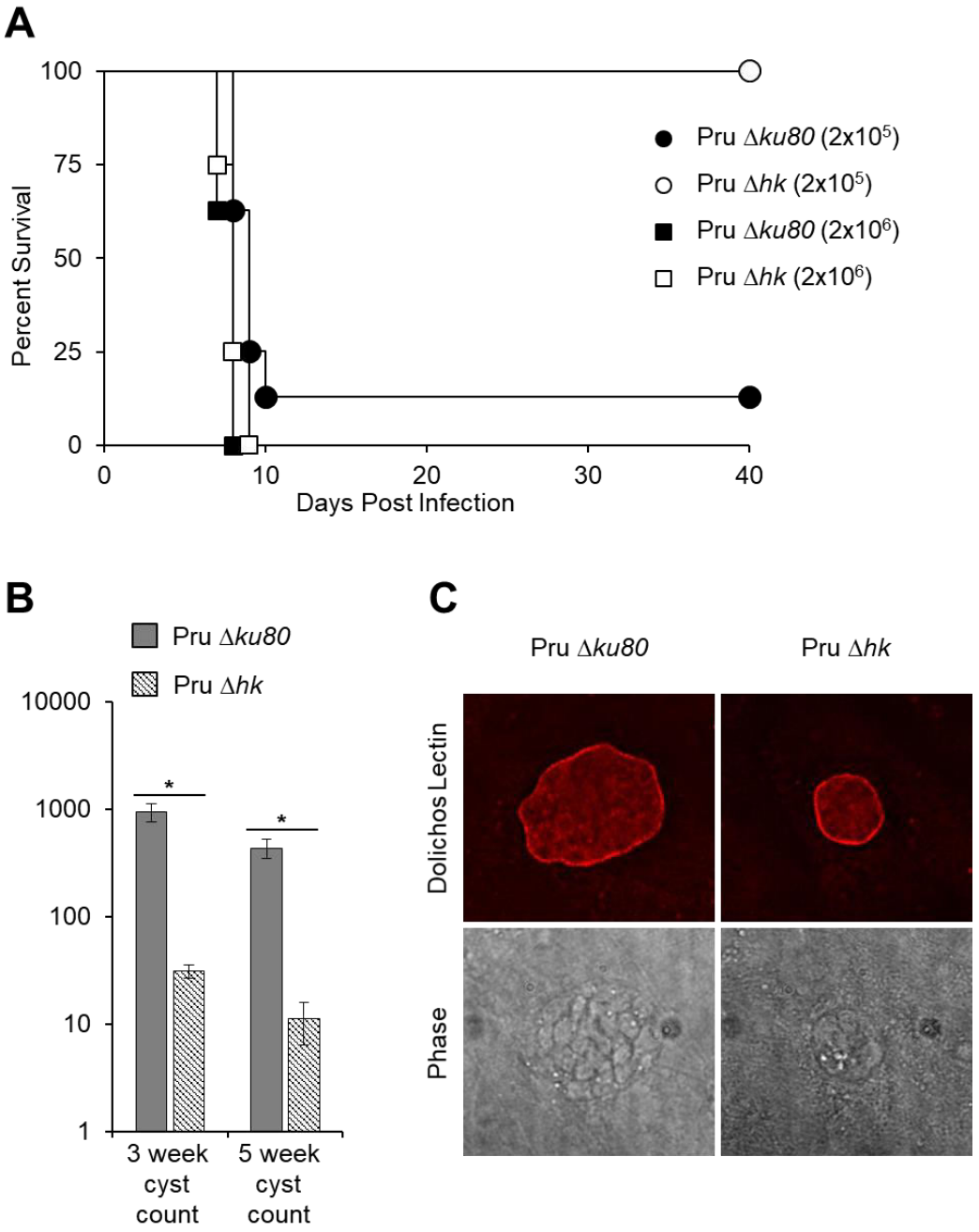

Figure 2.6: Acute virulence in mice and asexual differentiation of Pru Δku80 and Pru Δhk strains of T. gondii: *A, survival curves for mice following intra-peritoneal injection with either 2x105 or 2x106 tachyzoites of RH Δku80 or RH Δhk parasites respectively. B, estimation of cyst burden in mouse brain following establishment of chronic infection with Pru Δku80 and Pru Δhk parasites. * P value = 0.0001. C, dolichos bifluros lectin staining was done to visualize the presence of cyst wall polysaccharide during in vitro asexual differentiation of Pru Δku80 and Pru Δhk parasites. The vacuole formed by the Pru Δhk*

parasite is smaller owing to the decreased fitness of the mutant parasite. Staining was done after 1 week of growth in optimal conditions required for inducing bradyzoite differentiation in vitro.

In contrast to the outcome of acute infection, during chronic infection, mice infected with 200 Pru Δhk parasites showed a drastically reduced cyst burden (by ~97 %) [Fig. 2.6B] when compared to mice infected with parental wild type parasites. In order to determine whether the inability of Pru Δhk parasites to form productive tissue cysts in vivo was due to defective cyst wall formation, we checked to see if these parasites are capable of in vitro differentiation and cyst wall formation. Pru *wt* and Pru Δ*hk* infected host cells were maintained in low CO_2 conditions for a week and then stained for cyst wall formation using dolichos fibrous lectin [Boothroyd *et al*., 1997]. We observed that, the Pru Δ*hk* parasites were equally competent as Pru *wt* parasites in initiating bradyzoite differentiation and forming the cyst wall in vitro [Fig. 2.6C]. Therefore, it appears that glutamine metabolism can support cyst wall biogenesis and other metabolic requirements associated with early bradyzoite differentiation. However, deficient mature tissue cyst formation in vivo might indicate that glucose metabolism is essential for this process. Glycolysis is also probably essential for dissemination of tachyzoites to favorable tissue locations for productive tissue cyst formation and persistence in the host.

2.3.5 Metabolic impact of deficient glucose metabolism

To study the metabolic changes in Δ*hk* parasites we carried out metabolic labeling studies with extracellular tachyzoites. Following isotopic labeling, total metabolites were extracted from parasites and profiled by LC-MS. The kinetics of ^{13}C assimilation from $U^{13}C$-glucose and $U^{13}C$-$U^{15}N$-glutamine was tracked over a period of 2 hours. Our primary focus was to analyze metabolic intermediates from glycolysis, the pentose phosphate pathway and the Krebs cycle as these pathways are directly impacted by

glucose or glutamine availability and are the key pathways via which bulk assimilation of carbon is likely occurs in T. gondii [Oppenheim *et al*., 2014; MacRae *et al*., 2012].

When RH *wt* parasites were fed U^{13}C-glucose (in the presence of unlabelled glutamine), robust labelling was observed for intermediates of glycolysis and the pentose phosphate pathway, along with minimal labelling in Krebs cycle intermediates. The kinetics of ^{13}C- labeling for the isotypes of intermediates from glycolysis, pentose phosphate pathway and Krebs cycle, shown in [Fig. 2.7]. We noticed that +2^{13}C-acetyl-CoA derived from glucose was incorporated into citrate, as previously reported [Oppenheim *et al*., 2014]. On the other hand, when parasites were fed with U^{13}C-U^{15}N-glutamine (in the presence of unlabelled glucose), labelling was restricted to intermediates of the Krebs cycle only and no labelling was detected in any intermediates of glycolysis or the pentose phosphate pathway. This confirms that gluconeogenesis is inactive when glycolysis is active, as observed previously [Oppenheim *et al*., 2014].

Notably, acetyl-CoA remained unlabelled and there was no evidence for acetyl-CoA derived labelling of citrate. It is evident from these labelling patterns that glucose and glutamine have distinct metabolic fates in wild type *T. gondii* tachyzoites [Fig. 2.7]. In contrast to wt parasite, U^{13}C-glucose derived labelling was completely absent in Δ*hk* parasites, further confirming the inability of these parasites to metabolize glucose. Δ*hk* parasites readily incorporated ^{13}C- derived from U^{13}C-U^{15}N-glutamine into intermediates of the Krebs cycle. Importantly, unlike in *wt*, ^{13}C label was not restricted to the Krebs cycle, and significant levels of ^{13}C incorporation was also observed in intermediates of glycolysis and the pentose phosphate pathway [Fig. 2.7]. Thus, in Δ*hk* parasites gluconeogenesis is required for maintaining glycolytic and pentose phosphate pathway intermediates. The isotype labeling profile for each metabolite at the end of the experiment (i.e., after 120 minutes of labeling) is shown as Pie chart in [Fig. 2.8].

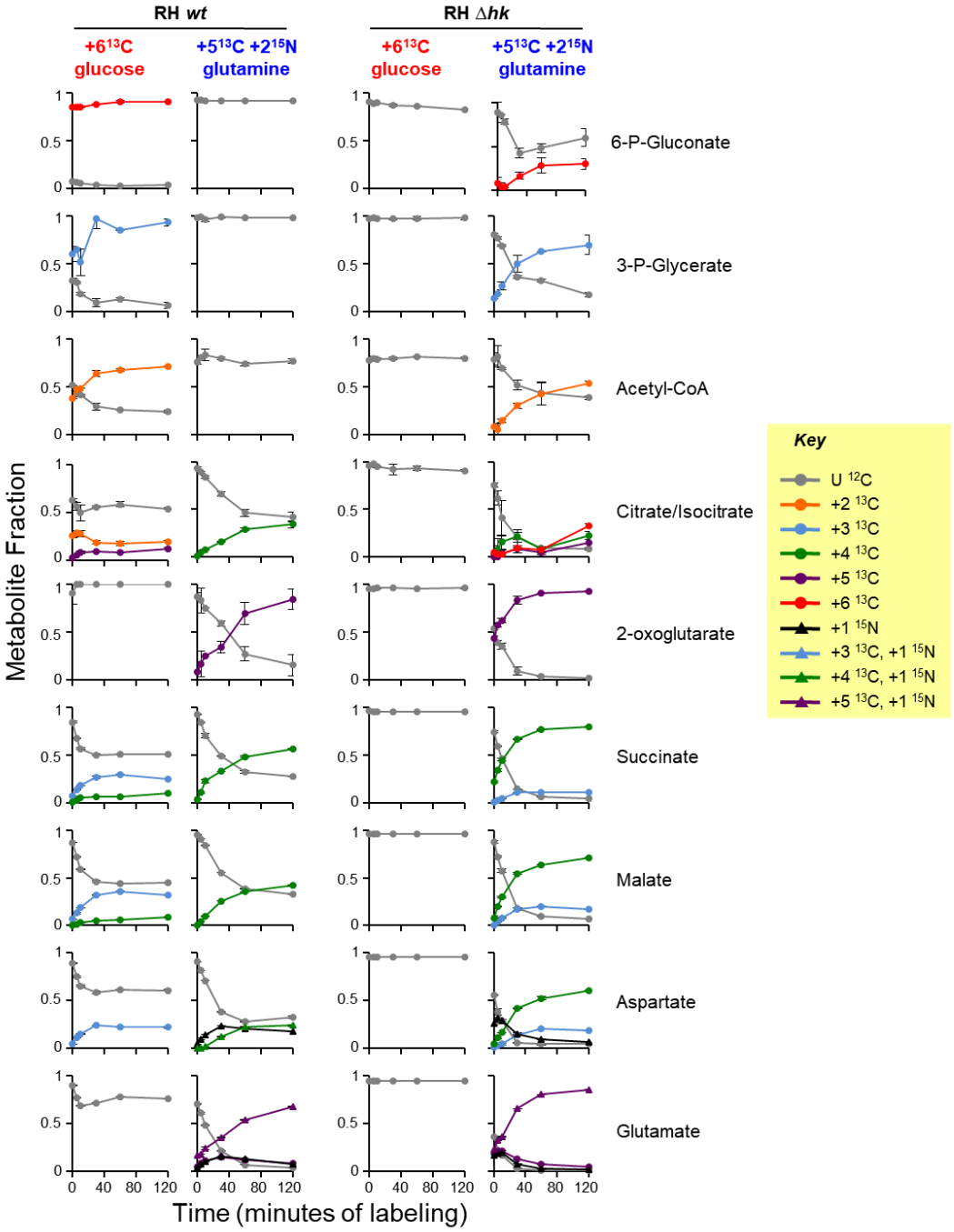

Figure 2.7: ^{13}C- metabolic labeling profiles for RH wt (left panel) and RH Δhk (right panel) parasites, using +6U-^{13}C-glucose and +5^{13}C+2^{15}N-glutamine. *Each plot depicts the fractional distribution of ^{12}C-parent and ^{13}C- isotopomers of each metabolite, for the given time points. The color code indicates the number of ^{13}C labeled carbons in each metabolite, and is shown in the key.*

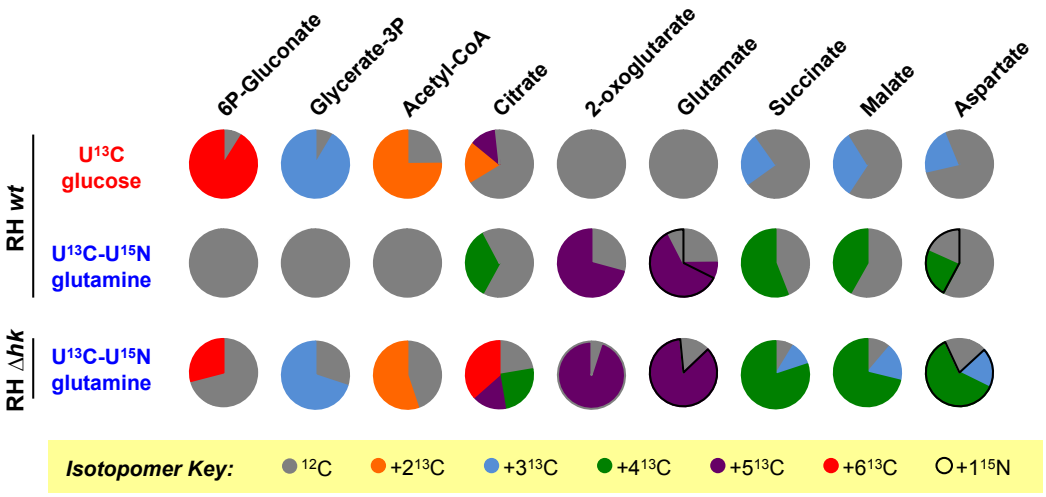

Figure 8: ***^{13}C isotopomer profile in RH wt and RH Δhk parasites.*** *Pie charts indicate the fraction of ^{13}C labeled isotopomers in total metabolite pool for key intermediates from pentose phosphate pathway, glycolysis and Krebs cycle after 120 minutes of labeling. The color scheme is shown as isotopomer key.*

Details of the isotype labeling patterns for selected intermediates from glycolysis, pentose phosphate pathway and Krebs cycle are summarized in [Fig. 2.9A] ($U^{13}C$-glucose labeling in wild type parasites), [Fig. 2.9B] ($U^{13}CU^{15}N$-glutamine labeling in wild type parasites), and [Figure 2.9C] ($U^{13}CU^{15}N$-glutamine labeling in Δ*Tghk* parasites).

2.3.6 Insights into the central carbon metabolism of *T. gondii*

The kinetics of ^{13}C- labeling for intermediates of glycolysis and Krebs cycle revealed the dynamics of carbon flux between these pathways. $+3^{13}C$-pyruvate derived from glycolysis is converted in the mitochondrion to $+2^{13}C$-acetyl-CoA, by the branched chain keto-acyl dehydrogenase [Oppenheim *et al*., 2014], and $+3^{13}C$-oxaloacetate, by pyruvate carboxylase enzyme [MacRae *et al*., 2012]. Although we do not detect oxaloacetate in our LC-MS method, we can infer its labeling pattern from the $+3^{13}C$- isotopomers detected for aspartate (formed by transamination of oxaloacetate), citrate and malate [Fig. 2.7].

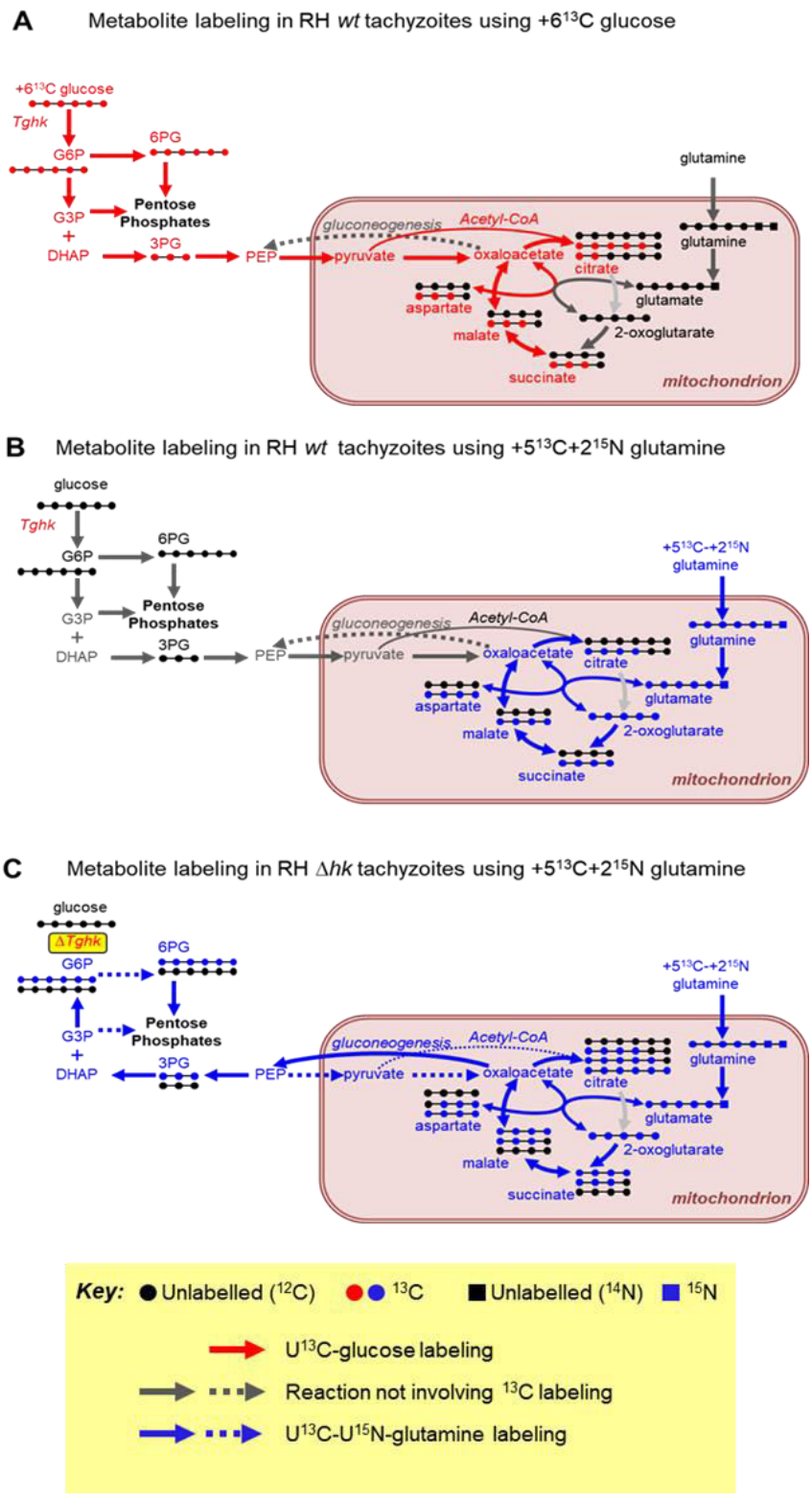

Figure 2.9: Schematic summary of 13C-labeled isotopomer profile in wt and Δhk parasites. *U-^{13}C-glucose labeling (red color) in RH wt parasites (A) and U^{13}C-U^{15}N-glutamine labeling (blue color) in RH wt (B) and RH Δhk parasites (C).*

We detected +2^{13}C and +5^{13}C isotopomers for citrate, indicating that +2^{13}C-acetyl-CoA was combining with both unlabeled and +3^{13}C-oxaloacetate to form citrate. Interestingly, we did not see any exchange of ^{13}C- between citrate and 2-oxoglutarate, and much of citrate remained unlabeled by glucose.

The labeling patterns observed with U^{13}C-glucose were well complemented by U^{13}C-U^{15}N-glutamine labeling patterns. First, U^{13}C-U^{15}N-glutamine is deaminated to +5^{13}C-+1^{15}N-glutamate, which is then transaminated to form +5^{13}C-2-oxoglutarate. Following this, +4^{13}C- isotopomers of succinate, fumarate, malate, oxaloacetate and citrate are formed. Unlabeled and +4^{13}C-oxaloactetate participate in the transamination of glutamate to aspartate, resulting in the formation of +1^{15}N- and +4^{13}C-+1^{15}N-aspartate [Figure 2.7]. The lack of glutamine derived ^{13}C- labeling in glycolytic intermediates and acetyl-CoA indicates that steady state glycolytic flux prevents gluconeogenesis. Here again, as in case of U^{13}C-glucose labeling, we did not observe any flux of ^{13}C- from citrate to 2-oxoglutarate. If +4^{13}C-citrate were to be converted to 2-oxoglutarate, since one of the carbon atoms derived from oxaloacetate is lost as CO_2, +3^{13}C-2-oxoglutarate should be formed. However, only +5^{13}C-2-oxoglutarate obtained from transamination of glutamate was detected, suggesting that citrate may not cycle back into the Krebs cycle.

It is likely that citrate is acting as a carbon sink in the mitochondrion, which can be shuttled out into the cytosol and be split into acety-CoA and oxaloacetate by the cytosolic ATP-citrate lyase enzyme [Oppenheim *et al*., 2014; Nitzsche *et al*., 2016; Tymoshenko *et al*., 2015]. Cytosolic oxaloacetate can be recycled to the mitochondrion via the citrate-malate shuttle, where oxaloacetate is first converted into malate, by cytosolic malate dehydrogenase (ToxoDB gene ID TGME49_318430), which is then imported into the mitochondrion via the 2-oxoglutarate/malate translocase (ToxoDB gene ID TGME49_274060).

When Δhk parasites were fed $U^{13}C$-$U^{15}N$-glutamine, the isotopomer profile of Krebs cycle intermediates resembled a combination of the profile obtained for glucose or glutamine labeling in wt parasites [Fig. 2.7, Fig. 2.8]. However, unlike in wt, we observed the formation of $+3^{13}C$-glycerate-3-phosphate and $+6^{13}C$-6-phospho gluconate, suggesting that gluconeogenesis is functional in Δ*hk* parasites. In addition to forming glycerate-3-phosphate (gluconeogenesis), PEP also facilitates the production of pyruvate, which is then converted to acetyl-CoA and oxaloacetate in the mitochondrion. This is supported by the formation of $+2^{13}C$-acetyl-CoA and $+3^{13}C$- isotopomers for malate, succinate and aspartate in Δ*hk* parasites, in the presence of $U^{13}C$-$U^{15}N$-glutamine. In *wt* parasites, a similar isotopomer profile for these metabolites is seen only in the presence of $U^{13}C$-glucose. Moreover, the formation of $+4^{13}C$-, $+5^{13}C$- and $+6^{13}C$- isotopomers of citrate suggests that $+3^{13}C$- and $+4^{13}C$- isotopomers of oxaloacetate and $+2^{13}C$-acetyl-CoA contribute to citrate formation [Fig. 2.7]. As in *wt* parasites, in Δ*hk* parasites also there was no evidence for the cyclic operation of Krebs cycle, as evidenced by the completed absence of $+3^{13}C$- isotopomer for 2-oxoglutarate. A summary of the metabolic circuitry in both wt and Δhk parasites, based on the observed ^{13}C- isotopmer profiles is elaborated in [Fig. 2.9].

2.3.7 Importance of glutamine in Δhk parasites

Replication, differentiation, and metabolic profiling studies with *wt* and Δ*hk* parasites revelaed that glutamine is a key nutrient for the parasite. We therefore tested glutamine essentiality in *wt* and Δ*hk* parasites. When *wt* tachyzoites were deprived of external glutamine (in the presence of glucose), they showed a slight, but consistent, fitness defect (doubling time ~8.8 hours) [Fig. 2.10A]. The fact that we see a fitness defect in the absence of glutamine, even when glucose is available, suggests a distinct metabolic role

for glutamine. This fitness defect was reversed by the addition of a cocktail of nonessential amino acids containing aspartate, alanine and glutamate, but lacking glutamine. Surprisingly, Δ*hk* parasites remain viable in the absence of glutamine, and exhibit a fitness defect (over that already imposed by lack of glycolysis; doubling time ~12.6 hours), which was reversed by the addition of a cocktail of non-essential amino acids [Fig. 2.10B]. Δ*hk* parasites probably survive in the absence of external glutamine by scavenging glutamine from the host cells. We tested this possibility by using the glutamine analog azaserine, which is an inhibitor of glutamine synthetase [Lea and Miflin, 1975; Rowell *et al*., 1977]. In the absence of exogenous glutamine, 10 µM azaserine completely inhibited *wt* parasite growth and resulted in their death; non-essential amino acids did not rescue parasites from azaserine mediated death [Fig. 2.11A], suggesting that glutamine is essential for parasite survival. We then carried out replication assays to show that tachyzoites fail to replicate even once in the presence of 10 µM azaserine, when deprived of of glutamine [Fig. 2.11B].

While performing glutamine deprivation experiments with Δ*hk* parasites, we noticed a dramatic reduction in the number of parasite vacuoles per microscopic field. We followed up on this observation further by performing plaque assays, and found that the plaquing efficiency of Δ*hk* tachyzoites was reduced by >95% in the absence of glutamine, suggesting a dramatic reduction in invasion efficiency, in comparison to *wt* parasites [Fig. 2.10C]. However, unlike intracellular growth, the invasion defect of extracellular Δ*hk* parasites was not reversed by non-essential amino acids. It is likely that ATP synthesis is compromised in extracellular Δ*hk* parasites in the absence of glutamine, as was previously reported in case of *wt* and Δ*gt1* parasites [Nitzsche *et al*., 2016; MacRae *et al*., 2012].

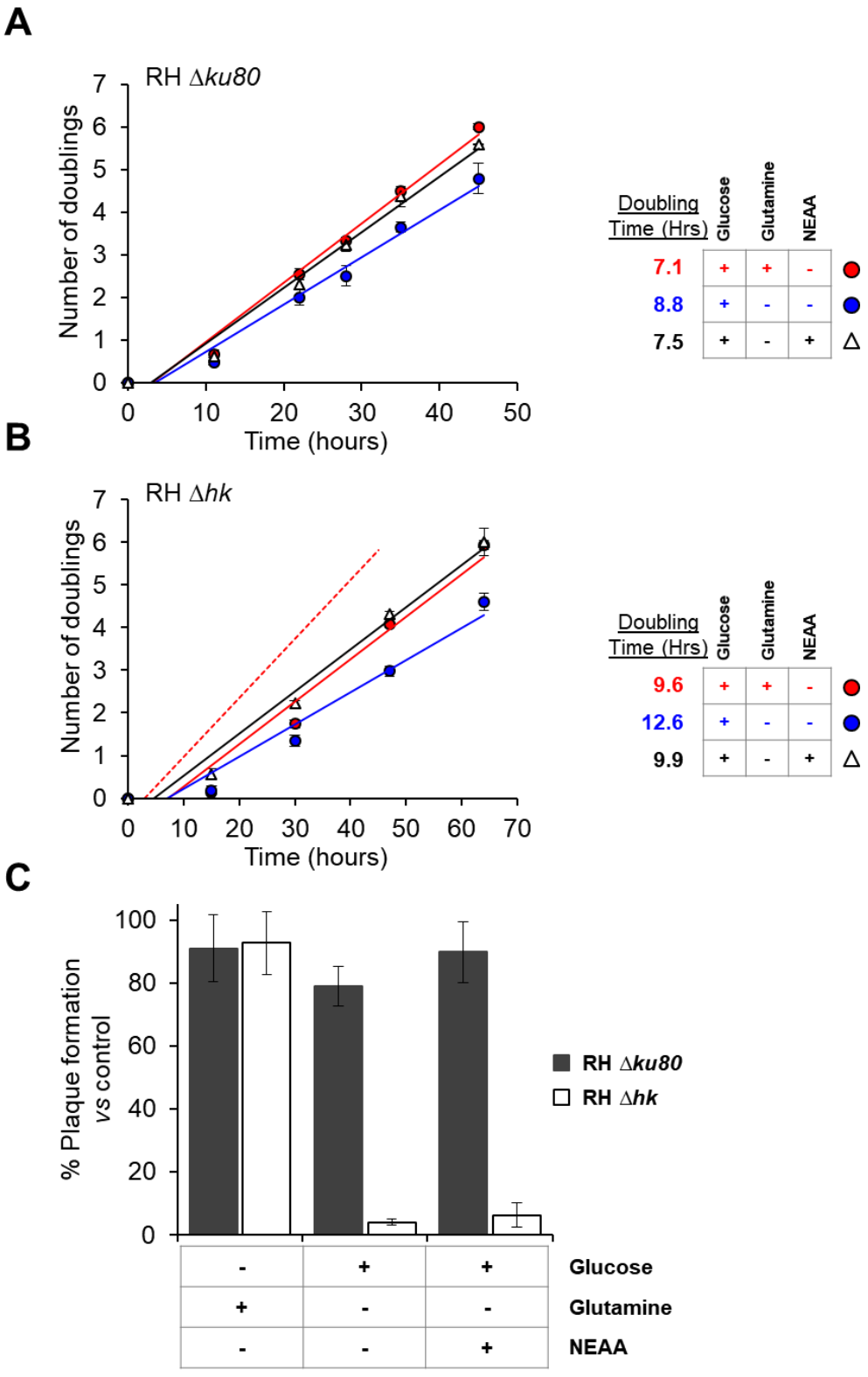

Figure 2.10: Replication kinetics and plaque formation assays following glutamine deprivation. *Replication assays for tachyzoite stage RH wt (A) and RH Δhk (B) parasites in the presence and absence of glutamine and nonessential amino acids. The red dashed line in B indicates the growth of RH Δku80 parental strain under optimal conditions. C, plaque formation assays were carried out to determine the*

ability of the parasites to invade and replicate within host cells in the absence of glutamine. The number of plaques formed was normalized to control cultures of respective parasites growing in complete media.

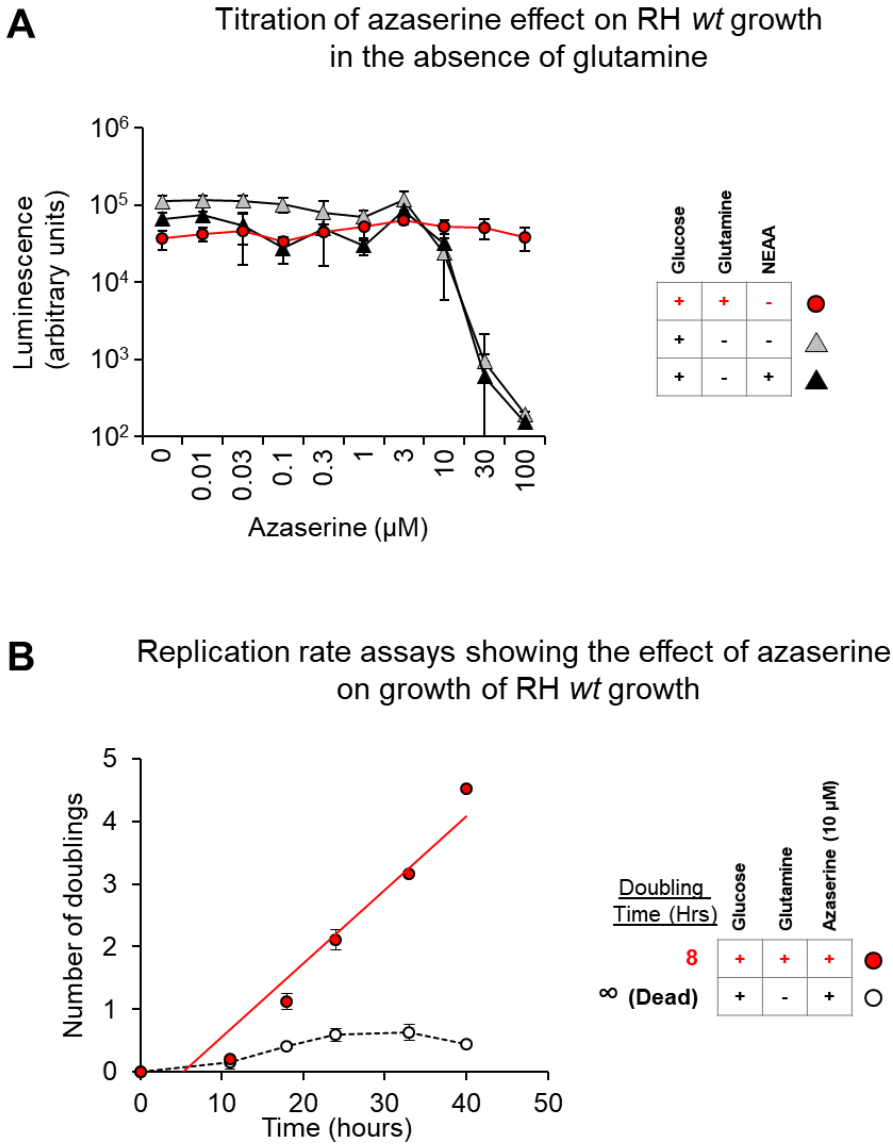

Figure 2.11: Growth kinetics of RH wt parasites treated with the glutamine analog azasurine. *A, titration of azaserine concentration to find its inhibition profile, in the presence and absence of glutamine and non-essential amino acids. B, Replication assays showing the inability of T. gondii tachyzoites to replicate in the presence of azaserine when glutamine is absent. Data shown in red indicates optimal growth in complete media.*

2.3.8 Conditional essentiality of *PEPCK* in *T. gondii*

It is apparent from our metabolic labeling studies that the PEPCK enzyme is critical for gluconeogenesis, and is likely essential for parasite growth in the absence of glycolysis. The role of PEPCK and its essentiality in Δ*gt1* parasites was previously reported [Nitzsche *et al*., 2017]. To further validate these findings and study ATP biogenesis in parasites deficient in gluconeogenesis, we generated mutant parasites lacking a functional *PEPCK* enzyme. Two isoforms of *PEPCK* are encoded by T. gondii, TgME49_289650 (*Tgpepck1*) and TgME49_289930 (*Tgpepck2*), of which only the former is expressed and likely functional in tachyzoites (Toxodb.org). Using the CRISPR/Cas9 mediated genome editing approach, we obtained *Tgpepck1* gene knockout (Δ*Tgpepck1*) parasites in the RH strain of *T. gondii* [Figure 2.12A]. The mutant genotype was confirmed by genomic PCRs, and lack of *Tgpepck1* mRNA expression was confirmed by cDNA PCRs [Fig. 2.12B].

Replication assays with Δ*pepck1* parasites revealed a marginal fitness defect under optimal growth conditions (doubling time ~9.5 h). While glutamine was not essential for RH Δ*pepck1* parasite growth (doubling time ~9.4 h), glucose deprivation was found to be lethal for these parasites [Fig. 2.12C]. Metabolic labeling studies on Δ*pepck1* parasites using $U^{13}C$-$U^{15}N$-glutamine revealed that the absence of gluconeogenic flux of ^{13}C- from Krebs cycle to glycolytic and pentose phosphate pathway intermediates [Fig. 2.12D]. These findings are in agreement with that previously reported using conditional expression of *Tgpepck1* in Δ*gt1* parasites [Nitzsche *et al*., 2017].

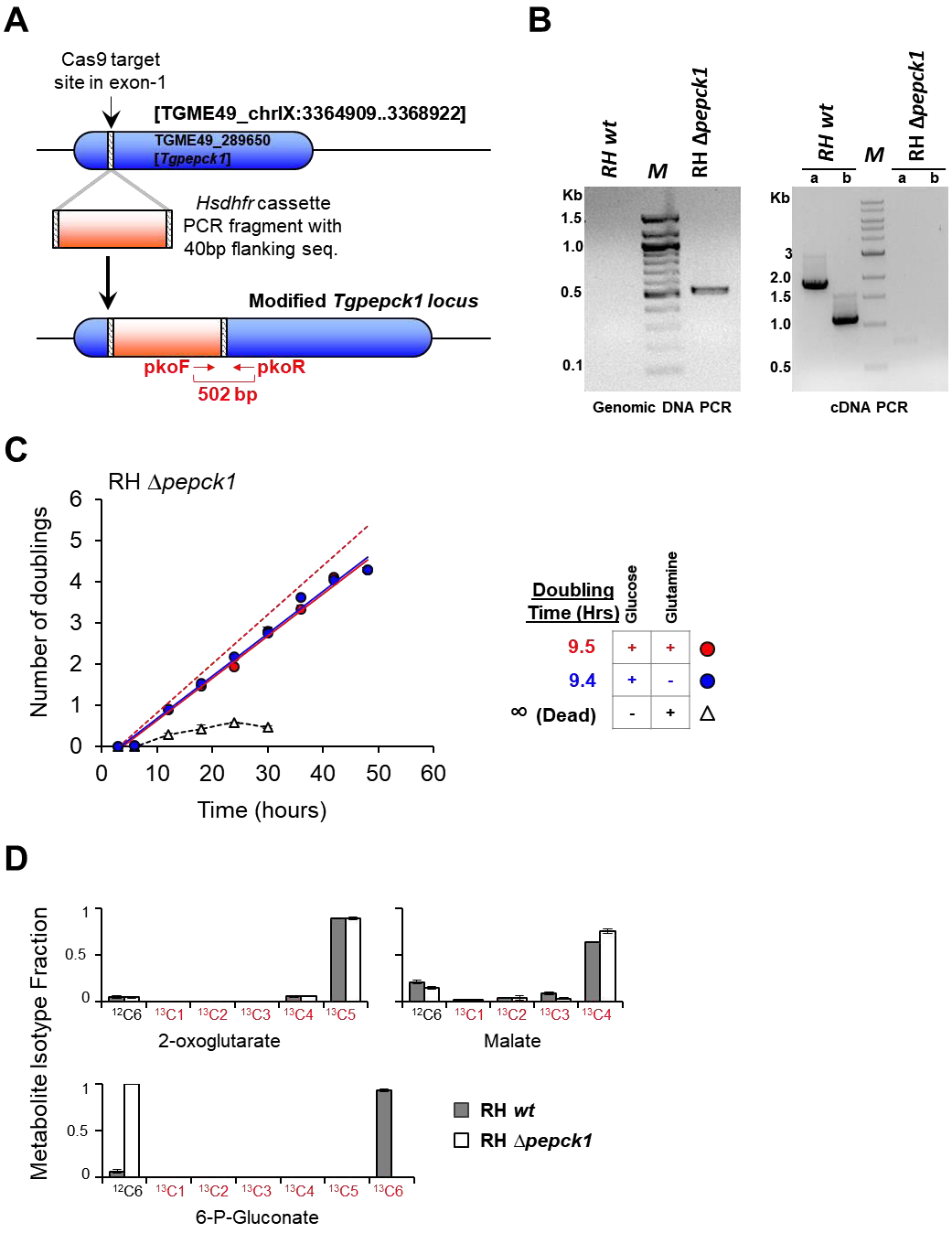

Figure 2.12: Tgpepck1 gene knockout studies. ***A****, schema depicts the strategy used for knocking out Tgpepck1 gene using the CRISPR/Cas9 system; the CRISPR guide RNA was designed to target exon-1 of the gene.* ***B****, confirmation of Tgpepck1 gene knockout by genomic DNA and cDNA PCRs. A 502 bp PCR product is amplified from genomic DNA of RH Δpepck1 parasites only, using the primer pairs pko1 and pko2 shown in* ***A****. M – 100 bp DNA marker ladder. In cDNA PCRs, exon specific primers were used to amplify two different PCR products, 1835 bp fragment (a) and 1079 bp fragment (b). M – 1 kb DNA marker ladder.* ***C****, replication assay for RH Δpepck1 tachyzoites in the presence and absence of glucose or*

glutamine. The black dashed line indicates that RH Δpepck1 parasites are killed by glucose deprivation. The red dashed line indicates the growth of RH wt parasites in complete media. ***D,*** *^{13}C labeling pattern derived from +5^{13}C-+2^{15}N glutamine in the absence of glucose for intermediates of Kreb's cycle (2-oxoglutarate and malate) and pentose phosphate pathway (6-P-gluconate) from RH wt and RH Δpepck1 parasites. Lack of $^{13}C6$ labeling for 6-P-gluconate demonstrates the absence of gluconeogenesis in RH Δpepck1 parasites.*

2.3.9 Confirming conditional essentiality of *Tgpepck1* in *T. gondii* by plaque forming assays

We performed plaque assays to demonstrate that the Δ*pepck1* parasites were actually dead and not merely growth arrested when deprived of glucose. For this, the Δ*pepck1* parasites were first grown in the absence of glucose for 24, 48 or 72 h, before again adding glucose to the culture and allowing the parasites to form plaques. We found that Δ*pepck1* parasites can survive glucose deprivation for up to 48 h, albeit with decreased plaque-forming efficiency. However, after 72 h of glucose deprivation, no plaque formation was observed, suggesting that the parasites cannot survive glucose deprivation beyond 48 h [Fig. 2.13].

2.3.10 Complementation of RH Δ*pepck1* parasites with *Tgpepck1* cDNA

While performing complementation studies with Δ*pepck1* parasites, we tested the possibility of using glucose deprivation as selection for transgenic parasites expressing *Tgpepck1*. When Δ*pepck1* tachyzoites were transfected with a plasmid encoding the *Tgpepck1* cDNA with an in-frame HA tag at the 3' end (*Tgpepck1-HA*), and allowed to replicate in minus glucose medium, the surviving parasites were found to be 100% positive for *TgPEPCK-HA* expression. The localization was cytosolic as confirmed by immunostaining with anti-HA antibodies [Fig. 2.14A]. *Tgpepck1* has a mitochondria

localization signal as predicted by TargetP 1.1 software. When a HA tag in added in the 3' end of the gene in the genomic locus and expressed from its native promoter, the *PEPCK1-HA* protein localized to the mitochondrion [Nitzsche *et al*., 2017].

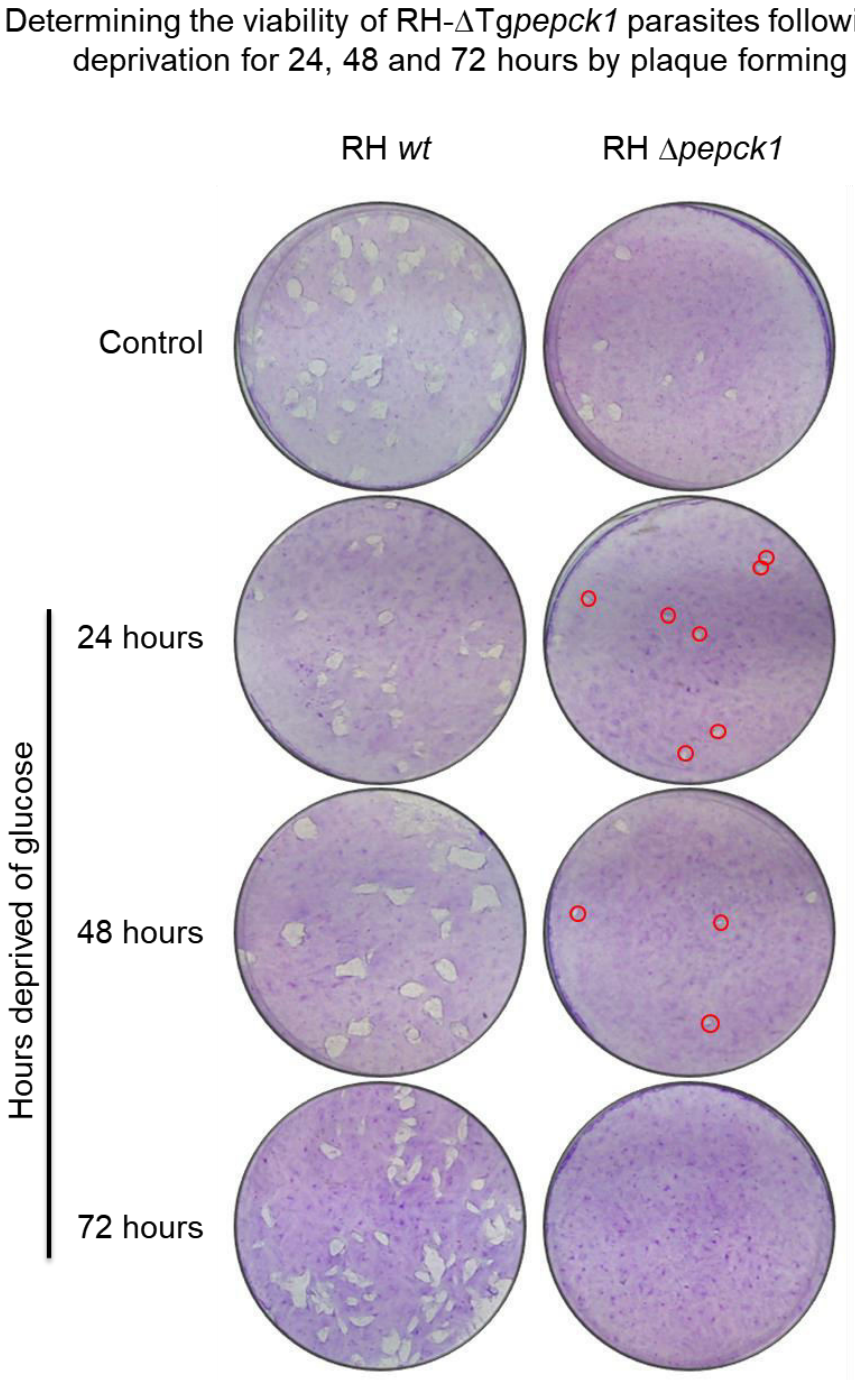

Figure 2.13: Confirming the death of RH Δpepck1 parasites in the absence of glucose*. ~50 RH Δpepck1 parasites were allowed to invade and replicate within HFF cells in 6 well plates. Glucose deprivation was done for 24, 48 and 72 hours, before changing to complete media, and continuing growth for plaque*

formation. Microscopically verified plaques formed by RH Δpepck1 parasites in 24 and 48 hour glucose deprived cultures is marked by red out lines.

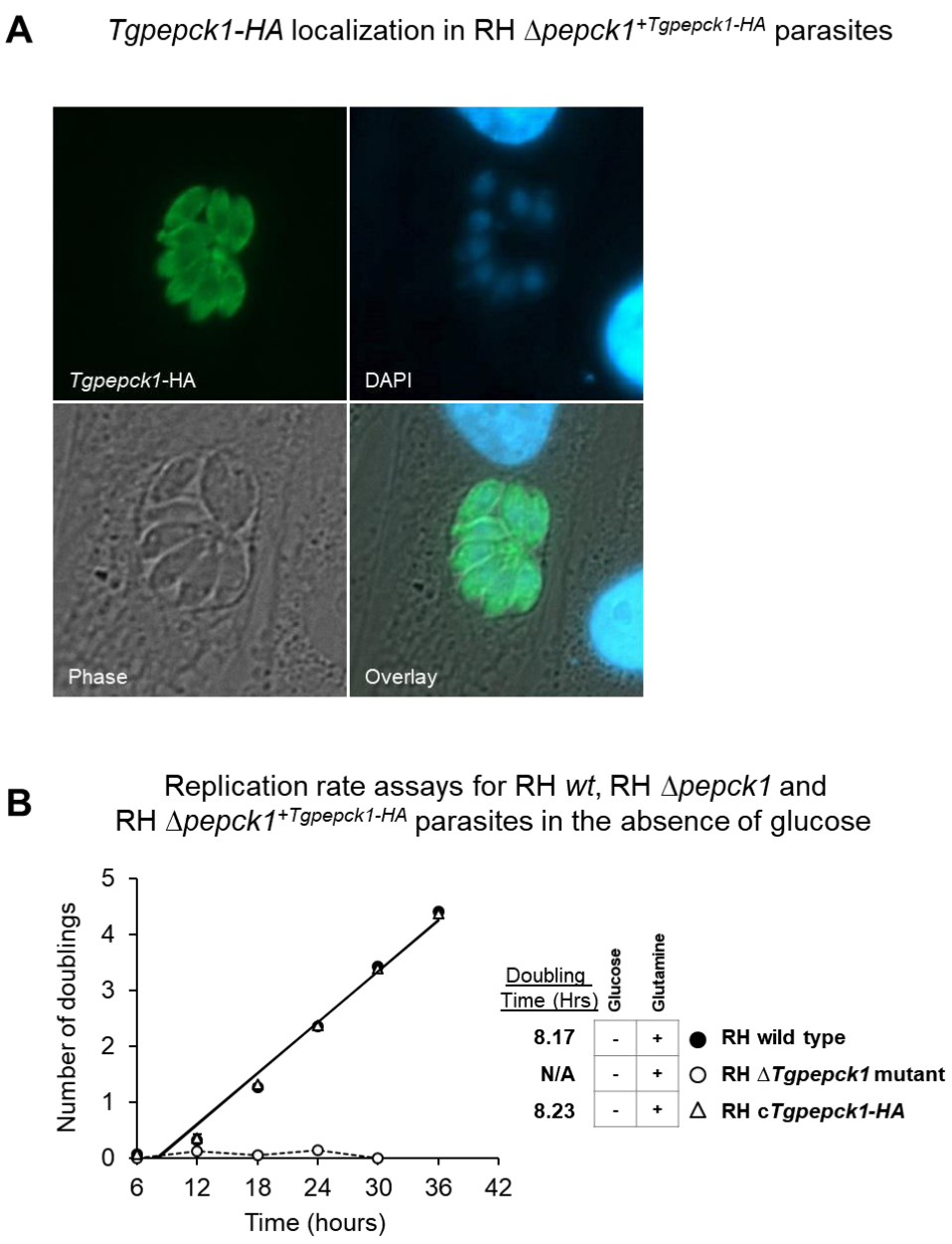

Figure 2.14: Complementation studies with RH Δpepck1 parasites. *A, localization of TgPEPCK-HA protein expressed ectopically in RH Δpepck1 parasites. Infected monolayers were stained with anti-HA antibodies (green) and counter stained with DAPI (blue). B, replication assays showing that the RH Δpepck1+Tgpepck1-HA parasites behave like RH wt parasites when subject to glucose deprivation.*

In our study, it appears that the overexpression of the *Tgpepck1-HA* cDNA from a plasmid using the β-tubulin promoter, has resulted in mis-localization to the cytosol. Nevertheless, the cytosol localized *PEPCK1-HA* protein functionally complemented the mutant phenotype. Replication assays carried out on complemented parasites (RH Δ*pepck1*$^{+Tgpepck1\text{-}HA}$) had comparable growth to *wt* parasites in the absence of glucose [Fig. 2.14B].

2.3.11 Effect of acetate supplementation on the growth of RH *wt*, RH Δ*hk* and RH Δ*pepck1* parasites

It has been reported that Δ*gt1* parasites can overcome their fitness defect by scavenging externally supplied acetate and incorporating it into lipid biomass [Nitzsche et al., 2016]. However, a similar rescue of the fitness defect was not observed in case of RH Δ*hk* parasites [Fig. 2.1]. To test this more rigorously, we performed replication rate assays in the absence of glucose [Fig. 15A], and plaque forming assays in the absence of glutamine [Fig. 2.15B], with RH *wt*, RH Δ*hk* and RH Δ*pepck1* parasites. One set of replicate cultures were supplemented with 2 mM Na-acetate. As seen from our results, acetate supplementation did not rescue RH Δ*pepck1* parasites from death in the absence of glucose. Similarly, the plaquing deficiency seen in case of RH Δ*hk* parasites was not rectified in the presence of acetate. Therefore, we conclude that, unlike in Δ*gt1* parasites, lipid biomass deficiency may not be a major reason for the observed phenotypic defects seen with RH Δ*hk* and RH Δ*pepck1* parasites, in the absence of glutamine and glucose, respectively.

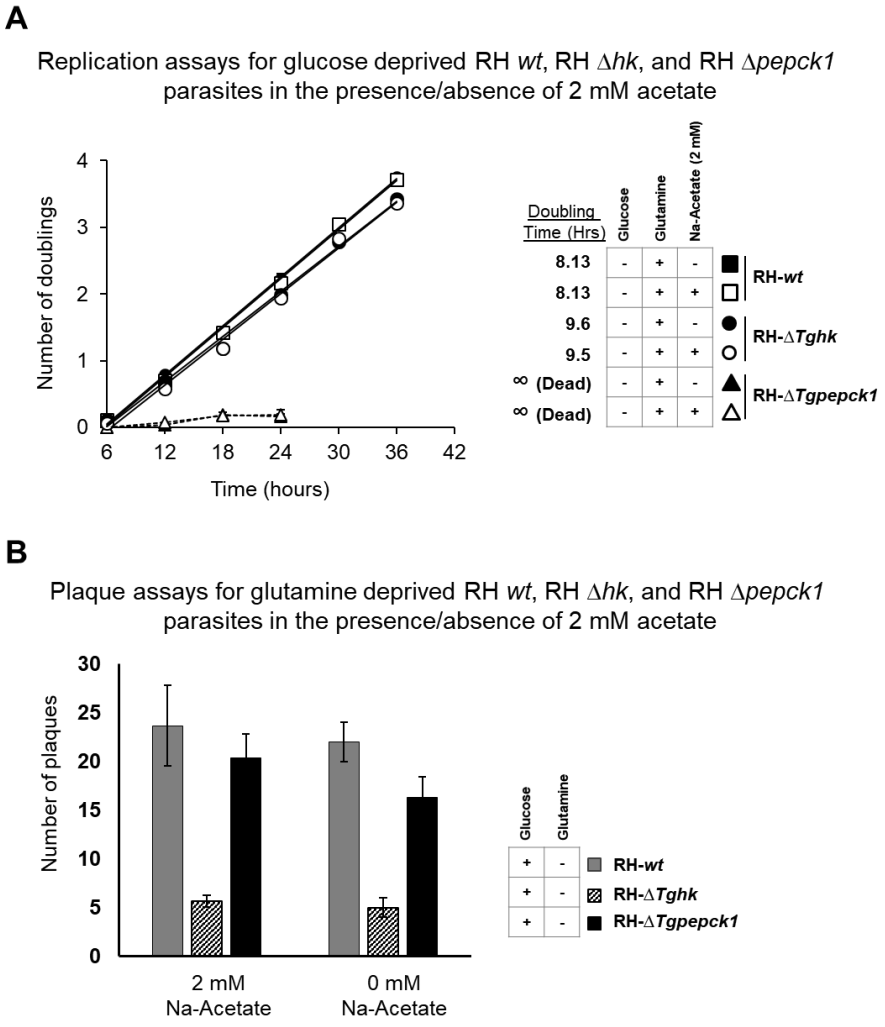

Figure 2.15: Acetate supplementation studies with extracellular RH wt, RH Δhk, and RH Δpepck1 parasites. *2 mM acetate was supplemented in all cases. A, replication assays showing that acetate cannot rescue RH Δpepck1 parasites from death in glucose deprived cultures. B, plaque assays showing that acetate cannot reverse the plaque forming deficiency seen with RH Δhk parasites in the absence of glutamine.*

2.3.12 Glutaminolysis facilitates mitochondrial oxidative phosphorylation

The F-type ATP synthase in apicomplexan mitochondrion is highly divergent [Gardner *et al*., 2002; Mather *et al*., 2007; Brayton *et al*., 2007; Reid *et al*., 2012] and many of its subunits are not readily detected by sequence comparison with yeast and

mammalian counterparts. However, evidence is now available for the existence of a functional F-type ATP synthase in T. gondii mitochondrion [Lin *et al*., 2011].

We reasoned that in the absence of glycolytic ATP, RH Δ*hk* parasites should be wholly dependent on mitochondrial ATP. This assumption is supported by our observation that extracellular Δ*hk* parasites deprived of glutamine are unable to invade host cells efficiently. In order to validate this, we tracked ATP synthesis in extracellular tachyzoites incubated in the presence and absence of glucose for 15 hours [Fig. 16A]. In *wt* parasites, ATP levels decreased to ~50% in 6 hours, coinciding with the half-life of extracellular parasite viability [Konrad *et al*., 2011]. Importantly, the kinetics of ATP loss in *wt* was similar in complete, minus glucose and minus glutamine medium, suggesting that either glucose or glutamine alone as a nutrient can sustain optimal cellular ATP levels. In Δ*hk* parasites, presence/absence of glucose had no effect on ATP homeostasis and the kinetics of ATP loss was similar to that of wt. However, when Δ*hk* parasites were deprived of glutamine, ATP levels declined dramatically; ~50% loss was seen in less than 2 hours, and by ~6 hours there was complete loss of ATP [Fig. 16B]. Non-essential amino acids could not rescue the ATP synthesis deficiency in Δ*hk* parasites.

We validated these findings using atovaquone, which inhibits oxidative phosphorylation [McFadden *et al*., 2000]. ATP synthesis in wt parasites, in the presence of glucose, was not inhibited by atovaquone. However, in the absence of glucose, glutamine dependent ATP synthesis was completely inhibited by 200 nM atovaquone in wt parasites [Fig. 2.16C]. This finding indicates that T. gondii tachyzoites are fully dependent on oxidative phosphorylation for ATP synthesis in the absence of glycolysis. In agreement with this finding, ATP synthesis in Δ*hk* parasites was sensitive to atovaquone even in the presence of glucose [Fig. 2.16D], and complemented Δhk^{+Tghk}

parasite resembled wild type parasites in their response to atovaquone treatment [Fig. 2.17]. As expected, ATP synthesis in Δ*pepck1* parasites, under the different test conditions was similar to that observed with *wt* parasites [Fig. 2.18].

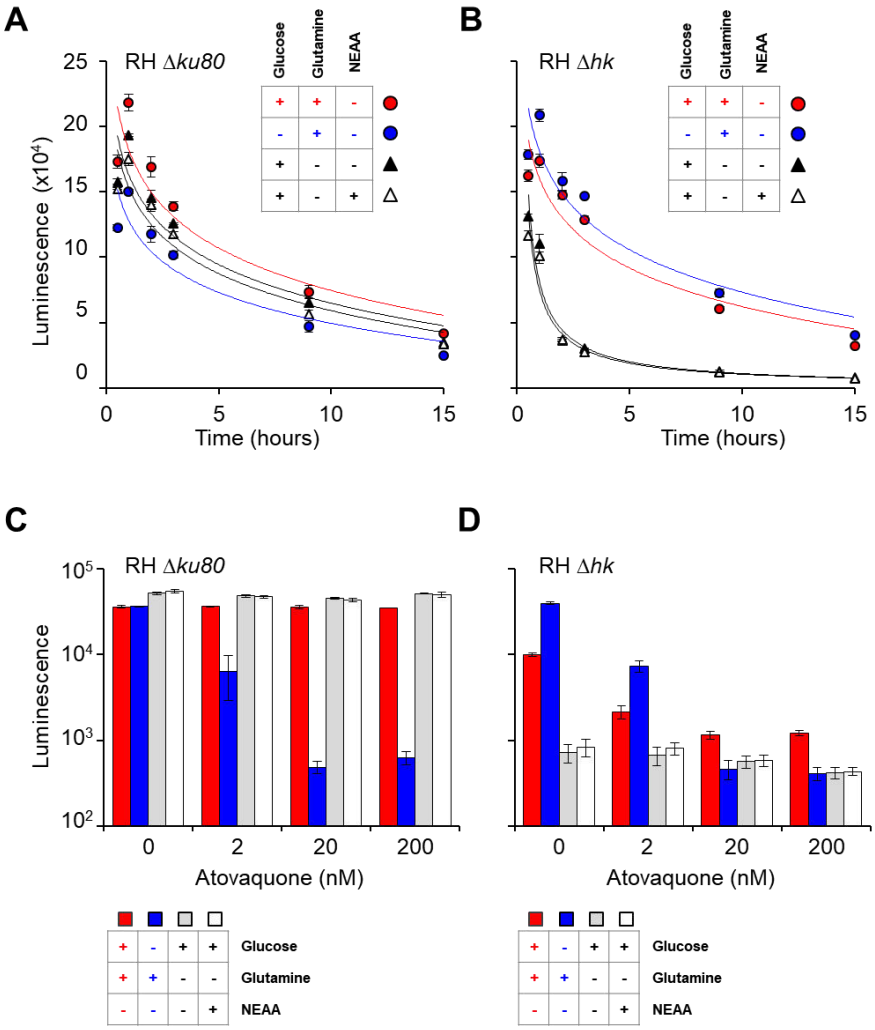

Figure 2.16: ATP synthesis assays on tachyzoite stage T. gondii. *Luciferase expressing, extracellular parasites were used to measure total cellular ATP content. Progressive loss of ATP with time can be seen in Rh wt (A) and RH Δhk (B) parasites incubated in complete and nutrient deficient media. Since RH Δhk parasites are always dependent on glutaminolysis for ATP synthesis, when deprived of glutamine, they exhibit a dramatic loss of cellular ATP, with a half-life of ~1-2 hours. C and D, effect of atovaquone on ATP synthesis in RH wt and RH Δhk parasites, following 2 hours of drug treatment. Here again, the parasites were incubated in complete and nutrient deficient media. ATQ – atovaquone; NEAA – mixture of nonessential amino acids.*

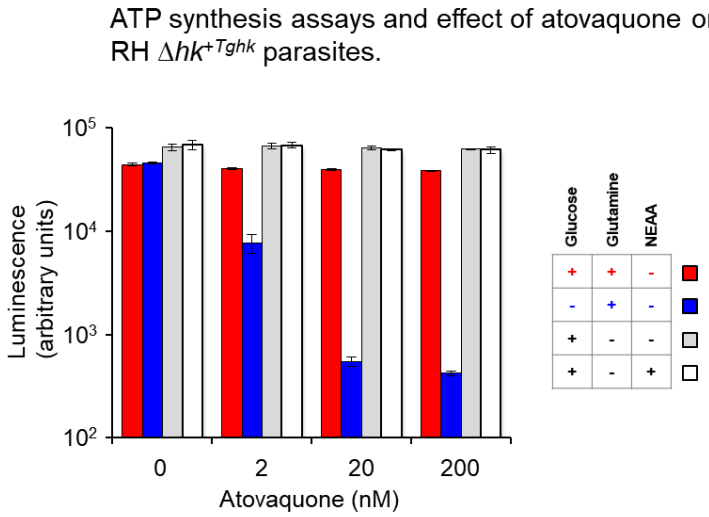

Figure 2.17: ATP synthesis assays with TgΔhk mutants complemented with a functional Tghk gene*. The data depicted in red and blue indicated the ATP synthesis observed in the complete and minus glucose medium respectively.*

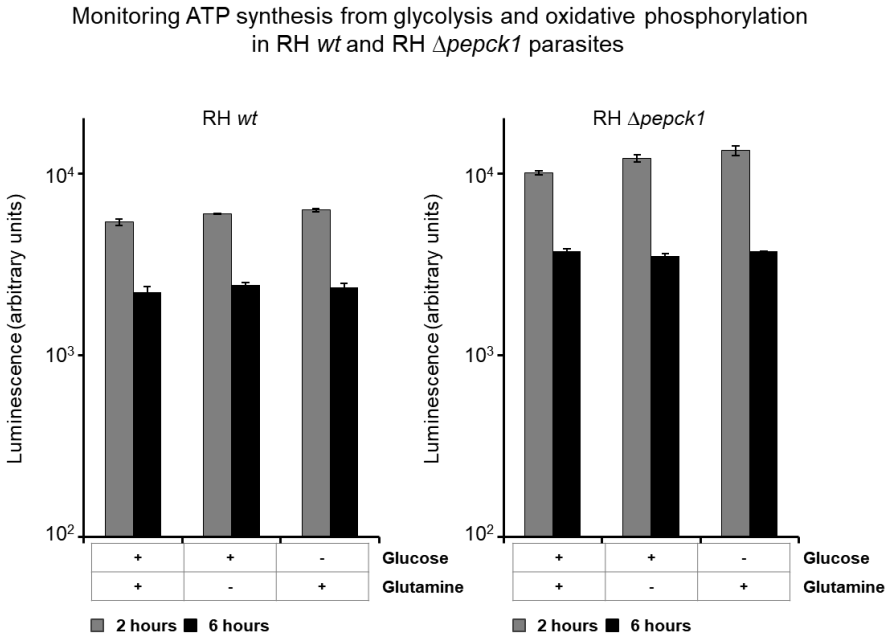

Figure 2.18: ATP synthesis assays with wild type (left panel) and ΔTgpepck1 (right panel) parasites. *105 tachyzoites were incubated in either complete culture media or in media lacking either glucose or glutamine, as indicated. After 2 and 6 hours of incubation, total cellular ATP content was determined using a luciferase assay system.*

2.4 Conclusion

As an obligate intracellular parasite, *T. gondii* is dependent on host-derived glucose and glutamine for survival. Glucose metabolism is well studied in tachyzoite stage *T. gondii*, where a robust glycolytic flux is the major source of carbon and energy (ATP) for the parasite [Al-Anouti *et al*., 2004; Saliba and Kirk, 2001; MacRae *et al*., 2012]. Although glucose is needed for optimal growth of *T. gondii*, it is not an essential nutrient. This was originally shown in studies using mutant parasites deficient in the major glucose transporter (Δ*gt1*), where glutaminolysis was found to support growth of tachyzoite stage parasites [Blume *et al*., 2009]. Moreover, genetic mutants of the glycolytic enzyme fructose 1,6 bisphosphate aldolase were viable, but only in the absence of glucose [Shen and Sibley, 2014]. To further validate the essentiality of glycolysis in *T. gondii*, and to determine its role for asexual development of the parasite, we generated mutant parasites deficient in glycolysis by knocking out the gene coding for hexokinase (Δ*hk*), which catalysis the first step in glycolysis.

Phenotypic studies with *wt* and Δ*hk* parasites revealed that glucose is required for optimal growth and robust replication of tachyzoite stage parasites, and glutamine and other carbon sources, such as acetate, succinate, pyruvate, glycerol and propionate, cannot compensate for the fitness defect [Fig. 2.1]. This is intriguing since, the fitness defect in glucose transporter (Δ*gt1*) mutants was overcome by acetate supplementation. Scavenged acetate was primarily incorporated into lipid biomass, suggesting that the fitness defect in Δ*gt1* parasites was primarily due to lipid biomass deficiency [Nitzsche *et al*., 2016]. In Δ*gt1* parasites, residual glycolytic activity is detectable, suggesting low levels of glucose entry into these cells. In contrast, the complete absence of glucose oxidation via glycolysis in Δ*hk* parasites, as seen in our metabolic labeling studies, indicates that acetate supplementation cannot compensate for complete loss of glycolysis in these

parasites. This was further confirmed by plaque forming assays on Δ*hk* mutants, with and without acetate supplementation [Fig. 2.15].

During asexual development, tachyzoite stage parasites convert to bradyzoites, which are responsible for the formation of tissue cysts in chronic infections [Dubey *et al*., 1998]. Bradyzoites are slow growing forms and probably are metabolically less active than tachyzoites [Lunghi *et al*., 2015]. Until now the role of glycolysis for bradyzoite formation was not studied. Here, we show that virulence associated with acute infection and mature tissue cyst formation during chronic infection is compromised in Type II Pru Δ*hk* parasites [Fig. 2.6]. These results suggest that for effective in vivo pathogenesis in mammalian host, *T. gondii* requires glycolysis. Diminished tissue cyst formation in vivo, however, was not due to defective cyst wall polysaccharide synthesis, since Pru Δ*hk* parasites were capable of differentiating into bradyzoites in vitro, and exhibit apparently normal cyst wall staining with dolichos biflorus lectin. As shown for tachyzoite stage parasites, glutamine alone as a nutrient appears to be sufficient for in vitro bradyzoite formation by *T. gondii*. Therefore the inability of these parasites to form mature bradyzoite tissue cysts in vivo might be due to insufficient availability of glutamine. This is supported by our observation that host cell invasion and plaquing efficiency are greatly diminished in Δ*hk* parasites in the absence of glutamine [Fig. 2.10C].

The metabolic changes in Δ*hk* parasites were tracked using ^{13}C labeling studies. In contrast to *wt* parasites, in Δ*hk* parasites there was complete absence of glucose derived ^{13}C labeling in intermediates of glycolysis, pentose phosphate pathway and Kreb's cycle. U^{13}C-U^{15}N-glutamine derived labeling patterns revealed that Δ*hk* parasites generate glycolytic and pentose phosphate pathway intermediates *via* gluconeogenesis [Figure 7, 8]. Only in Δ*hk* parasites, we observed the formation of glutamine derived +3^{13}C-isotopomers for aspartate, malate and succinate, in addition to the +4^{13}C- isotopomers.

This indicates that +3^{13}C-PEP, formed via the *PEPCK* reaction, is sequentially converted into +3^{13}C-pyruvate and +3^{13}C-oxaloacetate, which then equilibrates with aspartate, malate and succinate pools. Moreover, the formation of glutamine derived +6^{13}C- and +5^{13}C- isotopomers of citrate, in addition to the +4^{13}C- isotopomer, indicates the *BCKDH* mediated formation +2^{13}C-acetyl-CoA as previously reported [Oppenheim *et al*., 2014]. Taken together, our results from metabolic labeling studies with Δ*hk* parasites are in agreement with that previously reported for the glucose transporter mutants [Nitzsche *et al*., 2016], and validates the importance of glutaminolysis and gluconeogenesis for survival of *T. gondii* in the absence of glycolysis. A summary of the results from metabolic studies is shown in Figure 2.19.

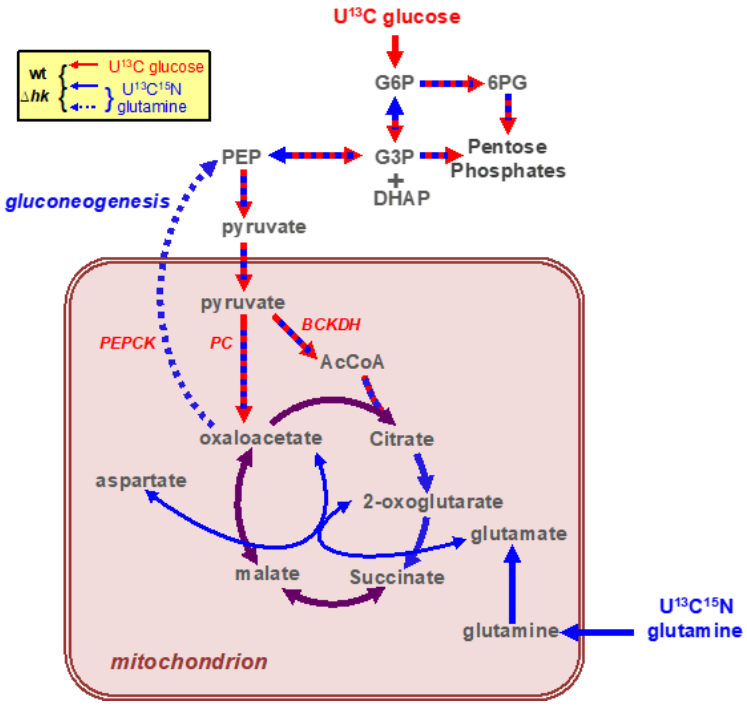

Figure 2.19: Schematic representation of results from metabolic labeling studies in T. gondii wild type and Δhk mutant parasites.

Surprisingly, despite its importance, glutamine deprivation was not lethal for intracellular survival of Δ*hk* parasites, although their fitness was greatly reduced [Fig.

2.10A]. It is likely that glutamine deprived intracellular Δ*hk* parasites scavenge glutamine/glutamate from within host cells. Also, Δ*pepck1* parasites, which are deficient in gluconeogenesis, failed to grow and replicate within host cells in the absence of glucose, suggesting that glutaminolysis derived gluconeogenesis is the only mechanism by which *T. gondii* tachyzoites can assimilate carbon in the absence of glycolysis. To find out whether *Tgpepck1* is essential for asexual differentiation of tachyzoites to bradyzoites, we attempted to disrupt the *Tgpepck1* gene from the Pru strain (Type II) of *T. gondii*, but failed to obtain the mutants despite repeated attempts using either gene replacement or CRISPR/Cas9 mediated gene editing using two different guide RNAs. While the essentiality of *PEPCK* enzyme in Pru strain *T. gondii* needs to be explored further, we however found no difference whatsoever between wt RH and *wt* Pru strains in metabolic labeling experiments with glucose and glutamine. Interestingly, fructose-1,6 bisphosphatase (*Tgfbp2*), which catalyzes the second reaction in gluconeogenesis, is essential for *T. gondii*, even in glucose replete conditions [Blume *et al*., 2015] and appears to mediate a futile cycle which regulates fructose-1,6 bisphosphate levels and carbon supply for synthesis of N-glycans, GPI anchor and amylopectin.

In contrast to intracellular Δ*hk* parasites, when extracellular Δ*hk* parasites are deprived of glutamine, they are greatly impaired in their ability to invade host cells and lose viability as observed in plaque forming assays [Fig. 2.10C]. This is likely due to loss of ATP synthesis, as confirmed by our experiments with atovaquone, which inhibits oxidative phosphorylation [McFadden *et al*., 2000]. *T. gondii* tachyzoites are capable of obtaining all of their ATP from either glycolysis or oxidative phosphorylation, and prior biochemical evidence suggests active mitochondrial oxidative phosphorylation in tachyzoites [Vercesi *et al*., 1998]. In *wt* and Δ*pepck1* parasites, atovaquone had no effect on ATP synthesis in the presence of glucose, in agreement with previous findings [Pomel

et al., 2008]. However, since oxidative phosphorylation is the only source of ATP for Δ*hk* parasites, atovaquone completely abolished ATP synthesis in this parasite, even in the presence of glucose [Fig. 2.16]. Overall, our findings suggest that *T. gondii* tachyzoite harbor a highly dynamic and essential mitochondrial oxidative metabolism, which can support parasite growth and differentiation in varying nutrient conditions. Further exploring the role of glycolysis and glutaminolysis in carbon and energy metabolism in the latent bradyzoite stages will help to reveal the metabolic requirements for tissue cyst formation and host persistence of this promiscuous parasite.

2.5 References:

Abdelbaset, AE. *et al*. (2017). Lactate dehydrogenase in Toxoplasma gondii controls virulence, bradyzoite differentiation, and chronic infection. PLoS One 12:e0173745.

Al-Anouti, F., Tomavo, S., Parmley, S., Ananvoranich, S. (2004) The expression of lactate dehydrogenase is important for the cell cycle of Toxoplasma gondii. J Biol Chem 279:52300-11.

Bahl, A. *et al*. (2010). A novel multifunctional oligonucleotide microarray for Toxoplasma gondii. BMC Genomics 11:603.

Barban, S. (1962). Studies on the mechanism of resistance to 2-deoxy-D-glucose in mammalian cell cultures. J Biol Chem 237:291-5.

Blume, M. *et al*. (2009). Host-derived glucose and its transporter in the obligate intracellular pathogen Toxoplasma gondii are dispensable by glutaminolysis. Proc Natl Acad Sci U S A 106:12998-3003.

Blume, M. *et al*. (2015). Toxoplasma gondii Gluconeogenic Enzyme Contributes to Robust Central Carbon Metabolism and Is Essential for Replication and Virulence. Cell Host Microbe 18:210-20.

Bohne, W. *et al*. (1998). Targeted disruption of the bradyzoite-specific gene BAG1 does not prevent tissue cyst formation in Toxoplasma gondii. Mol Biochem Parasitol 92:291-301.

Boothroyd, JC. *et al*. (1997). Genetic and biochemical analysis of development in Toxoplasma gondii. Philos Trans R Soc Lond B Biol Sci 352:1347-54.

Brayton, KA. *et al*. (2007). Genome sequence of Babesia bovis and comparative analysis of apicomplexan hemoprotozoa. PLoS Pathog 3:1401-13.

Chambers, MC. *et al*. (2012). A cross-platform toolkit for mass spectrometry and proteomics. Nat Biotechnol 30:918-20.

Clasquin, MF., Melamud, E., Rabinowitz, J. D. (2012). LC-MS data processing with MAVEN: a metabolomic analysis and visualization engine. Curr Protoc Bioinformatics Chapter 14:Unit14.11.

Cobbold, SA. *et al*. (2013). Kinetic flux profiling elucidates two independent acetyl-CoA biosynthetic pathways in Plasmodium falciparum. J Biol Chem 288:36338-50.

Crawford, MJ. *et al*. (2006). Toxoplasma gondii scavenges host-derived lipoic acid despite its de novo synthesis in the apicoplast. EMBO J 25:3214-22.

Donald, RG., Carter, D., Ullman, B., Roos, D. S. (1996). Insertional tagging, cloning, and expression of the Toxoplasma gondii hypoxanthine-xanthine-guanine

phosphoribosyltransferase gene. Use as a selectable marker for stable transformation. J Biol Chem 271:14010-9.

Dubey, JP. (1997). Bradyzoite-induced murine toxoplasmosis: stage conversion,pathogenesis, and tissue cyst formation in mice fed bradyzoites of different strains of Toxoplasma gondii. J Eukaryot Microbiol 44:592-602.

Dubey, JP., Lindsay, DS., Speer, CA. (1998). Structures of Toxoplasma gondii tachyzoites, bradyzoites, and sporozoites and biology and development of tissue cysts. Clin Microbiol Rev 11:267-99.

Dubey, JP. (2008). The history of Toxoplasma gondii-the first 100 years. J Eukaryot Microbiol 55:467-75.

Ferguson, DJ., Hutchison, WM. (1987). An ultrastructural study of the early development and tissue cyst formation of Toxoplasma gondii in the brains of mice. Parasitol Res 73:483-91.

Fleige, T. *et al*. (2007). Carbohydrate metabolism in the Toxoplasma gondii apicoplast: localization of three glycolytic isoenzymes,the single pyruvate dehydrogenase complex, and a plastid phosphate translocator. Eukaryot Cell 6:984-96.

Fleige, T., Pfaff, N., Gross, U., Bohne, W. (2008). Localisation of gluconeogenesis and tricarboxylic acid (TCA)-cycle enzymes and first functional analysis of the TCA cycle in Toxoplasma gondii. Int J Parasitol 38:1121-32.

Foth, BJ. *et al*. (2005). The malaria parasite Plasmodium falciparum has only one pyruvate dehydrogenase complex, which is located in the apicoplast. Mol Microbiol 55:39-53.

Fox, BA. *et al*. (2009). Efficient gene replacements in Toxoplasma gondii strains deficient for nonhomologous end joining. Eukaryot Cell 8:520-9.

Fox, BA. *et al*. (2011). Type II Toxoplasma gondii KU80 knockout strains enable functional analysis of genes required for cyst development and latent infection. Eukaryot Cell 10:1193-206.

Gardner, MJ. *et al*. (2002). Genome sequence of the human malaria parasite Plasmodium falciparum. Nature 419:498-511.

Jensen, MD., Conley, M., Helstowski, LD. (1983). Culture of Plasmodium falciparum: the role of pH, glucose, and lactate. J Parasitol 69:1060-7.

Knoll, L. J., Boothroyd, J. C. (1998). Isolation of developmentally regulated genes from Toxoplasma gondii by a gene trap with the positive and negative selectable marker hypoxanthine-xanthine-guanine phosphoribosyltransferase. Mol Cell Biol 18:807-14.

Köhler, S. *et al*. (1997). A plastid of probable green algal origin in Apicomplexan parasites. Science 275:1485-9.

Konrad, C., Wek, RC., Sullivan, WJ. Jr. (2011). A GCN2-like eukaryotic initiation factor 2 kinase increases the viability of extracellular Toxoplasma gondii parasites. Eukaryot Cell 10:1403-12.

Lea, PJ., Miflin, BJ. (1975). Glutamate synthase in blue-green algae. Biochem Soc Trans 3:381-4.

Lin, SS. *et al*. (2011). Extracellular Toxoplasma gondii tachyzoites do not require carbon source uptake for ATP maintenance, gliding motility and invasion in the first hour of their extracellular life. Int J Parasitol 41:835-41.

Lu, W. *et al*. (2010). Metabolomic analysis via reversed-phase ion-pairing liquid chromatography coupled to a stand alone orbitrap mass spectrometer. Anal Chem 82:3212-21.

Lunghi, M., *et al*. (2015). Expression of the glycolytic enzymes enolase and lactate dehydrogenase during the early phase of Toxoplasma differentiation is regulated by an intron retention mechanism. Mol Microbiol 96:1159-75.

MacRae, JI. *et al*. (2012). Mitochondrial metabolism of glucose and glutamine is required for intracellular growth of Toxoplasma gondii. Cell Host Microbe 12:682-92.

Mather, MW., Henry, KW., Vaidya, AB. (2007). Mitochondrial drug targets in apicomplexan parasites. Curr Drug Targets 8:49-60.

McFadden, GI., Reith, ME., Munholland, J., Lang-Unnasch, N. (1996). Plastid in human parasites. Nature 381:482.

McFadden DC., Tomavo S., Berry EA., Boothroyd JC. (2000). Characterization of cytochrome b from Toxoplasma gondii and Q(o) domain mutations as a mechanism of atovaquone-resistance. Mol Biochem Parasitol 108(1):1-12.

Melamud, E., Vastag, L., Rabinowitz, JD. (2010). Metabolomic analysis and visualization engine for LC-MS data. Anal Chem 82:9818-26.

Nitzsche, R., Zagoriy, V., Lucius, R., Gupta, N. (2016). Metabolic Cooperation of Glucose and Glutamine Is Essential for the Lytic Cycle of Obligate Intracellular Parasite Toxoplasma gondii. J Biol Chem 291:126-41.

Nitzsche, R. *et al*. (2017). A plant/fungal-type phosphoenolpyruvate carboxykinase located in the parasite mitochondrion ensures glucose-independent survival of Toxoplasma gondii. J Biol Chem pii: jbc.M117.802702.

Olszewski, KL. *et al*. (2009). Host-parasite interactions revealed by Plasmodium falciparum metabolomics. Cell Host Microbe 5:191-9.

Oppenheim, RD. *et al*. (2014). BCKDH: the missing link in apicomplexan mitochondrial metabolism is required for full virulence of Toxoplasma gondii and Plasmodium berghei. PLoS Pathog 10:e1004263.

Polonais, V., Soldati-Favre, D. (2010). Versatility in the acquisition of energy and carbon sources by the Apicomplexa. Biol Cell 102:435-45.

Pomel, S., Luk, FC., Beckers, CJ. (2008). Host cell egress and invasion induce marked relocations of glycolytic enzymes in Toxoplasma gondii tachyzoites. PLoS Pathog 4:e1000188.

Ralph, SA. *et al*. (2004). Tropical infectious diseases: metabolic maps and functions of the Plasmodium falciparum apicoplast. Nat Rev Microbiol 2:203-16.

Reid, AJ. *et al*. (2012). Comparative genomics of the apicomplexan parasites Toxoplasma gondii and Neospora caninum: Coccidia differing in host range and transmission strategy. PLoS Pathog 8:e1002567.

Rommereim, LM. *et al*. (2014). Genetic manipulation in Δku80 strains for functional genomic analysis of Toxoplasma gondii. J Vis Exp (77):e50598.

Roos, DS. *et al*. (2002). Mining the Plasmodium genome database to define organellar function: what does the apicoplast do? Philos Trans R Soc Lond B Biol Sci 357:35-46.

Roos, DS. *et al*. (1994). Molecular tools for genetic dissection of the protozoan parasite Toxoplasma gondii. Methods Cell Biol 45:27-63.

Roth, E. Jr. (1990). Plasmodium falciparum carbohydrate metabolism: a connection between host cell and parasite. Blood Cells 16:453-60

Rowell, P., Enticitt, S., Stewart, WDP. (1977). Glutamine synthetase and Nitrogenase activity in the blue-green algae Anabaena cylindrical. The New Phytologist 79: 41-54

Saliba, K. J., Kirk, K. (2001). Nutrient acquisition by intracellular apicomplexan parasites: staying in for dinner. Int J Parasitol 31:1321-30.

Sander, JD. *et al*. (2014). CRISPR-Cas systems for editing, regulating and targeting genomes. Nat Biotechnol 32:347-55.

Seeber, F. (2003). Biosynthetic pathways of plastid-derived organelles as potential drug targets against parasitic apicomplexa. Curr Drug Targets Immune Endocr Metabol Disord 3:99-109.

Seeber, F., Soldati-Favre, D. (2010). Metabolic pathways in the apicoplast of apicomplexa. Int Rev Cell Mol Biol 281:161-228.

Shen, B., Brown, K. M., Lee, TD., Sibley, LD. (2014). Efficient gene disruption in diverse strains of Toxoplasma gondii using CRISPR/CAS9. MBio 5:e01114-14.

Shen, B., Sibley, LD. (2014). Toxoplasma aldolase is required for metabolism but dispensable for host-cell invasion. Proc Natl Acad Sci U S A 111:3567-72.

Sidik, SM. *et al*. (2014). Efficient genome engineering of Toxoplasma gondii using CRISPR/Cas9. PLoS One 9:e100450.

Tymoshenko, S., *et al*. (2015). Metabolic Needs and Capabilities of Toxoplasma gondii through Combined Computational and Experimental Analysis. PLoS Comput Biol 11:e1004261.

Ufermann, CM. *et al*. (2017). Toxoplasma gondii plaque assays revisited: Improvements for ultrastructural and quantitative evaluation of lytic parasite growth. Exp Parasitol 180:19-26.

van Dooren, GG., Stimmler, LM., McFadden, GI. (2006). Metabolic maps and functions of the Plasmodium mitochondrion. FEMS Microbiol Rev 30:596-630.

Vercesi, AE. *et al*. (1998). Respiration and oxidative phosphorylation in the apicomplexan parasite Toxoplasma gondii. J Biol Chem 273:31040-7.

Wassmer, SC., Grau, GE. (2017). Severe malaria: what's new on the pathogenesis front? Int J Parasitol 47:145-152.

Woo, YH., *et al*. (2015). Chromerid genomes reveal the evolutionary path from photosynthetic algae to obligate intracellular parasites. Elife. 4:e06974.

Chapter 3

Studying the atovaquone mode of action using metabolic and genetic approaches & identification of novel atovaquone analogs with conserved mode of action

3.1 Introduction

The last decade has seen significant improvement in detection, treatment and confinement of malaria worldwide, which has reduced the mortality and morbidity due to this deadly disease. Effective use of combination therapies, and mosquito repellent nets were the driving force for this success [WHO Malaria Report 2016]. However, the continued emergence of resistant parasites in malaria hot spot areas in the world is becoming an alarming situation. Reports on emergence of artemisinin resistant parasites in South East Asia is becoming more frequent and has raised the concern of spreading this resistance to the other parts of the world, and an estimated 100,000 people are under threat of being infected by artemisinin resistance malaria [Lubell *et al*., 2014]. Being the frontier line clinical drug recommended by WHO against malaria, artemisinin resistance has created a large vacuum between the drug discovery and future malaria treatment.

Extensive efforts have been done for identification of novel targets, conserved parasite pathways and functions to develop new therapeutic interventions. Screening large small-molecule libraries against different stages of malaria parasite and carrying out mechanistic studies has provided many novel molecular scaffolds which can be developed into future antimalarial drugs [Gamo *et al*., 2010; Plouffe *et al*., 2008; Guiguemde *et al*., 2010; Baldwin *et al*., 2005]. In malaria parasites, mitochondrial functions, pathways and proteins are bona fide and validated targets. One of the most prominent mitochondrion targeting antimalarial drug is atovaquone, which is a structural analog of ubiquinone. Atovaquone targets the essential CYTb protein, which is part of the Electron Transport Chain (ETC) Complex III (bc_1 complex) and therefore has a vital function in mitochondrial respiration of the malaria parasites. Atovaquone is very potent and its estimated EC_{50} value is ~1 nM [Fry *et al*., 1992; Hudson *et al*., 1993; (a) Srivastava *et al*., 1999; Hunte *et al*., 2008]. The wide use of this effective drug active

against all sexual and asexual stages of the parasites has been prevented due to its higher cost, malarial parasites ability to evolve resistance easily and toxicity in humans in higher dose and prolonged use [Chiodini *et al*., 1995; Looareeuwan *et al*., 1996]. Atovaquone binds with high affinity and specificity as a competitive inhibitor to the Q_o site in Cytb protein, which is the ubiquinone binding site, to inhibit the function of respiratory Complex III by preventing the oxidation of ubiquinol to ubiquinone. This ultimately blocks the Q-cycle of mitochondrial ETC, collapsing the potential gradient across the mitochondrial inner membrane [Srivastava *et al*., 1997; (b) Srivastava *et al*., 1997; Hunte *et al*., 2008].

It has been demonstrated that the most important function associated with mitochondria is biosynthesis of pyrimidine base [Painter *et al*., 2007]. The pyrimidine biosynthesis pathway enzyme dihydroorotate dehydrogenase (DHOD) oxidises dihydroorotate into orotate. The reduction of oxidized ubiquinone, which is the H+ to acceptor, facilitates this reaction [Gutteridge *et al*., 1979]. Therefore, when the mitochondrial Q cycle is blocked, it results in inhibition of the essential pyrimidine biosynthesis, and this ultimately leads to death of the parasite [Painter *et al*., 2007]. Using transgenic *P. falciparum* expressing the cytosolic yeast DHOD enzyme which uses fumarate as H+ acceptor, thus effectively decoupling pyrimidine biosynthesis from the mitochondrion, it was demonstrated elegantly that the inhibitory effect of atovaquone was completely nullified [Painter *et al*., 2007]. These studies on the mode of action atovaquone confirmed the importance of mitochondrial respiratory chain for the survival of *P. falciparum*.

It has been demonstrated conclusively that both rodent and human malaria parasites readily acquire resistance to atovaquone by mutating the *cytb* gene [Srivastava et al., 1999; Syafruddin *et al*., 1999]. It has been shown that *Pfcytb* mutations conferring

atovaquone resistance resulted in decreased efficiency of the respiratory chain and fitness of the parasite, but was not leathal for the survival of blood stages of the parasite. The mutant *Pfcytb* parasites were however found to be incapable of differentiating to sexual stages and developing into sporozoites within mosquitos, and thus, interestingly the mutant parasite appeared to be incapable of malaria transmission [Peters *et al*., 2002; Goodman *et al*., 2016]. This finding is of significance with respect to the malaria disease, since wild type parasites will die upon exposure to atovaquone and mutatant parasites, which escape atovaquone treatment, will be unable to survive in the mosquito and continue the infection cycle by transmission. Many different mutations in *Pfcytb*, which result in decreased efficacy of atovaquone, have been shown to block parasite development at specific life cycle stages. For example, Y268N, M133I and V259L mutations in *Pfcytb*, which are most commonly associated with atovaquone resistance, block gametocyte maturation, while Y268C and M133I mutations block the differentiation of oocysts into sporozites [Fig 3.1] [Goodman *et al*., 2017]. These findings highlight the importance of the mitochondrion associated functions as antimalarial drug targets, and has resulted in renewed interest in discovering novel inhibitors targeting the parasite mitochondrion, especially the mtETC and pyrimidine biosynthesis [Goodman et al., 2017]. There is also interest in developing novel analogs of atovaquone having low toxicity, high specificity to parasite CYTb and less prone to development of resistance by the parasite. Novel inhibitors targeting the parasites DHOD are also much sought after [Stickles *et al*., 2016; Phillips *et al*., 2015].

In case of atovaquone resistant parasites, many different mutations have been mapped to the *Pfcytb* gene, it is not readily clear how these mutations affect the overall functioning of the mtETC. Since pyrimidine metabolism is dependent on proper functioning of the mtETC, how *Pfcytb* gene mutations affect this pathway is not clear.

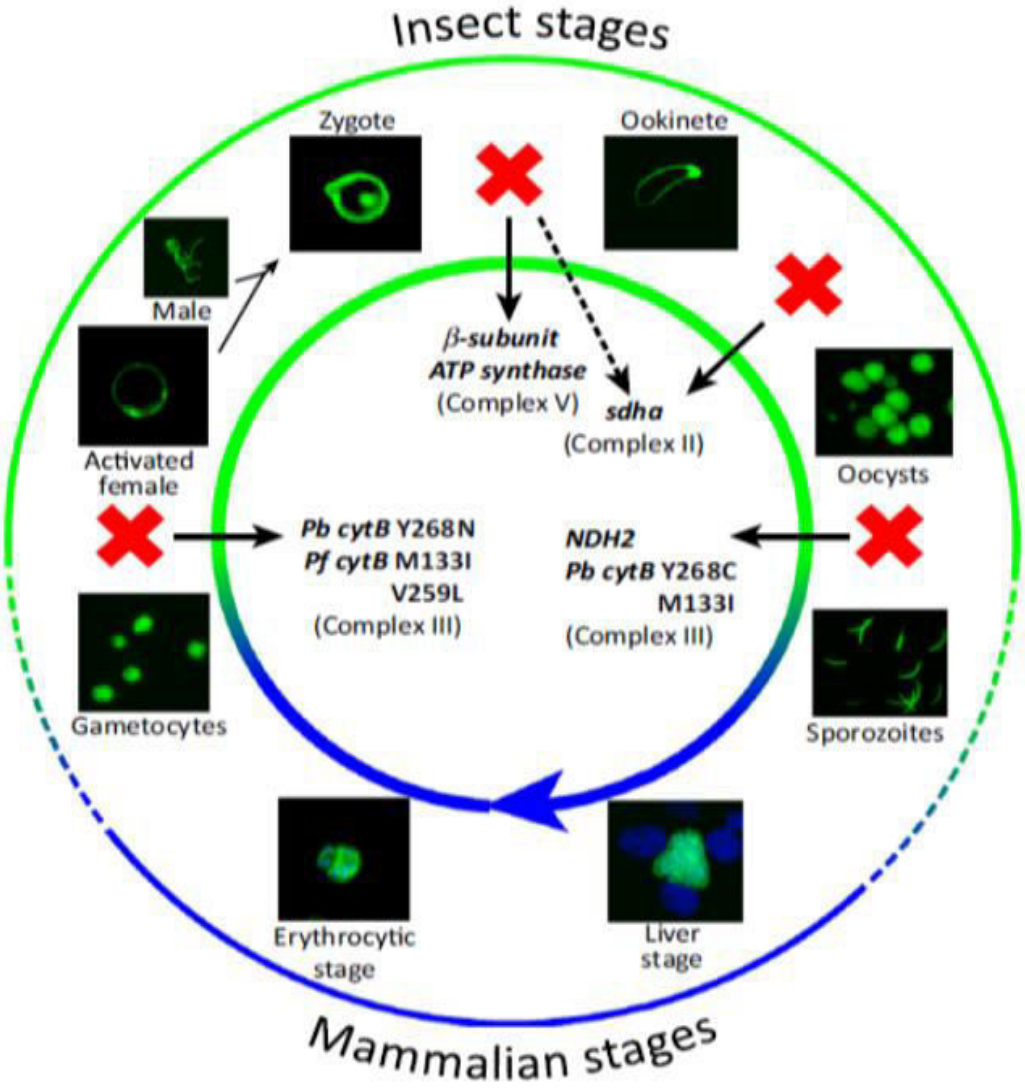

Figure 3.1 Pfcytb mutations affecting life cycle progression in P. falciparum. *The point mutations in cytb Y268N, M133I and V259L hinders gametocyte maturation while the mutations Y268C and M133I affect transformation of oocysts to sporozoites in P. falciparum. Reproduced from Goodman et al., 2017.*

The fact that the mutant parasites are alive and replicating would suggest that the mutations in *Pfcytb* gene conferring atovaquone resistance only reduce the efficiency of mtETC, and do not completely abolish it. Suboptimal functioning of mtETC appears to be sufficient for driving pyrimidine biosynthesis. The asexual and sexual stages of the parasite differ in their ability to survive with mutations in *Pfcytb* gene; while asexual stages can survive with suboptimal mtETC, sexual stages appear to be compromised in

their development in mosquitos [Goodman *et al*., 2016]. It is also probable that the parasites have alternate pathways to maintain their mitochondrial membrane potential [Painter *et al*., 2007]. Thus, it is important to characterize how mtETC and pyrimidine biosynthesis are altered in atovaquone resistant parasites.

In this study we tried to address this long pertaining question of the status of mitochondrial metabolism, pyrimidine biosynthesis in mutant parasites by generating malaria parasite tolerant to atovaquone with novel mutation in *Pfcytb* gene. We comprehensively studied the status of mitochondrial metabolism, pyrimidine metabolism in the mutant in comparison to wild type parasites. We also screened class of atovaquone and naphthoquinone anlogs with good efficacy and conserved target, hitting *Pfcytb*. We found the analogs to be equally potent in *Pfcytb* mutant parasites in comparison to wild type parasites. We also looked in detail the effect of novel mutation on the function of *Cytb* and atovaquone binding using homologous modelling studies.

3.2 Methodology

3.2.1 Parasite culturing and synchronization

Asexual blood stage 3D7 strain *P. falciparum* was maintained in continuous culture using modified protocol [Trager and Jensen. 2005; Radfar *et a*l., 2009]. In brief, the parasites were cultured using complete malaria culture media (CMCM) composed of RPMI1640 supplemented with 5% albumax-II, 2 mM glutamax, 734 µM hypoxanthine, 12.5 mM HEPES and 20 ml 7.5% sodium bicarbonate L-1 (Invitrogen). The hematocrit was maintained at ~2.5% by feeding the cultures with fresh and washed human RBCs when required, and parasitemia was allowed to reach a maximum of 10%, at which point the culture was split. Early rings or late trophozoite and schizont stage parasites were

obtained using 5% sorbitol synchronization or 70% percoll enrichment methods, respectively [Trager and Jensen. 2005; Radfar *et a*l., 2009].

3.2.2 Antimalarial screening and EC_{50} estimation

To test the potency of atovaquone analogs, a modified SYBR Green dye based DNA quantification assay was performed [Smilkstein *et al*., 2004; Bennett *et al*., 2004]. We incubated 3D7 wild type parasites in optimal growth conditions with molecules at fixed concentration of 10 µM in triplicate in 96 well format for 60 hrs for primary screening. In these assays, ~2.5% haematocrit and ~2% parasitemia was maintained in CMCM. Atovaquone or chloroquine (at 1 µM each) were used as positive controls and 1% DMSO as negative control for growth inhibition. After 60 hrs of incubation, culture plates were stained with 25 µl of 0.5% Triton-X100 with 10X SYBR Green-I dye (Invitrogen) in 1X phosphate buffered saline (PBS), pH 7.4 and incubated for 15 minutes before taking reading on Promega GloMax fluorescence plate reader. The obtained data were analysed in Microsoft excel spreadsheet and percentage growth inhibition was calculate for each molecule. The potent inhibitors from the primary screen were taken for EC50 estimation using the same protocol from 10 µM to 0.001 µM concentration and dose response was calculated in Microsoft Excel Spread sheet.

3.2.3 Extraction of metabolites from *P. falciparum*

To capture the perturbed metabolites pool from inhibitor treated parasites, mass spectrometry based metabolomics was performed using modified protocol from Allman et al [Allman *et al*., 2016]. In brief, *P. falciparum* wild type or atovaquone resistant trophozoite stage parasites were percoll enriched (>90% enrichment) and incubated in CMCM for 1 h before starting the inhibitor treatment. Five replicates of 10^8 parasites

each for control and inhibitor treatment were setup. Atovaquone was used at 100 nM and the atovaquone like molecules (Lawson analogs) were used at 1 µM concentration, and incubation was carried out for 4 h in optimal growth condition. After the incubation parasites were pelleted by centrifugation at 5000 rpm for 1 min, followed by a quick wash with 500 µl ice cold PBS to quench metabolism and immediately extracted with 200 µl of chilled 90% Methanol in water. The solvent was spiked with PIPES for technical normalization. The samples were mixed by vortexing briefly in extraction buffer and incubated in ice for 5 minutes. Then the samples were sonicated for 15 minutes in ice chilled water bath sonicator at 50 Hz and centrifuged at 14,000 rpm for 5 minutes. The extraction solvent containing metabolites were gently collected in glass vials. The insoluble pellets were extracted twice with 100 µl of extraction buffer by vortexing and sonicated for 5 minutes, to effect complete extraction of the metabolites. The collected metabolites was stored in -80°C deep refrigerator till further analysis.

3.2.4 LC-MS based metabolic profiling and Data analysis

The mass profile data from inhibitor treated or untreated parasites extract was acquired using UPLC (Accela 1250) coupled to Q-Exactive (Themo Scientific) bench top high resolution mass spectrometer. Reverse phase chromatography with Thermo accucore C18 column (150 mm X 2.1 mm, 2.6 µ particle size) was utilized for metabolite separation. Biphasic separation was performed using 0.1% Formic acid buffered water as solvent "A" and acetonitrile as solvent "B" with gradient starting from 10 % solvent B which was ramped up to 15% by 3rd min, 20%, at 6th, 50% at 10th, 60% at 12th, 90% at 13th minute and hold there till 15th minutes which was ramped down to 10% solvent B at 15.5 minutes and hold there till 20th minutes. The flow rate was maintained at 200 µL/minutes. The mass data was acquired in negative ionization mode from 85-1000 mass

to charge (m/z) scan range. The mass spectrometers instrumentation was kept similar to published protocol used by Melamund et al [Lu *et al*., 2010; Melamund *et al*., 2010].

The mass profile data output form the mass spectrometer was converted from .RAW format to universal .mzXML format using the Proteowizard program default parameters [Chambers *et al*., 2012]. These files from different treatments and replicates were further analysed using freely available MAVEN software for mass peak alignment, peak picking and data output for further statistical analysis at default parameters and mass error window of 10 ppm. The quality of mass peaks detected from extracted ion chromatogram was ascertained by the quality of peak, retention time and m/z matched to available pure commercial standards compounds. The metabolites from each replicate were grouped at chromatographic retention window of 0.5 minutes and mass error window of 10 ppm with minimum intensity count of 5000. The mass intensity matrix for each metabolite was exported to Microsoft Excel spread sheet for further statistical analysis. The overall replicate data quality was checked using Pearson correlation and any replicated with less than 0.90 score was omitted from further analysis. Each metabolites intensity from inhibitor treated sample verses control was compared, fold difference was calculated and the variation was statistically validated with student t-test.

3.2.5 Generation of atovaquone tolerant *P. falciparum*

A chemogenomics approach was used in order to validate the possible mode of action of the atovaquone analogs. For this atovaquone resistant parasites were generated. *In vitro* resistant selection was performed as per previously described protocol [Kato *et al*., 2016]. In brief approximately 1×10^8 *P. faclciparum* (3D7) parasites were subjected to atovaquone drug pressure at 10 nM (10X EC_{50}) for 4 days until no live parasites were

detectable by microscopy. The drug was then washed off and the parasites were allow to recover in complete RPMI medium. Once parasitemia reached to 3-5%, two rounds of intermittent drug pressure at 10X EC_{50} were given, followed by three rounds of increased drug pressure at 100X EC_{50}) [Fig 3.2]. Development of drug resistance was confirmed by measuring EC_{50} value by SYBR Green method as described earlier. Drug resistant parasites were then cloned out by limiting dilution method. The genomic DNA from resistant parasite was extracted using QIAmp DNA Blood Mini Kit (Qiagen, USA), and the *Pfcytb* gene was amplified by PCR using the primers shown in Table 3.1, using the conditions previously reported by Fisher *et al*., 2012. The amplified *Pfcytb* gene was cloned into the pGMT-Easy vector (Promega) for identifying the mutation by sequencing.

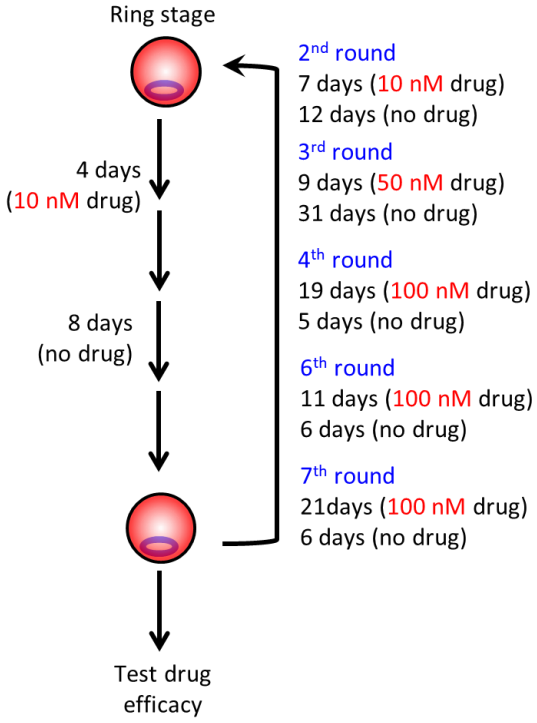

Figure 3.2 Schematic work flow to generate atovaquone tolerant P. falciparum. *The figure depicts the pulsed treatment of P. falciparum cultures with increasing atovaquone pressure for 7 rounds. After each round the sensitivity of the parasites to atovaquone was tested. Atovaquone pulsing was stopped after 7 rounds when the resistance appeared to be stable.*

PfCytb Forward	ATGAACTTTTACTCTATTAATTTAG
PfCytb Reverse	TATGTTTGCTTGGGAGCTGTAATC

Table 3.1 Primers used to PCR amplify P. falciparum Cytb gene. The primers are shown in 5' to 3' orientation.

3.2.6 Effects of atovaquone and analogs on atovaquone resistant parasites

P. falciparum parasites tolerant to atovaquone were cloned out and tested for their susceptibility to chloroquine, atovaquone and atovaquone analogs. The dose dependent killing assay was performed and the EC_{50} concentration was estimated as explained in section 3.2.

3.2.7 Characterization of mtETC function

Multiple clonal lines of atovaquone tolerant *P. falciparum* were isolated and their mutations in *Pfcytb* gene was mapped by sequencing. One of the resistant lines $Pfcytb^{mut4}$, which had a mutation in the heme binding site and had one of the best resistance profile was selected for further studies on mtETC and pyrimidine biosynthesis. These studies were conducted in the presence or absence of atovaquone and one of the best analogs called Lawso-16.

3.2.7.1 Mitochondrial membrane potential studies using JC1 dye

The JC-1 dye is frequently used to monitor the mitochondrial membrane potential [Reers *et al*., 1995; Perry *et al*., 2011]. The dye selectively aggregates into viable cells with intact mitochondrial membrane potential and gives sharp red colour fluorescence while the monomer has diffused green colour fluorescence. We treated the wild type and

*Pf*cytb^{mut4} parasites with 100 nM atovaquone or 1 µM Lawson-16 for 6 and 12 h respectively, and then stained with 1 µM JC-1 dye for 30 minutes in dark [Pasini *et al*., 2013]. The JC-I stained parasites were then visualized by live cell microscopy to monitor the mitochondrion associated red fluorescence.

3.2.7.2 Total Cellular ATP estimation

To monitor the biochemical functionality of the parasite mitochondrion, total cellular ATP was quantified. This was done in cultures where glucose was the only nutrient source and in cultures were glucose and glutamine were present and nutrients. Each of the cultures also had control and inhibitor treatments. Total cellular ATP was measured using Promega ATP monitoring kit, using manufacturer's standard protocol. In brief, 10^8 parasitized RBCs were saponine lysed, and intact parasites were recovered and incubated with inhibitors for 30 min or 1 h, lysed with 50 µl assay lysis buffer and incubated for 10 minutes. After incubation, 100 µl ATP monitoring reagent (Luciferin and Luciferase enzyme mix) was added and the resulting luminescence emitted was measured using a Thermo Vario Skan plate reader. All experiments were performed in 5 replicates.

3.2.7.3 Pyrimidine biosynthesis in resistant parasites

Mass spectrometry based metabolomics was performed to understand the functional status of pyrimidine biosynthesis in *Pfcytb*^{mut4} parasites in comparison to wild type parasites treated with 100 nM atovaquone or 1 µM Lawson16. Both these inhibitors collapses the parasite mitochondrial membrane potential thus affect pyrimidine biosynthesis. This indeed was the case in wild type parasites. To study pyrimidine biosynthesis in *Pf*cytb^{mut4} parasites, which are tolerant to atovaquone, we incubated percoll enriched 10^8 parasites with 100 nM atovaquone or 1 µM Lawson-16, and after 4 h

these parasites were processed for LC-MS analysis. Metabolite extracts were prepared from five replicates for each condition, and pyrimidine biosynthesis intermediate dihydroorotate and end product UMP were measured.

3.3 Result

3.3.1 Lawson and NDS series of atovaquone analogs are potent anti-malarial compounds with mode of action similar to that of atovaquone

We screened many naphtoquinone derivatives from the Lawson series and other synthetic atovaquone analogs synthesised in-house at CSIR-NCL. In primary screening, at fixed concentration of 10 µM, we found six Lawson analogs (Lawson-15, 16, 17, 18, 20 and 21), which completely inhibited the growth of *P. falciparum* wild type parasites in a standard SYBR Green based killing assay. Similarly, we also tested several NDS atovaquone analogs (NCL in-house molecules) and identified 14 molecules showing >80% growth inhibition on wild type parasites [Fig 3.3]. We further took these primary hits for evaluating their antimalarial potency and estimating their EC_{50} values. Three molecules, Lawson-16, Lawson-17 and Lawson-21 showed nanomolar efficacy, while Lawson-20 had its EC_{50} value around 1.4 µM [Fig 3.4]. None of the NDS molecules exhibited antimalarial potency at low micromolar or nanomolar range.

It is important to study whether the mode of action of the selected atovaquone analogs is similar to that of atovaquone. The target for atovaquone binding is the *P. falciparum* mitochondrial electron transport chain complex III protein cytochrome b. Inhibition of *Pfcytb* by atovaquone is known to collapse the inner mitochondrial membrane potential thus ultimately inhibiting pyrimidine biosynthesis due to a block in the Q-cycle of mtETC [Srivastava *et al*., 1997; (b)Srivastava *et al*., 1997 Hunte *et al*., 2008].

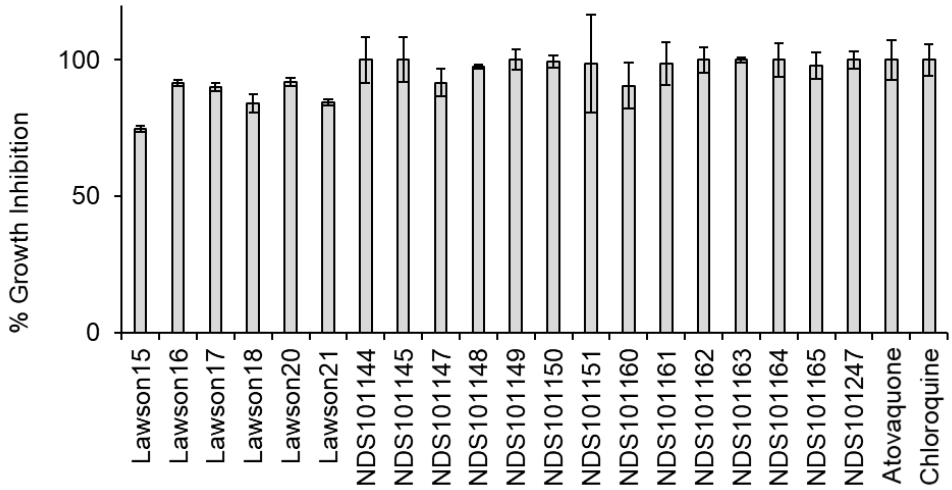

Figure 3.3 Growth inhibition values for hits identified from primary growth inhibition assay using atovaquone and its analogs. *5 Lawson and 14 NDS group of molecules were observed to possess >90 growth inhibitory effect on P. falciparum in growth inhibition assay. Standard anti-malarial drugs, chloroquine and atovaquone were used as positive controls for parasite growth inhibition and 1% DMSO was used as negative control. Number of replicates n = 3.*

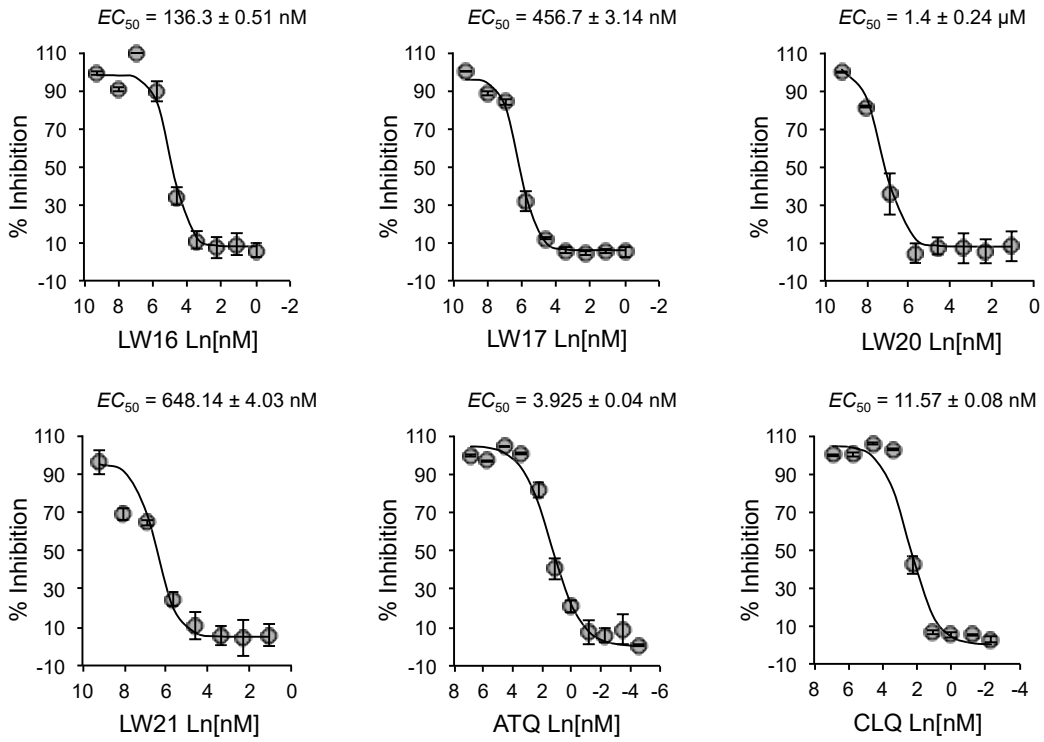

Figure 3.4 Estimating antimalarial potency of atovaquone and its selected analogs . *Results are plotted for four of the best analogs of atovaquone exhibiting micromolar and sub-micromolar potency. LW16,*

Lawson 16; LW17, Lawson 17; LW20, Lowson 20; LW21, Lawson 21. Along with atovaquone (ATQ) the standard anti-malarial drug chloroquine (CLQ) was used as positive control for parasite growth inhibition and 1% DMSO as negative control. Number of replicates n = 2. The EC_{50} values determined for the respective compounds is shown above the plots.

This in turn causes the accumulation of the intermediate metabolite dihydroorotate and depletion of the end product uracil monophosphate (UMP) levels in the parasite. These changes in metabolite levels can be captured with accuracy using mass spectrometry [Fig 3.5]. We used the same approach as previously described [Cobbold *et al*., 2016; Allman *et al*., 2017] to monitor this signature perturbation in pyrimidine biosynthesis intermediates due to atovaquone treatment of *P. falciparum* and compared it to the effect of three of the best analogs, Lawson 16, 17 and 21. We observed more than thousand fold accumulation of dihydroorotate and many fold depletion of UMP when treated with atovaquone and its Lawson analogs in comparison to untreated control *P. falciparum* blood stage parasites [Fig 3.6]. This observation confirmed that the analogs are acting on the same target as that of atovaquone, which is the *Pf*CYTb protein present in parasite mitochondrion.

3.3.2 Generating and characterizing atovaquone resistant *P. falciparum* mutants

We generated *P. falciparum* mutant strains in the laboratory, which were resistant to atovaquone. The protocol used for this is given in methods section. Briefly, after pulse exposure of *P. falciparum* to atovaquone at 10 nM and at 100 nM concentration for multiple cycles, mutant parasites were obtained, which were tolerant to atovaquone in high micromolar concentration, in contrast to wild type parasites which have an EC_{50} of 3.925 ± 0.04 nM [Fig 3.4]. We isolated two clonal lines of the resistant parasites by serial dilution method and these were used in further experiments.

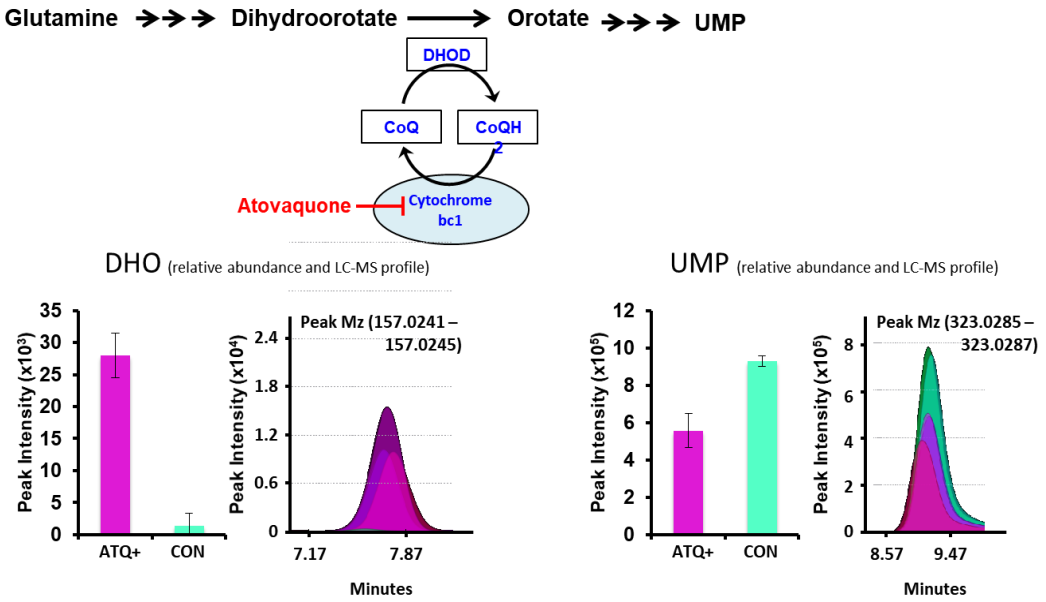

Figure 3.5 Studying the metabolic effect of atovaquone by mass spectrometry. *The top panel shows the metabolic coupling between mtETC and pyrimidine biosynthesis in P. falciparum and the site of atovaquone action. The bottom panel shows the LC-MS data depicting the change in metabolite profile in atovaquone treated parasites with respect to untreated control. Number of replicates n = 3.*

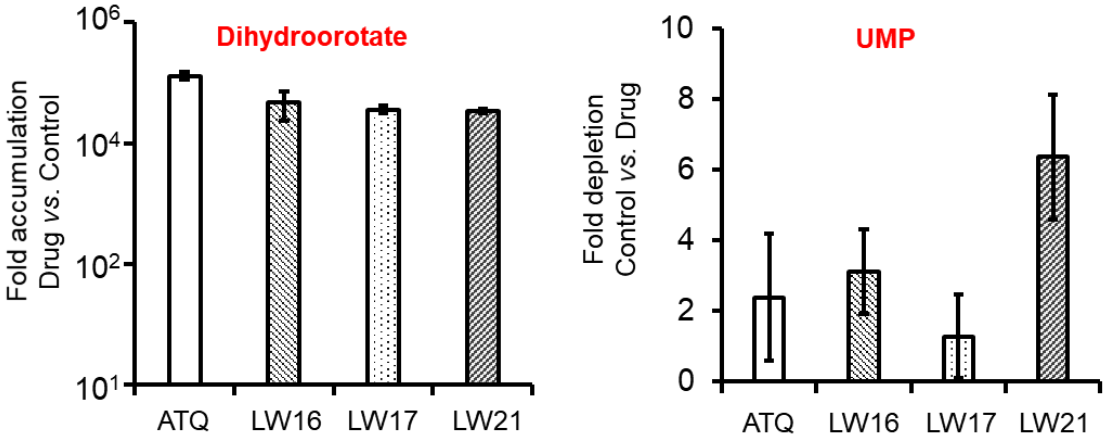

Figure 3.6 LC-MS based mode of action studies for atoaquone and its analogs. *LC-MS data depicting the change in metabolite profile in atovaquone, Lawson-16 (LW16), Lawson-17 (LW17) and Lawson-21 (LW21) treated parasites with respect to untreated control. Accumulation of dihydroorotate and depletion of UMP levels with respect to untreated control confirms that the analogs have a similar mode of action as that of atovaquone. Number of replicates n = 3.*

We first carried out a comparative study of the antimalarial efficacy of the atovaquone resistant mutant isolates using the Lawson analogs of atovaquone. We also tested chloroquine to see if the resistance was specific to atovaquone. The *Pfcytb*^{mut2} mutant line showed high levels of resistance to atovaquone (EC_{50} = 3.4 ± 1.01 µM) [Fig 3.7]. This represents at least a 1000 fold increased tolerance of the drug by the mutants.Expectedly, the *Pfcytb*^{mut2} mutant showed increased tolerance to the atovaquone analogs as well and the respective EC_{50} values are shown on top of the plots in Fig 3.7. Similarly, the *Pfcytb*^{mut4} mutant line also showed high levels of resistance to atovaquone (EC_{50} = 2.4 ± 0.28 µM) [Fig 3.8]. Interestingly, eventhough once again increased tolerance was seen with this mutant for the various atovaquone analogs, Lawson-16 appeared to retain its antimalarial activity with nano molar potency. The respective EC_{50} values for the molecules tested are shown on top of the plots in Fig 3.8. We also found that both the mutant parasite lines retained their sensitivity to chloroquine [Fig 3.7 & 3.8], and this confirmed that the resistance developed was very specific to the atovaquone and its analogs to varying degrees and was not broad spectrum in nature.

3.3.3 Mapping the mutations in *Pfcytb* gene from the two atovaquone resistance clonal isolates of *P. falciparum*.

Prior studies have shown that atovaquone resistance in *P. falciparum* is acquired mainly by mutating the *Pfctyb* gene, which tends to affect the binding of the drug to *Pf*CYTb protein, which is the target for this inhibitor. *Pfctyb* gene is encoded in the mitochondrial genome of the parasite and is a highly conserved gene, across the apicomplexan phylum [Srivastava *et al*., 1997; (b) Srivastava *et al*., 1997 Hunte *et al*., 2008]. In clinical isolates from the field and in *in vitro* developed drug resistant strains, it

has been found that the parasite frequently mutates the region close to the site at which atovaquone is known to bind to CYTb, i.e., the atovaquone binding pocket. The binding motif is flanked by transmembrane helices C, D and F and surface helices cd1 and ef, which harbor the catalytic motif PEWY [Birth *et al*, 2014]. Mutations in this region appear to prevent the binding of atovaquone to its target and thus helping the parasite to escape from the deleterious effect of drug [Akhoon *et al*., 2014; Hunte et al., 2008; Birth *et al*., 2014].

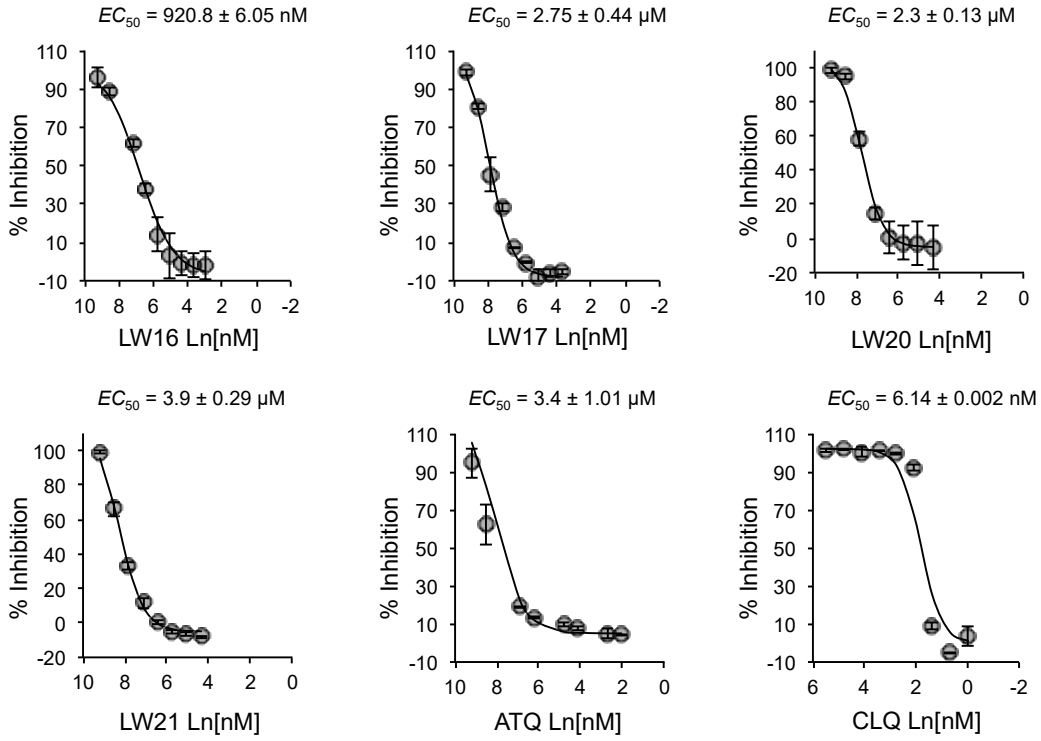

Figure 3.7 Testing the antimalarial efficacy of atovaquone and its analogs on the Pfcytb^{mut2} mutant strain. *Each plot shows the % inhibition observed against a dilution series of the respective molecules. Molecule name abbreviations are the same as in Fig 3.4. Results from representative experiment plotted. Number of replicates n = 2. The EC_{50} values determined for the respective compounds is shown above the plots.*

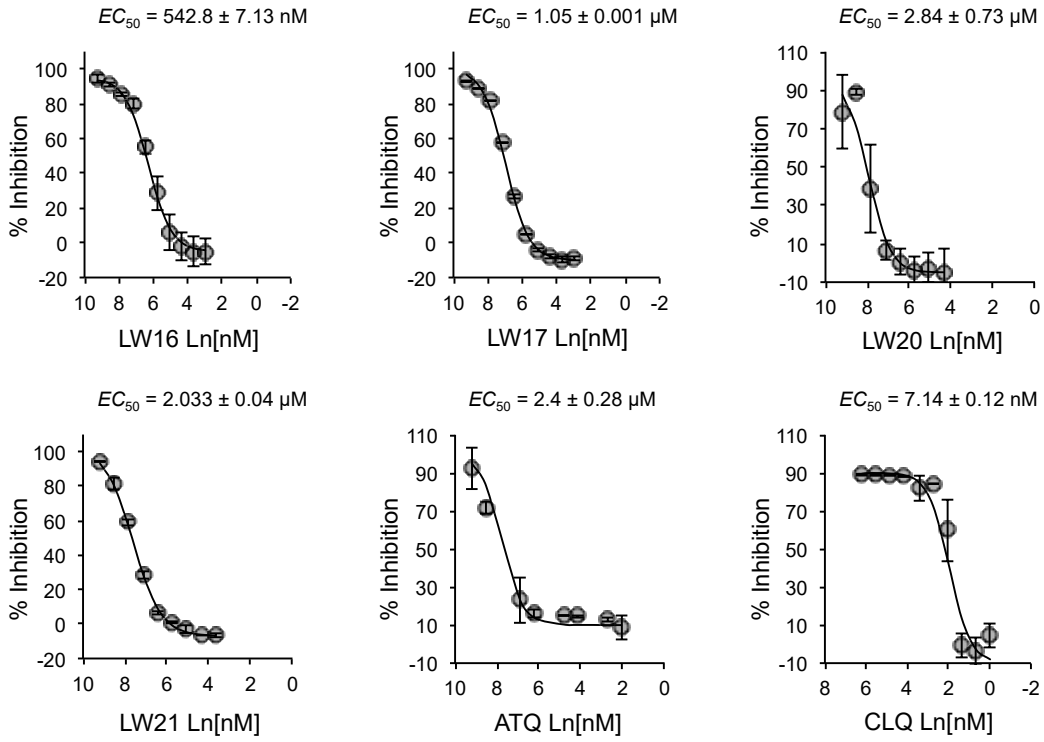

Figure 3.8 Testing the antimalarial efficacy of atovaquone and its analogs on the Pfcytb^{mut4} mutant strain. *Details of the experiment and data representation is the same as in Fig 3.7. Results from representative experiment plotted. Number of replicates n = 2. The EC_{50} values determined for the respective compounds is shown above the plots.*

We proceeded to confirm whether the tolerance exhibited for atovaquone and its analogs by the two mutant isolates *Pfcytb^{mut2}* and *Pfcytb^{mut4}* is due to mutations in *Pfcytb* gene. For this, we PCR amplified and sequenced the full length gene from wild type and the two resistant strains. Upon analysis we observed the both *Pfcytb^{mut2}* and *Pfcytb^{mut4}* strains had novel mutations is *Pfcytb* gene. The mutation were present in highly conserved regions; L31R in *Pfcytb^{mut2}* and in P177L *Pfcytb^{mut4}*. The *Pfcytb^{mut4}* mutant strain was of particular interest to us since it exhibited the highest tolerance and the P177L mutation mapped to the heam binding BL domain of the protein [Fig 3.9]. These findings confirmed that the two parasite starins had acquired aovaquone resistance by

mutating the *Pfcytb* gene. Interestingly, the mutations found in these two strains are novel, and different from previously reported and frequently observed Y268S or I133M mutations associated with atovaquone resistance in *P. falciparum* [Birth *et al*., 2014; Goodman *et al*., 2017]. It is also interesting that the methodology we have used to generate atovaquone resistant parasites has triggered the formation of more than one type of mutation in the *Pfcytb* gene. It is likely that the original mutant population used for the clonal isolation of the two resistant strains, could have other types of mutations as well in the *Pfcytb* gene.

Figure 3.9 ***Sequence alignment of Pfcytb gene from wild type and Pfcytb mutants.*** *Pfcytb gene was PCR amplified and sequenced. Sequence alignments with reference sequence was done to identify the mutations responsible for resistance in atovaquone tolerant Pfcytb^{mut2} and pfcytb^{mut4} clonal isolates.*

3.3.4 The atovaquone resistant parasite *Pfctyb*^{mut4} possesses a functional pyrimidine biosynthesis pathway in asexual blood stages

The various mutations in *Pfcytb*, previously reported from atovaquone resistant parasites were found to impose fitness defect on the parasite. The efficiency with which the mtETC operates in atovaquone tolerant parasites is reported to be nearly 10 times less in Y268S mutant in comparison to wild type parasites [Fisher *et al*., 2012]. While this appears not to be a problem for the growth of blood stage *P. falciparum*, mutant parasites are compromised in their ability to complete the sexual development in the mosquito host [Goodman *et al*., 2016]. Studies on the resistant parasites link the essentiality of mtETC for pyrimidine biosynthesis, as the parasites are dependent on *de novo* synthesis of pyrimidine and are unable to scavenge from the mosquito host [Painter et al., 2007]. In asexual blood stages, the parasites are not affected by the decreased efficiency of mtETC probably due to minimal activity of the pathway [Goodman *et a*l., 2016; Goodman *et al*., 2017]. It is also reported that the deleterious effect of the non-functional *Pfcytb* can be overcome by ectopically expressing yeast dihydroorotate dehydrogenase, which is not dependent on mtETC [Painter et al., 2007].

We reasoned that the *Pfcytb* mutations in the *Pfcytb*^{mut4} mutant isolated in this study, may not totally inhibit mtETC but make it inefficient. To understand the status of pyrimidine biosynthesis in *Pfcytb*^{mut4} parasites, we analyzed pyrimidine biosynthesis by measuring the relative abundance of UMP and dihydroorotate in the mutant parasites treated with either atovaquone (100 nM) or Lawson-16 (1 µM) for 4 h. To our surprise, the pyrimidine biosynthesis pathway was unaffected in mutant parasites and we did not observe any accumulation of dihydroorotate or depletion of UMP levels [Fig 3.10]. This finding indicates that either the mutation has minimal effect on the function of mETC complex III

or the minimal activity of the mtETC, due to the mutation in *Pfcytb* gene, is sufficient to support pyrimidine biosynthesis in the parasite. In addition, we also observed that although Lawson-16 had retained significant antimalarial activity against the *Pfcytb*^{mut4} mutant, it did not appear to significant affect pyrimidine biosynthesis in the mutant. This observation hints that the *Pfcytb* mutation has affected efficient binding of both atovaquone and Lawson-16 molecule to the *Pf*CYT protein. It is also likely that the short duration of inhibitor treatment used in this study (4 h) is in sufficient for the lower affinity binding of Lawson-16 molecule to mutant *Pf*CYT protein to exhibit its metabolic effect, in similar manner to that seen in wild type parasites. Therefore, we become interested in assessing the integrity of mtETC in *Pfcytb*^{mut4} parasites.

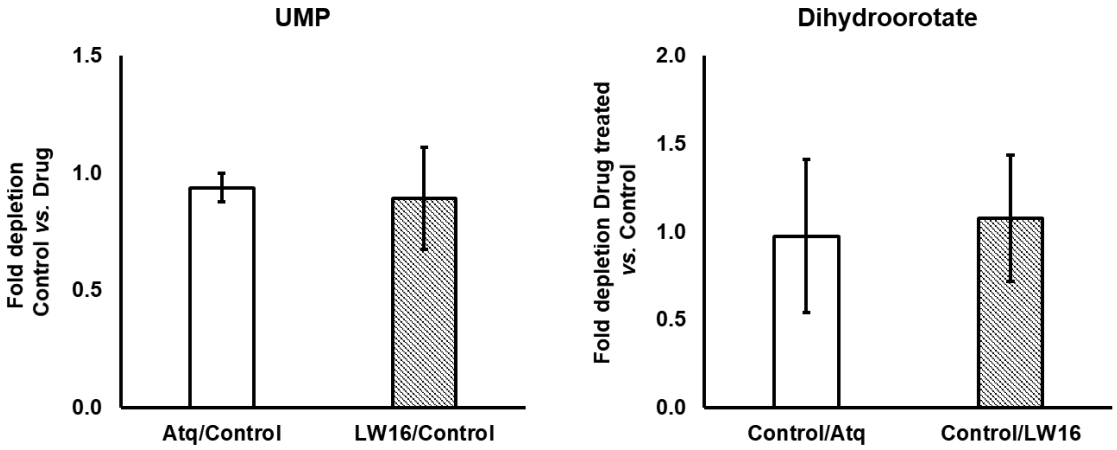

Figure 3.10 Status of Pyrimidine biosynthesis in Pfcytb^{mut4} mutant parasites. *LC-MS data to show the status of functional pyrimidine biosynthetic pathway in atovaquone tolerant parasite clone Pfcytb^{mut4}. There is no accumulation of dihydroorotate and depletion of UMP levels with respect to untreated control in 4 hours of treatment with either 100 nM atovaquone or 1 µM LW16. This confirms that the Pfcytb gene mutation has not affected the ability of the mtETC to facilitate pyrimidine biosynthesis in the mutant parasites.*

3.3.5 *Pfcytb*^{mut4} parasites maintain mitochondrial membrane potential in presence of atovaquone but are sensitive to Lawson-16 analog

Pyrimidine biosynthesis and many other important cellular functions are dependent on the maintenance of mitochondrial membrane potential. To understand the effect of *Pfcytb* gene mutation on maintenance of mitochondrial membrane potential, we used the fluorescent probe JC-1 [Pasini *et al*., 2013]. The dye is specific to mitochondrial membrane potential and aggregates in live parasites with intact mitochondrial membrane potential to give intense red fluorescence, but in dead cells with loss of membrane potential, the dye is present in monomeric form as gives a diffused green fluorescence. Wild type *P. falciparum* showed red fluorescent staining in the mitochondrion with the JC-1 dye, which was abolished in the presence of the atovaquone and Lawson-16 inhibitors [Fig 3.11]. We observed that the mutant *Pfcytb*^{mut4} parasites were also maintaining mitochondrial membrane potential, as evident from JC-1 staining and this was not abolished by 100 nM atovaquone. However, the mutant parasites were sensitive to 1 µM Lawson-16 treatment and lost the mitochondrion associated red fluorescence due to JC-1 accumulation [Fig 3.11].

3.3.6 Assessing mitochondrial ATP in *Pfcytb*^{mut4} parasites

We measured total cellular ATP synthesis in saponine lysed intact parasites treated with atovaquone or Lawson-16 in both wild type and *Pfcytb*^{mut4} parasites, in the presence of glucose only or in the presence of glucose and glutamine as nutrient source. Wild type parasites showed ~40% reduction in total cellular ATP in presence of atovaquone, in comparison to untreated parasites, in both nutrient conditions [Fig 3.12]. In contrast, mutant parasites are less effected by atovaquone treatment; especially when glutamine is available as a nutrient they show only ~20% decreased cellular ATP compared to

untreated parasites. This indicates that the mitochondrial ATP synthesis, which is driven by glutamine in apicomplexan parasites, is affected less by atovaquone in the mutant parasites.

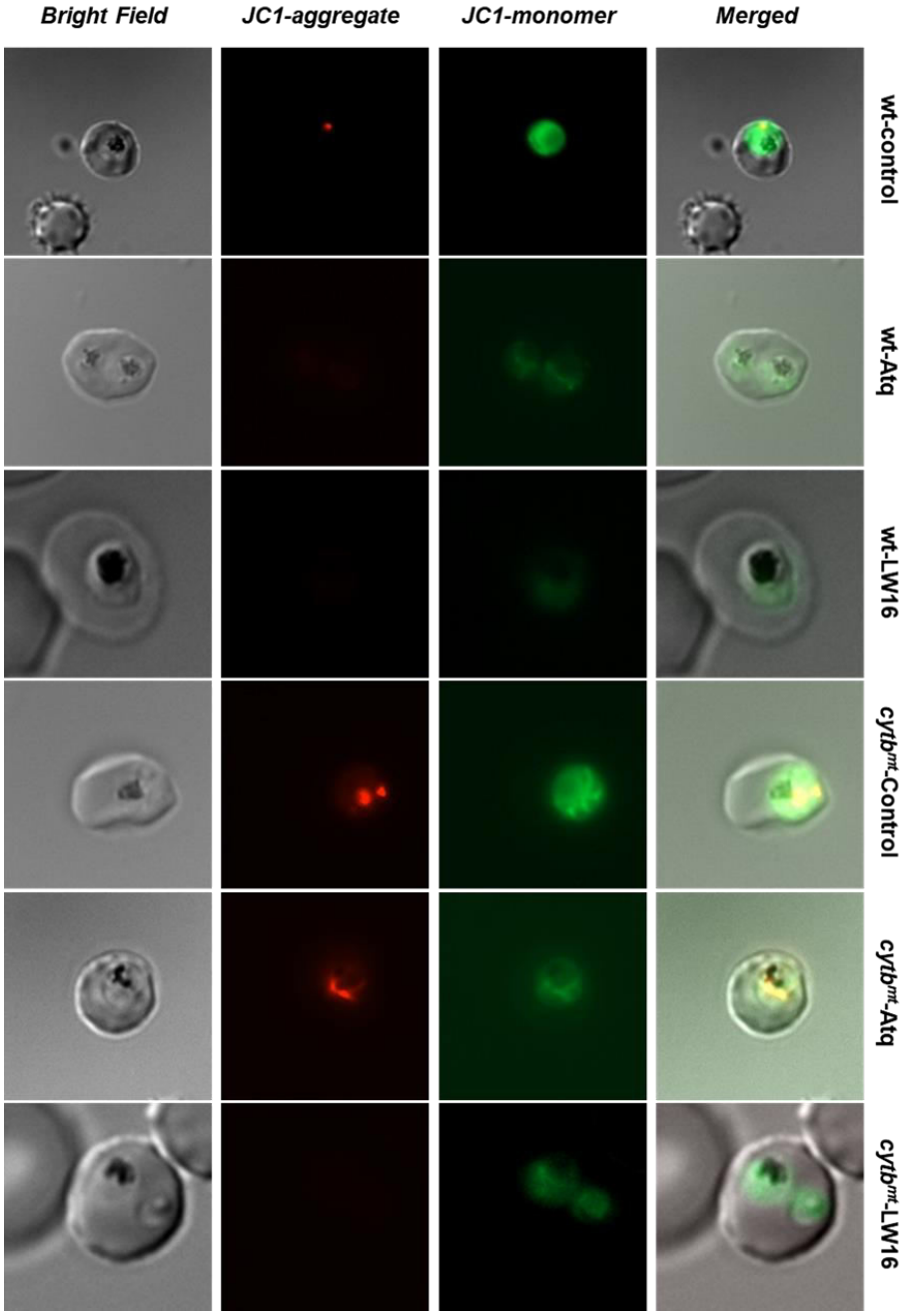

Figure 3.10 P. falciparum mitochondrial membrane potential staining by JC-1 dye. *Aggregation of red fluorescent JC-1 dye indicates intact mitochondrial membrane potential. Control, no drug treatment; Atq, 100 nM Atovaquone; LW16, 1 µM Lawson-16, wt, wild type atovaquone sensitive parasites; cytb^{mt}, atovaquone tolerant clone Pfcytb^{mut4}. Pictures shows the decreased mitochondrial membrane potential in*

wild type parasites in the presence of atovaquone. The atovaquone resistant parasites have retained their mitochondrial membrane potential and atovaquone treatment does not affect it. However, both wild type and mutant parasites are susceptible to Lawson-16 molecule.

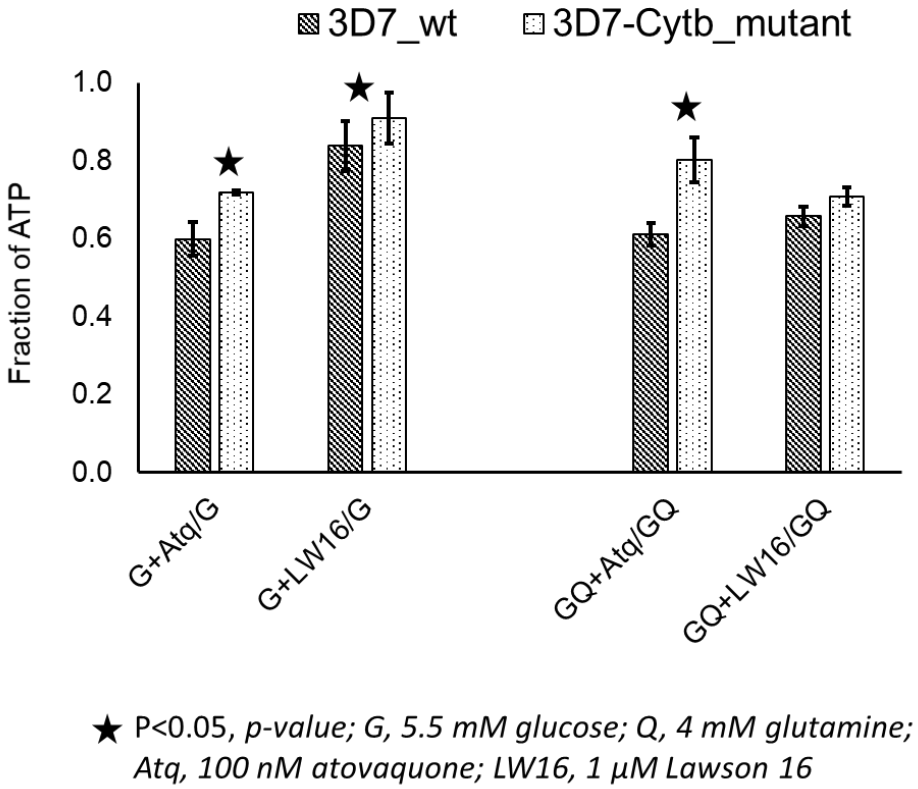

Figure 3.12 ATP quantification in wild type and atovaquone resistant parasites. *Total cellular ATP was quantified in intact parasite isolated by saponin treatment of infected RBCs. The fraction of total luminescence emitted (proxy for ATP quantity) from Pfcytb^{mut4} in the presence of glucose only or glucose supplemented with glutamine as nutrient source is depicted. Atovaquone (100 nM) and Lawson-16 (1 µM) were used to test their effects on ATP synthesis in wild type and mutant parasites. Parasites prepared by saponine treatment of infected RBCs were incubated with drug for 1 hour. Number of replicates n=5. The stars indicate P-value of <0.05 showing the significance of the difference seen between drug treated vs. untreated samples.*

Overall the ability of Lawson-16 inhibitor to affect total cellular ATP levels was minimal in both wild type and *Pfcytb^{mut4}* parasites, when glucose metabolism was the

only source of ATP. But glutamine was also available, Lawson-16 was able to inhibit ATP synthesis more robustly in both wild type and *Pfcytb*^{mut4} parasites. These results once again confirm that the mutation in *Pfcytb* gene is specific towards atovaquone binding and inhibtion of mtETC. Thus, although the atovaquone analog Lawson-16 appears to act *via* targeting *Pf*CYTb protein, its binding site maybe different from that of atovaquone and hence is able to affect mitochondrial membrane potential and kill the parasite with similar efficacy, in both wild type and *Pfcytb*^{mut4} parasites. Thus, our study emphasizes the usefulness of developing novel naphthoquinone class of antimalarial compounds that can be used in combination with atovaquone

3.4 Conclusion

The emergence of drug resistance in *P. falciparum* is big threat at the global level and concern has been raised that this might lead to increase in malaria related mortality and morbidity. It is the need of the time to identify drugs with higher specificity, with improved pharmacology and efficiency. The process of drug development is lengthy, costly and consumes lot of resources. Any drug whose target is known provides scope to use medicinal chemistry to develop new molecules with better efficacy. Thus target based drug discovery is an advantage and at the same time it can help us better understand the underlying biological function and its essentiality in parasite life cycle. Atovaquone, once regarded as an excellent multistage active and was proposed to be used as a frontline antimalarial drug lost its usefulness due to the emergence of clinical resistance rapidly. However, recent findings have shown that atovaquone resistance imposes a fitness defect on the parasite rendering them defective in their ability to complete the sexual cycle in mosquito. The target for atovaquone, mitochondrial genome coded “Cyt b”, a mitochondrial electron transport chain complex III component, whose function is

important for maintenance of membrane potential across in mitochondrial membrane and recycling for ubiquinone. The mitochondrial Q-cycle in *P. falciparum* is important for the biosynthesis of pyrimidine as the enzyme dihydroorotate dehydrogenase (DHOD) needs oxidised ubiquinone (Q) as an electron receptor (converts to reduced QH_2) to oxidise DHO to orotate.

Pyrimidine biosynthesis is essential for the survival of parasites as they are auxotrophic for pyrimidines and loss of DHOD functions blocks this pathway. It was unclear, how the atovaquone resistant *Pfcytb* mutant parasites manages to drive the biosynthesis of pyrimidine in asexual erythrocyte stages of the life cycle? Whether the mutated Cytb are still maintaining residual activity, and hence maintaining the Q-cycle necessary for pyrimidine biosynthesis has not been explored in detail. To address some of these unanswered questions we generated atovaquone resistant malaria parasites, which were capable of tolerating µM levels of the drug. We isolated two clonal lines from the resistant population and found the atovaquone resistance can be mapped to two novel mutations in the mitochondrial gene *Pfcytb*. Upon analysis we found that the resistance developed was specific for the atovaquone and its analogs only. The mutant parasites were equally susceptible as wildtype parasites to the antimalarila drug chloroquine.

In the mutant parasites, the mitochondrial membrane potential was found to be intact even upon atovaquone treatment, as indicated by the active accumulation of the JC-1 dye in the parasite mitochondrion. The red fluorescence associated with the mitochondrion due to accumulation of the JC-1 dye in mutant parasites indirectly proves that the mutant parasites are capable of maintaining their proton gradient and mutation in Cytb has minimal effect on the mtETC of the parasite. Interestingly, this finding was further supported by the finding that pyrimidine biosynthesis was unaffected in $Pfcytb^{mut4}$ upon incubation with atovaquone in contrast to wild type parasites which are killed due to

blocked pyrimidine biosynthesis. These findings point towards the notion that the *Pfcytb* gene mutation in the *Pfcytb*^{mut4} line (P177L) specifically imparts atovaquone resistance without affecting essential functions associated with the mtETC.

This conclusion was further supported by studies on ATP synthesis by the parasite, where the wild type parasites showed upto ~40 % loss in total cellular ATP when incubated with atovaquone drug for one hour. In comparison, mutant parasites were less affected. Overall, these studies prove that the mutation in *Pfcytb* gene generated in this study specifically conferred resistance to atovaquone while preserving mitochondrial memebrane potential and pyrimidine biosynthesis. It is likely that this may be the case for the other *Pycytb* gene mutations which have been reported previously to confer atovaquone resistance. While these mutations seem to allow the parasite to survive in asexual intraerythrocyte stages, albeit with a less efficient mtETC, the essentiality of this metabolic function becomes apparent during the sexual development in the mosquito host.

We further tested various analogs of atovaquone for their ability to inhibit growth of blood stage *P. falciparum*. We identified five analogs from the Lawson series (LW16, LW17, LW18, LW20 and LW21) and one other in-house molecule (NDS1001249) which were active against wild type parasites. We shortlisted few of the Lawson molecules for further studies based on their low micromolar to nanomolar potency. Metabolomics studies captured the signature accumulation of DHO and depletion of UMP levels in the parasite when treated with Lawson-16, -17 and -21 molecules. Similar profiles are seen with atovaquone, thus confirming that the target for these novel molecules is *Pf*CYTb protein. We tested these analogs against the two atovaquone resistant strains of *P. falciparum* and found that the mutant parasites have gained resistance to the analogs as well. We also made the interesting observation that the Lawson-16 analogs retained its

efficacy for killing the *Pfcytb*^{mut4} mutant parasites. This was confirmed by the finding that Lawson-16, the most potent atovaquone analog, was able to collapse the mitochondrial membrane potential, as indicated by the lack of red fluorescence in the parasite mitochondrion in the presence of the JC-1 dye, in both wild type and *Pfcytb*^{mut4} mutant parasites. Thus, our findings provide evidence that novel atovaquone analogs, based on the napthoquinone scaffold, can be developed as potent antimalarial compounds, and these can be used as partner drugs in combination therapy with atovaquone. Such a treatment strategy may help in mitigating the chance of parasite developing resistance. Our studies also once again validate the importance of mtETC and pyrimidine biosynthesis as antimalarial drug targets.

3.5 References

(a)Srivastava, IK. et al. (1999). Resistance mutations reveal the atovaquone-binding domain of cytochrome b in malaria parasites. Mol. Microbiol. 33, 704–711.

(b)Srivastava, IK. & Vaidya, AB. (1999). A mechanism for the synergistic antimalarial action of atovaquone and proguanil. Antimicrob. Agents Chemother. 43, 1334–1339.

Akhoon BA. *et al*. (2014). Understanding the Mechanism of Atovaquone Drug Resistance in Plasmodium falciparum Cytochrome b Mutation Y268S Using Computational Methods; PLoS ONE 9(10): e110041.

Allman EL. *et al.* (2016). Metabolomic profiling of the Malaria Box reveals antimalarial target pathways. Antimicrob Agents Chemother 60:6635– 6649.

Baldwin J. *et al*. (2005). High-throughput screening for potent and selective inhibitors of Plasmodium falciparum dihydroorotate dehydrogenase. J Biol Chem. 280(23):21847–53.

Barton, V. *et al*. (2010). Inhibiting Plasmodium cytochrome bc1: a complex issue. Curr. Opin. Chem. Biol. 14, 440–446.

Bennett TN. *et al*. (2004). Novel, rapid, and inexpensive cell-based quantification of antimalarial drug efficacy. Antimicrob Agents Chemother 48:1807-10.

Birth D., Kao WC., Hunte C (2014). Structural analysis of atovaquone-inhibited cytochrome bc1 complex reveals the molecular basis of antimalarial drug action; Nature Communications, 5, 4029.

Chambers MC. *et al*. (2012). A cross-platform toolkit for mass spectrometry and proteomics. Nat Biotechnol. 30(10):918-20.

Chiodini PL. et al. (1995). Evaluation of atovaquone in the treatment of patients with uncomplicated Plasmodium falciparum malaria. J Antimicrob Chemother. 36(6):1073–8.

Cobbold SA. *et al*. (2016). Metabolic Dysregulation Induced in Plasmodium falciparum by Dihydroartemisinin and Other Front-Line Antimalarial Drugs; The journal of Infectious Diseases, 213:276-286.

Fisher N. *et al*. (2012). Cytochrome b Mutation Y268S Conferring Atovaquone Resistance Parasite bc1 Catalytic Turnover and Protein Expression; JBC, 287:(13); 9731-9741.

Fry, M. & Pudney, M. (1992). Site of action of the antimalarial hydroxynaphthoquinone, 2-[trans-4-(40-chlorophenyl) cyclohexyl]-3-hydroxy- 1,4-naphthoquinone (566C80). Biochem. Pharmacol. 43, 1545–1553.

Gamo FJ. *et al*. (2010). Thousands of chemical starting points for antimalarial lead identification. Nature 465:305–310.

Goodman CD., Buchanan HD., McFadden GI (2017). Is the Mitochondrion a Good Malaria Drug Target? Trends in Parasitology, 33 (3), 185-193.

Goodman, C.D. et al. (2016). Parasites resistant to the antimalarial atovaquone fail to transmit by mosquitoes. Science 352, 349–353.

Guiguemde WA. *et al*. (2010). Chemical genetics of Plasmodium falciparum. Nature 465:311–315.

Gutteridge WE, Dave D, Richards WH. (1979). Conversion of dihydroorotate to orotate in parasitic protozoa. Biochim Biophys Acta. 582(3):390–401.

Hudson, AT. *et al*. (1993) Atovaquone - a novel broad-spectrum anti-infective drug. Parasitol. Today 9, 66–68.

Hunte, C., Solmaz, S., Palsdottir, H. & Wenz, T. (2008). A structural perspective on mechanism and function of the cytochrome bc1 complex. Results Probl. Cell. Differ. 45, 253–278.

Kato N. *et al*. (2016). Diversity-oriented synthesis yields novel multistage antimalarial inhibitors; Nature 538, 344-349.

Looareesuwan S. *et al*. (1996). Clinical studies of atovaquone, alone or in combination with other antimalarial drugs, for treatment of acute uncomplicated malaria in Thailand. Am J Trop Med Hyg. 54(1):62–6.

Lu W. et al. (2010). Metabolomic analysis via reversed-phase ion-pairing liquid chromatography coupled to a stand alone orbitrap mass spectrometer. Anal Chem. 82(8):3212-21.

Lubell, Y. *et al*. (2014). Artemisinin resistance--modelling the potential human and economic costs. Malar. J. 13, 452.

Melamud E, Vastag L, Rabinowitz JD. (2010). Metabolomic analysis and visualization engine for LC-MS data. Anal Chem. 1;82(23):9818-26.

Painter, HJ. *et al*. (2007). Specific role of mitochondrial electron transport in blood-stage Plasmodium falciparum. Nature 446, 88–91.

Pasini EM., Ierssel D., Vial HJ., Kocken C HM (2013). A novel live-dead staining methodology to study malaria parasite viability; Malaria Journal, 12:190.

Peters, JM. *et al*. (2002). Mutations in cytochrome b resulting in atovaquone resistance are associated with loss of fitness in Plasmodium falciparum. Antimicrob. Agents Chemother. 46, 2435–2441.

Perry SW. *et al*. (2011). Mitochondrial membrane potential probes and the proton gradient: a practical usage guide. Biotechniques; 50(2):98-115.

Phillips, MA. *et al*. (2015). A long-duration dihydroorotate dehydrogenase inhibitor (DSM265) for prevention and treatment of malaria. Sci. Transl. Med. 7, 296ra111.

Plouffe D. et al. (2008). In silico activity profiling reveals the mechanism of action of antimalarials discovered in a high-throughput screen. Proc Natl Acad Sci U S A 105:9059–9064.

Reers M. *et al*. (1995). Mitochondrial membrane potential monitored by JC-1 dye. Methods Enzymol; 260:406-17.

Smilkstein M. *et al*. (2004). Simple and inexpensive fluorescence-based technique for high-throughput antimalarial drug screening. Antimicrob Agents Chemother 48:1803-6.

Srivastava, IK., Rottenberg, H. & Vaidya, AB. (1997). Atovaquone, a broad spectrum antiparasitic drug, collapses mitochondrial membrane potential in a malarialparasite. J. Biol. Chem. 272, 3961–3966.

Stickles, A.M. *et al*. (2016). Atovaquone and ELQ-300 combination therapy: A novel dual-site cytochrome bc1 inhibition strategy for malaria. Antimicrob. Agents Chemother. 22;60(8):4853-9.

Syafruddin D., Siregar JE., Marzuki S. (1999). Mutations in the cytochrome b gene of Plasmodium berghei conferring resistance to atovaquone. Mol Biochem Parasitol; 30;104(2):185-94.

World Health Organization. Fact Sheet: World Malaria Report 2016 (WHO, 2016). available at http://www.who.int/malaria/media/world-malaria-report-2016/en/.

Chapter 4

Untargeted LC-MS metabolomics studies to understand drug mechanism of action in Plasmodium falciparum

4.1 Introduction: Untargeted metabolomics to study drug mode of action

In the past decade, there has been great interest in ramping up drug discovery efforts against malaria and other protozoan parasites, partly due to the fact that parasites have been gaining resistance against various drugs in clinical use. There have been efforts to identify small molecules with specificity and potency against parasite using large scale phenotypic screenings. The results have been very encouraging and hundreds of drug like small molecules with nano molar or sub-micromolar efficacy have been identified [Gamo *et al*., 2010; Duffy and Avery et al., 2012; Spangenberg *et al*., 2013; Paiardini et al., 2015; Von Voorhis *et al*., 2016]. These molecules belong to diverse chemical classes, with many novel drug scaffolds. One such example is collection of antimalarial molecules called Malaria Box, which was assembled by Medicines for Malaria Venture (MMV), Geneva, through collaboration between academic laboratories and pharmaceutical companies [Gamo *et al*., 2010; Spangenberg *et al*., 2013; Paiardini et al., 2015; Von Voorhis *et al*., 2016]. Although the Malaria Box collection includes many potent antimalarial compounds, their mode of action still remains unknown. For a realistic chance of these molecules becoming next generation antimalarial drugs, it is of foremost importance to completely understand the mode of action of these molecules and identify their targets. This will also help in addressing the specificity and selectivity of these molecules. Knowing the target for these molecules will also help in improving their drug-like and pharmacological properties by medicinal chemistry.

For some MMV Malaria Box molecules, mode of action studies have been carried out for targets involved in isoprenoid biosynthesis, peptide degradation, protein translation, thioredoxin systems, pyrimidine biosynthesis, folate biosynthesis pathways [Bowman *et al*., 2014; Paiardini *et al*., 2015; Tiwari *et al*., 2016; Wu *et al*., 2015; Ahyong *et al*., 2016]. The identity of these target was known from pre-existing knowledge target

inhibitor interaction, while some where discovered by way of making resistant mutants. However, this approach is time consuming, difficult and is carried out for one inhibitor/target pair at a time. Despite the technical difficulties, generating resistant mutants is a good way to study mode of action for antimalarial compounds and this has been have been successfully achieved for different class of molecules such as decoquinates, spiroindolone, KAF156, DDD107498 and most recently for a set of MMV malaria box molecules [Cowell AN. *et al*.,2018; Rottmann *et al*., 2010; Nam *et al*., 2011; McNamara *et al*., 2013; Spillman *et al*., 2013; Kuhen *et al*., 2014; Baragaña *et al*., 2015; Flannery *et al*., 2015]. Typically, the approach involves sequencing the whole genome of the resistant mutants to map the mutations responsible for resistance.

Thus, the above described studies implemented either genomics, drug resistant line generation or classical biochemical approaches to elucidate mode of action of the molecules under study. However, alternative methods which are unbiased, untargeted and greatly enhance the coverage on the number of molecules that can be studied have been tested, and one such approach involves studies on metabolic perturbations using mass spectrometry. Using untargeted metabolomics approach, one can capture cellular metabolism by detecting and carrying out relative quantification of thousands of small molecules. This approach has been used to classify many antiprotozoal compounds according to their mode of action in unbiased and rapid manner [Gao *et al*., 2007; Scalbert *et al*., 2009; Creek et al., 2012; Halouska *et al*., 2012; Dun *et al*., 2012; Beyoğlu and Idle., 2013]. Similarly, untargeted metabolomics has been implemented on a large scale to classify >100 MMV Malaria BOX antimalarial molecules based on their signature metabolic profiles in two separate studies [Allman et al., 2016; Creek *et al*., 2016]. Put together, these studies have established the usefulness of mass spectrometry

based metabolomics in elucidating the mode of action of novel antimalarial compounds and identifying their likely metabolic target.

We have implemented this powerful technique to interrogate the metabolic effects of two novel and powerful antimalarial compounds. These two compounds are cladosporine and halofuginone, which are known to inhibit parasite protein synthesis by targeting lysyl and prolyl tRNA synthetases, respectively. Along with these compounds, we used two standard antimalarial drugs chloroquine and pyrimethamine, for comparing and contrasting the respective metabolic profiles. The main goal of this work is to generate, signature metabolic profiles for these compounds, which can be used as a benchmark for comparing the mode of action of parent compounds with structural analog molecules, as part of antimalarial hit to lead development activities. A brief introduction to the antimalarial inhibitors used in this study is discussed below.

Chloroquine: This drug belongs to the chemical class of 4-aminoquinolines, discovered by Hans Andersag in 1934, and has been included on the list of essential Medicines by the WHO [List of essential medicine list 2017, WHO]. It has been widely used for the treatment of malaria until early 1960s, when resistance to this drug was first reported. Although, WHO doesn't recommend chloroquine alone as a frontline antimalarial treatment anymore, it is still a very effect antimalarial drug, especially for vivax malaria [List of essential medicine list 2017, WHO]. It interferes with the biocrystalization of heam (released by the proteolytic digestion of haemoglobin), thus preventing the detoxification of heam and production of hemozoin pigment in the parasites food vacuole [Hempelmann *et al*., 2007; Combrinck *et al*., 2013]. *P. falciprum* resistance to chloroquine is facilitated by mutation in *Pf*CRT and *Pf*MDR1 genes [Lehane *et al*., 2008; Petersen *et al*., 2011; Sidhu *et al*., 2006; Venkatesan et al., 2014].

Pyrimethamine: The drug is widely used to treat toxoplasmosis and uncomplicated malaria in combination with sulphadaizine [Blasco *et al*., 2017]. Pyrimethamine was discovered by Nobel Prize winning scientist Gertrude Elion in 1952 and was made available for medical use since 1953 [Vasudevan *et al*., 2013]. This folic acid antagonist inhibits folate biosynthesis by targeting the enzyme dihydrofolate dehydrogenase (DHFR), inhibiting the regeneration of tetrahydrofolic acid from dihydrofolate [Osborne *et al*., 2001]. This regeneration is important for the synthesis of DNA and RNA in many organisms including in *P. falciparum* and *T. gondii* [Gregson *et al*., 2005]. Monotherapy with pyrimethamine was stopped after reports of mutation in DHFR gene and development of rapid resistance against the drug in the field [Kateera *et al*., 2016].

Halofuginone: It is a derivative of the quinazolinone-type alkaloid febrifugine, which is naturally found in the Chinees herb *Dichora febrifuga* [Ryley *et al*., 1973]. Halofuginone shows less cytotoxicity and is currently in use to treat veterinary pathogens like *Eimeria* and *Cryptosporidium* [Ryley *et al*., 1975; Linder *et al*., 2007; Jain *et al*., 2015]. Other uses for halofuginone have also been reported; for example, it was found to be effective in treatment of scleroderma, cancer, and fibrotic diseases [Elkin *et al*., 1999; Halevy *et al*., 1996; McGaha *et al*., 2002; Pines *et al*., 1998; Pines *et al*., 2003]. Mechanistically, halofuginone has been shown to target the enzyme prolyl-tRNA synthetase (PRS), from humans, [Keller *et al*., 2012; Son *et al*., 2013], and from the malaria parasite, for which it appears to have higher affinity and specificity [Kikuchi *et al*., 2006; Jain *et al*., 2014; Jain *et al*., 2015].

Cladosporine: Protein biosynthesis is multi-step and complex process involving many enzymes and many antiparasitic agents target this process. Many antimalarials, including tetracycline and doxycycline, block protein synthesis by interfering with the binding of aminoacyl-tRNA to 30s ribosome. Isoleucyl-tRNA synthetase targeting mupirocin is used to cure methicilline-resistant *Staphylococcus aureus* infection [Istvan *et al*., 2011; Caswell *et al*., 1987]. In the same note, the fungal secondary metabolite cladosporin isolated from *Aspergillus flavus* and *Cladosporium cladosporiodes* was identified to target lysyl-tRNA synthetase (LysRS) [Scott *et al*., 1971; Kimura *et al*., 2012]. Similar to halofuginone, it also found to be active against diverse class of pathogens and has shown insecticidal, antifungal, antibacterial, plant growth inhibitor as well as mouse anti-inflammatory activities [Kimura *et al*., 2012; Springer *et al*., 1981; Anke et al., 1979; Miller *et al*., 2010]. Cladosporin became an interesting candidate drug molecule because of its efficacy against both liver and blood stage of malarial parasites. Reverse genetic approaches identified the target for this compound as Lysyl-tRNA synthetase (KRS1) enzyme from *P. falciparum*, with >100 fold specificity towards *Pf*KRS in comparison to the human counterpart [Plouffe *et al*., 2008; Hoepfner *et al*., 2012; Sharma *et al*., 2014].

Though both halofuginone and cladosporin have been shown to primary target PRS and KRS enzymes, in both humans and *P. falciparum* parasites, respectively, its wide ranging bioactivity against other pathogenic and non-pathogenic species indicates that it these drugs may be operating by hitting other secondary targets as well. Thus, we carried out this study to identify drug induced changes in metabolite profiles, and to find out if this can be useful in identifying alternate mode of action for these molecules. For this work, we used untargeted metabolomics as the method of choice to capture the metabolic effects of these inhibitors on blood stage *P. falciparum* parasites.

4.2 Methodology

4.2.1 *P. falciparum* culture

Refer to chapter 3 section 3.2.1

4.2.2 Experimental setup with drugs and extraction of metabolites

To capture the alterations in metabolite levels in inhibitor treated parasites, mass spectrometry based metabolomics was performed using a modified protocol [Olszewski *et al*., 2013]. In brief, wild type *P. falciparum* trophozoite stage parasites were percoll enriched (>90% enrichment) and incubated with CMCM for 1 h before starting the inhibitor treatment. 1 X 10^8 parasites for used for each drug, and incubations were done in 5 replicates. Parasites were treated with 100 nM each for chloroquine, cladosporine, halofuginone or 1 µM of pyrimethamine for 4 hours, in standard growth condition. After the incubation parasites were pelleted by centrifugation at 5000 rpm for 1 min, followed by a quick wash with 500 µl ice cold PBS to quench the metabolism, and metabolite extraction was initiated by the addition of 200 µl ice chilled 90% methanol in water. The extraction buffer was spiked with PIPES for technical normalization. Samples were vortexed briefly after addition of extraction buffer before incubating in ice for 5 minutes. Then, samples were further sonicated for 15 minutes in ice chilled sonicator water bath at 50 Hz and centrifuged at 14,000 rpm for 5 minutes. The extracted metabolites were carefully collected into glass vials. The pellet were again extracted with 100 µl of extraction buffer, by vortexing and sonicating the samples for 5 minutes. The extract was recovered as before and pooled with the earlier one. The process was repeated twice for complete extraction of the metabolites. The collected metabolites was stored in -80°C refrigerator till analysis by LC-MS.

4.2.3 Acquisition of MS profile and data analysis

Refer to chapter 3 section 3.2.3

4.2.4 Statistical analysis

In order to obtain a global picture of the metabolome and to find the metabolites whose levels have been altered due to drug treatment, the following analysis was performed and overall data distribution, clustering and important features, untargeted multivariate data analysis was performed. The raw data was analysed using the MAVEN software and metabolite data was exported out in excel spread sheet format. The raw peak intensity values were $\log_2$ transformed and used for various global analysis. We first analysed the correlation between the five replicate datasets for control and inhibitor treated samples. Then, pairwise difference in the average log2 values, with a Student's T-test significance values of ≤ 0.001, was used to identify the metabolites showing inhibitor specific variation in abundance.

The tabulated mass features with respective intensities obtained from MAVEN analysis were also processed with online statistical analysis platform Metaboanalyst as per published protocol [http://www.metaboanalyst.ca/; Xia *et al*., 2016]. In brief, data was normalized using "Sum" method and scaled on "Pareto" scaling for normal distribution of the metabolites and further statistical analysis. Hierarchical clustering was performed to group the drug treatment according to their class and based on metabolic response. A multivariate data analysis algorithm, called as Sparse-Orthogonal-Partial Least Square-Discriminate Analysis (sOPLS-DA), was used to identify important mass features responsible for grouping and segregating all replicate samples. This analysis helped to identify the features (i.e., m/z values in this case) based on which the samples can be

grouped into either 'drug-treated like' or 'control 'groups. Further in-depth analysis was performed to identify mass features specific to each of inhibitor treatments.

4.3 Results

4.3.1 Number of metabolites detected, data quality and sample correlation studies

Based on the scan range set during data acquisition by the mass spectrometer, we obtained a mass distribution between 100 Da to 1000 Da. A total of 9697 mass features (metabolites) were detected across all samples and a distribution of these metabolites, by binning them on their m/z values, showed that 50% of the metabolites detected were < 290 Da and 75% of the metabolites were < 413 Da [Fig. 4.1]. This suggested that the methods used for metabolite extraction, chromatographic separation and mass spectrometric analysis primarily identified low molecular weight metabolic intermediates.

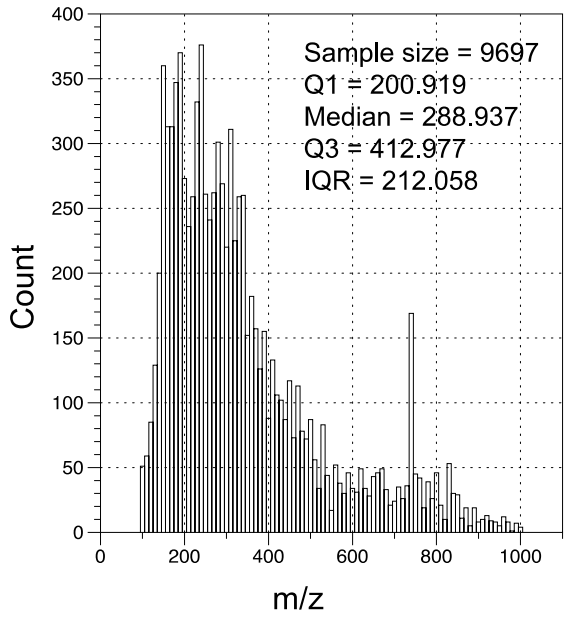

Figure 4.1. ***Distribution of metabolites identified from all samples analysed in this study****. A total of 9697 mass features (metabolites) were identified from each sample. The m/z values corresponding to median, quartile 1 (Q1), quartile 3 (Q3) and the interquartile region (IQR) are shown. m/z denotes the mass by charge ratio of the metabolites. For this and other subsequent analysis, z was assumed to be equal to 1.*

We then ascertained the quality of the data by looking the distribution of the peak intensity values for all mass features from each sample, as shown in [Fig. 4.2]. The results indicate that the dynamic range of the peak intensity distribution is very similar, thus indicating that the data quality is good and the correlation between the different samples is likely to be high. This also pointed to the fact the variation in metabolite abundance between the various samples is likely to be minimal. This is expected, since the design of the experiment was such that, we were interested in detecting only very early metabolic changes associated with inhibitor treatment and accordingly trophozoite stage *P. falciparum* were treated with the different inhibitors for a period of only 4 h.

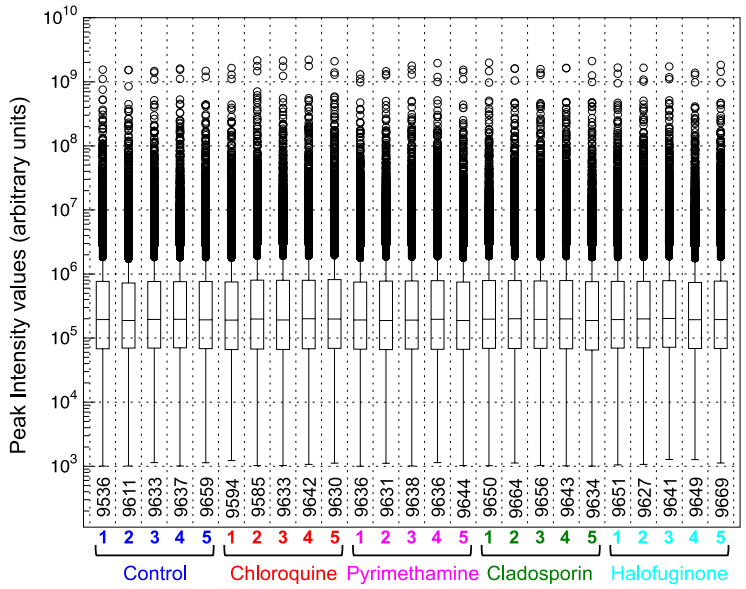

Figure 4.2. ***The dynamic range of the peak intensity values for metabolites.*** *Data for each of the five replicate samples for control and inhibitor treatment is shown. The numbers shown next to the x-axis refer to the number of metabolites for which the data was plotted. The number of metabolites are varying since any metabolite with less than 1000 intensity value was excluded.*

Next, we carried out Pearson correlation analysis to look at the 1:1 correlation between all samples. This is important, since untargeted LC-MS data tends to be noisy and this analysis will give an idea of how similar or dissimilar two samples are. In any global

analysis in biological system (such as metabolomics and transcriptomics), one would expect that only a fraction of the features show statistically significant changes between test conditions; for example, not all genes are expected to have altered expression levels between control and inhibitor treated samples. This assumption can be extended to metabolomics data also. We performed Pearson correlation analysis using the metabolite data obtained from the MAVEN software and obtained high correlation values (>0.9) between replicates of a particular treatment and within a minimum correlation value of >0.8 for all other replicates [Fig. 4.3].

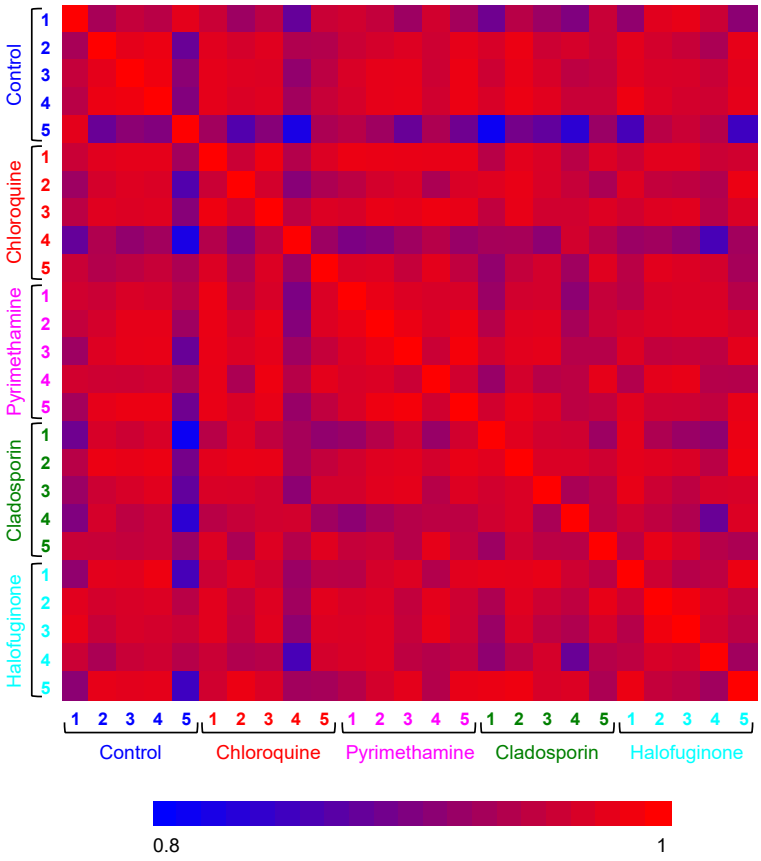

Figure 4.3. ***Pearson correlation for metabolite levels shown as a heatmap between the five replicates sample for control and each drug treatment.*** *The color for the heatmap is shown below the figure.*

We then used the average $\log_2$ transformed values to carry out a 1:1 correlation between control and the four different inhibitor treated samples. In all cases we obtained a linear fit with an R^2 value >0.9, which once again confirmed that only a fraction of the

metabolites are showing difference in their abundance values in response to inhibitor treatment [Fig. 4.4].

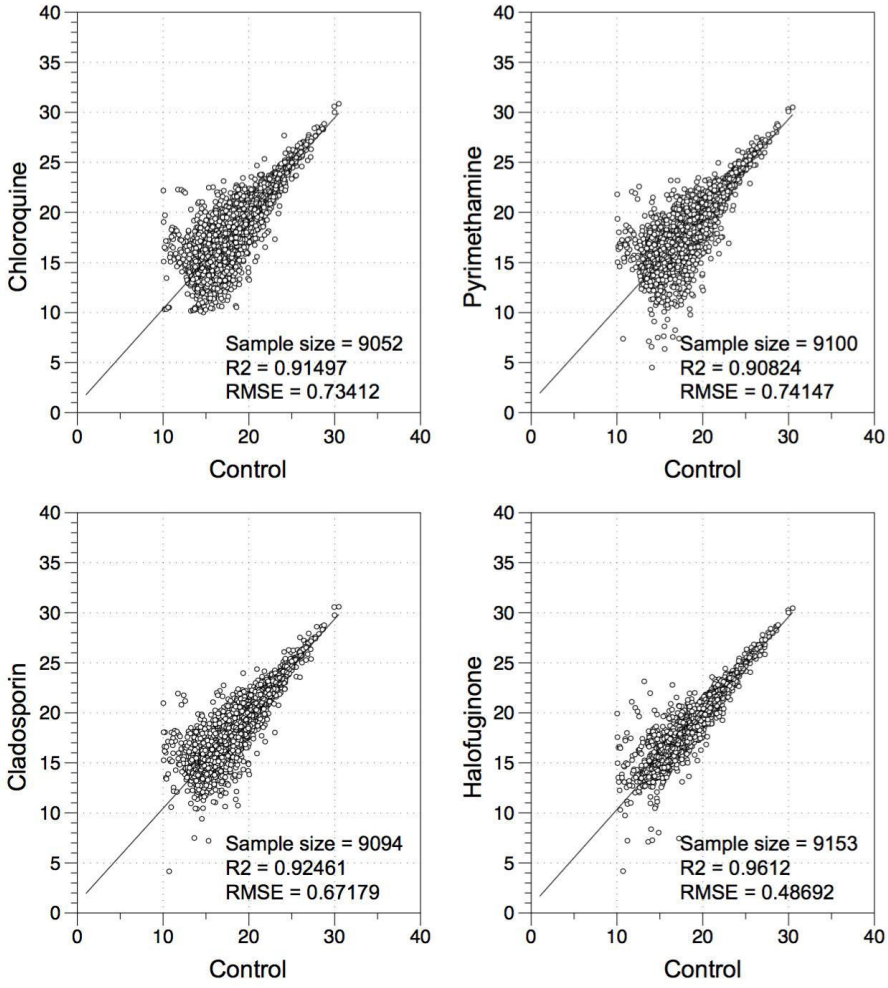

Figure 4.4. ***Comparing the abundance of individual metabolites between control and inhibitor treated samples.*** *The log_2 transformed peak intensity values corresponding to each metabolite was compared between the control and various inhibitor treated samples. A data plots were fitted with a linear equation and the R^2 and root mean square error (RMSE) values are shown. While all 9697 mass features are plotted in each graph and the sample size indicates the number of metabolites minus outliers that were used for deriving the fit. Outliers were excluded using $\sigma = 1.5$.*

4.3.2 Multivariate data analysis

Since untargeted metabolomics data are multidimensional in nature, we used two multivariate data analysis approaches to identify the differences between the control

and inhibitor treated samples. The two approaches which we have used are the hierarchical clustering and Principle component analysis (PCA) methods.

4.3.2.1 Hierarchical clustering of control and drug treated samples

To evaluate global differences in metabolite profile between drug treated and untreated *P. falciparum* blood stage parasites, we performed hierarchical clustering of the sample datasets, based on their relatedness. The clustering showed a clear segregation between control and drug treated samples [Fig. 4.5]. We also observed a clear segregation between different inhibitor treated samples by and large; the metabolic inhibitors, chloroquine and pyrimethamine and the protein synthesis inhibitors cladosporin and halofuginone were grouped separately [Fig. 4.5]. This indicates that, in addition to differences between control and inhibitor treated samples, the metabolite profiles are also good enough to segregate the samples by inhibitor mode of action. We then confirmed this further by performing PCA analysis.

4.3.2.2 PCA analysis of control and drug treated samples

A standard PCA analysis was performed for the control and inhibitor treated samples. The result shown in Fig. 4.6 clear shows that the control and inhibitor treated samples cluster together and are also significantly different from each other. Interestingly, it can be observed from the results that the data coming from treatment of protein synthesis inhibitors halofuginone and cladosporin are more similar to controls when compared to the metabolic inhibitors chloroquine and pyrimethamine. To some extent, this indicates that the metabolic perturbations due to the potent and very fast acting antimalarial compounds chloroquine and pyrimethamine is more pronounced in

comparison to the protein synthesis inhibitors, as the time lag for detectable metabolic effects to take place in this case is expected to be longer.

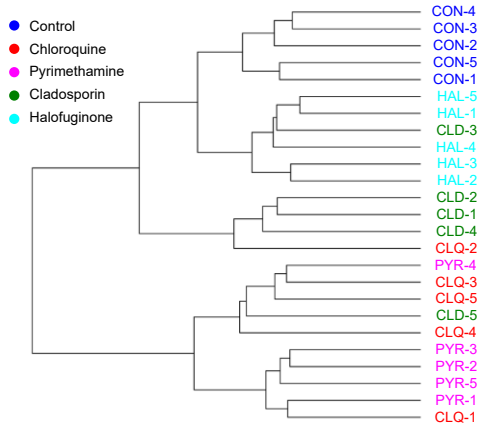

Figure 4.5 Hierarchical clustering of mass profiling data. *The figure illustrate the clustering of mass profiling data obtained from control and inhibitor treated P. falciparum samples***.**

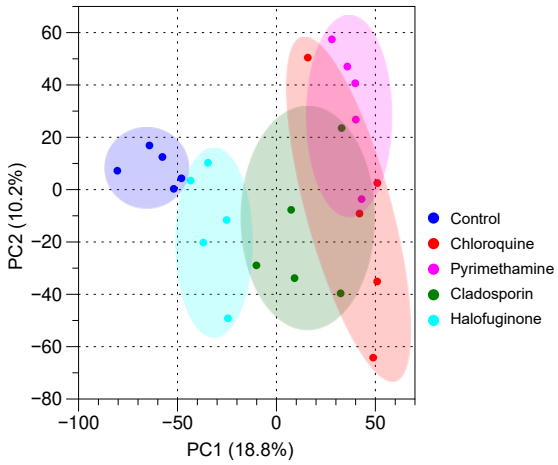

Figure 4.6 Principal component analysis of mass profiling data. PCA analysis was perfomed on all 25 datasets corresponding to 5 replicate datasets for each sample. The PCA analysis was carried out using the statistical tools implemented in Clustvis (https://biit.cs.ut.ee/clustvis/) [Metsalu T. *et al.*, 2015].

4.3.2.3 Identification of variables (mass features) specific to inhibitor treatments

To further identify the specific mass features or metabolites whose abundance was subject to significant changes in correlation with inhibitor treatment of *P. falciparum*

blood stage parasites, we used of the variant of the PCA analysis called as the Spars Partial Least Square-Discriminate Analysis (sPLS-DA). This statistical algorithm is used to identify important mass features from complex untargeted metabolomics data. This analysis once again validated and confirmed our earlier finding that the metabolite profile for replicate datasets was more similar to each other for each treatment type and showed clearly that control and inhibitor profiles are quite distinct [Fig. 4.7]. Moreover, this analysis also once again confirmed that the protein synthesis inhibitors exhibit lesser perturbations in metabolite levels when compared to the metabolic inhibitors over the 4 h period for which trophozoite stage *P. falciparum* were treated with the inhibitors.

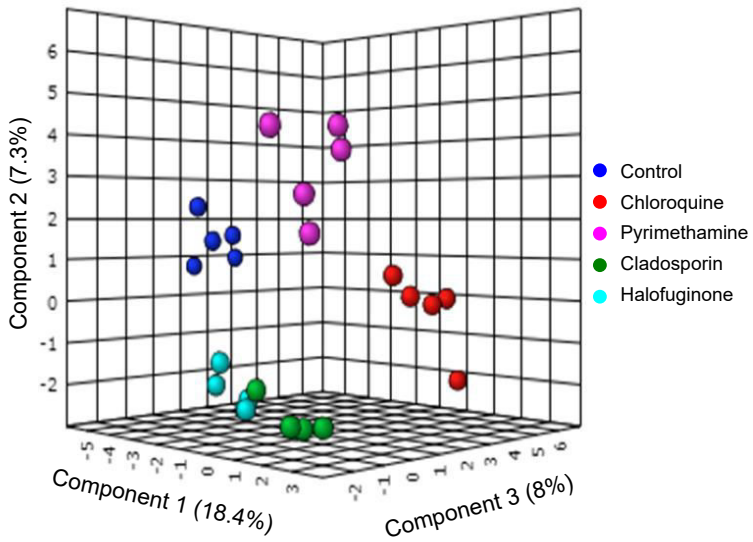

Figure 4.7 sPLS-DA analysis of mass features. *The 3D score plot clearly indicate that replicate datasets from each sample type group together and the replicate set for each sample type are culstered seperately from each other. It can be observed the data from the two samples pertaining to the two protein synthesis inhibitor treatment fall into the same 3D space while the rest occupy a completely different 3D space on the graph. The different coordinates of the plot give the sPLS-DA scores and each dimension indicates one of the three components responsible for the separation and grouping for the individual datasets. The contribution of each component in terms of percentage is also given. Data was generated using the Metaboanalyst software.*

The sPLS-DA analysis also identifies the mass features which are responsible for the differences between the samples. These mass features are identified as Variable Important for Projection (VIP) and are associated with a score. This gives the most significant masses and their corresponding statistical values with respect to each sample type. From this global analysis, the mass features or metabolites which showed maximum deflection in their intensities across the different inhibitor treated *P. falciparum* samples as shown in [Fig. 4.8]. Further identification of these compound might give important biological function associate with either related to drug target or their secondary effects on the parasites. This needs generation of extensive mass libraries and MS/MS profiles for further confirmation of the identities of the mass features.

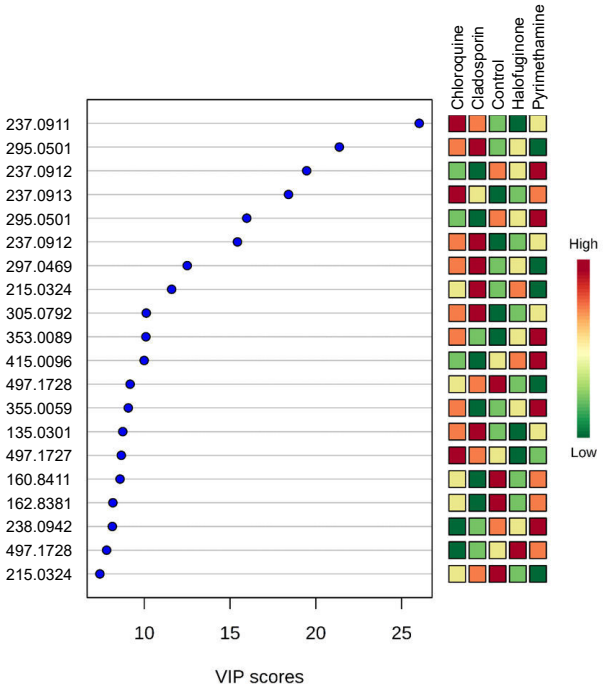

Figure 4.8 Top scoring mass features based on which the variations between the samples are projected. *The Variable important to Projection (VIP) score is determined based on the sPLS-DA analysis, which identifies the most important mass features that are responsible for the distinct mass profile of each sample. Here, 20 selected mass features whose VIP scores are more than 2 are shown.*

4.3.2.4 Identifying key metabolites responsible for unique metabolite profiles associated with inhibitor treatment.

We carried out one is to one comparison of the intensity values for the mass features derived from inhibitor treated samples. This was done in order to find out molecules which are uniquely altered in response to treatment with a particular inhibitor or which are altered in multiple drug treatment conditions. We carried out this analysis in order to find out the signature metabolite profile specific to each inhibitor treatment. Once again we compared the $\log_2$ transformed metabolites peak intensity values and the results indicated that the metabolite profile between samples derived from chloroquine and pyrimethamine treatment are the most similar to each other, suggesting that the metabolic response of *P. falciparum* to potent metabolic inhibitors is very comparable. Among the comparisons, the R^2 value for the linear fit of the data was the highest for chloroquine *vs* pyrimethamine (R^2 = 0.97521; RMSE = 0.40529), while the largest difference was seen between chloroquine *vs* halfuginone comparison (R^2 = 0.93926; RMSE = 0.60412) [Fig. 4.9].

We then identified those metabolites which are showing a difference of at least 2 $\log_2$ values (i.e., a fold change value of at least 4) between control and the four different inhibitor treated samples. Only those metabolites with a pValue of at least 0.001 were taken ahead further. From this analysis we were able to shortlist 261, 262, 162 and 32 mass features from comparisons between control and chloroquine, pyrimethamine, cladosporin and halofuginone, respectively [Fig. 4.10]. Some of the metabolites showed more than 4 fold change in abundance in more than one inhibitor treated sample and we think that these metabolites indicate a generic response by the parasite to various stress conditions, including responding to antimalarial interventions. Thus, after accounting for metabolites shared between the four different inhibitor treatment conditions, we ended up

identifying 335 unique metabolites which are showing significant changes in their abundance in response to inhibitor treatment. A heatmap of the fold change values for all 335 molecules is shown in [Fig. 4.11].

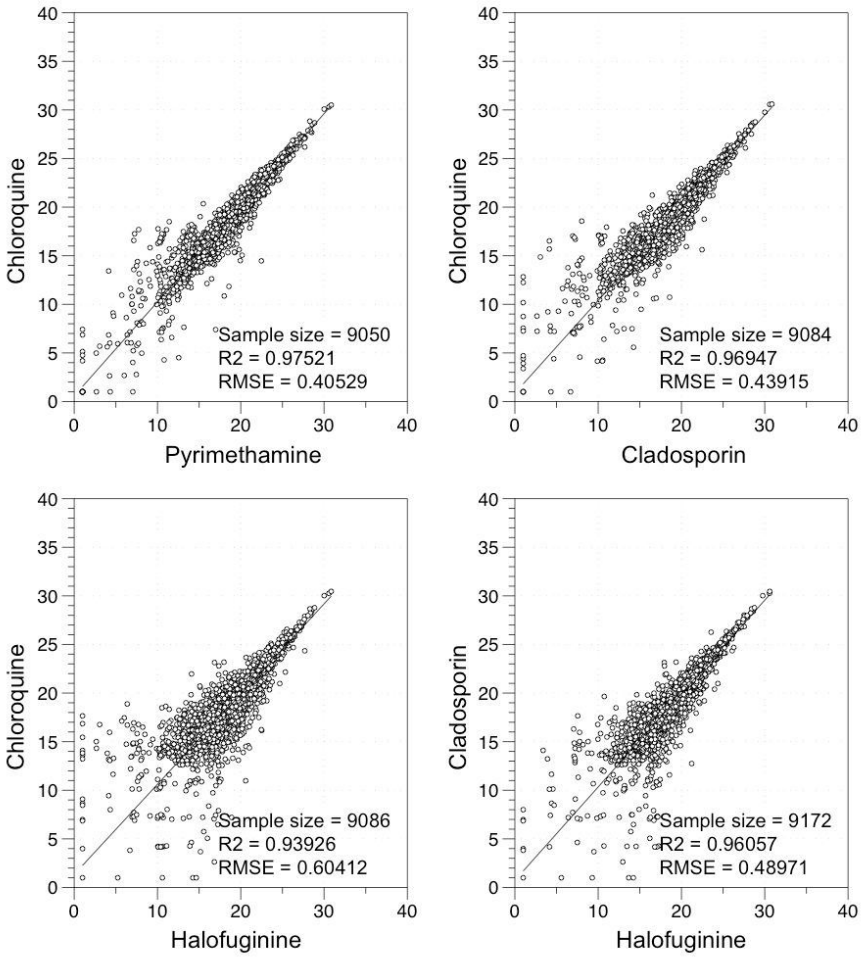

Figure 4.9 Similarity of metabolite intensity values between the various inhibitor treated samples. *The scatter plots depict the similarity in metabolite intensity between the different inhibitor treated samples. The log_2 transformed values of the metabolite intensity were used to generate the plots. All 9697 mass features were plotted but the samples sizes are shown to be different since we eliminated outliers (σ = 1.5) for generating the fit.*

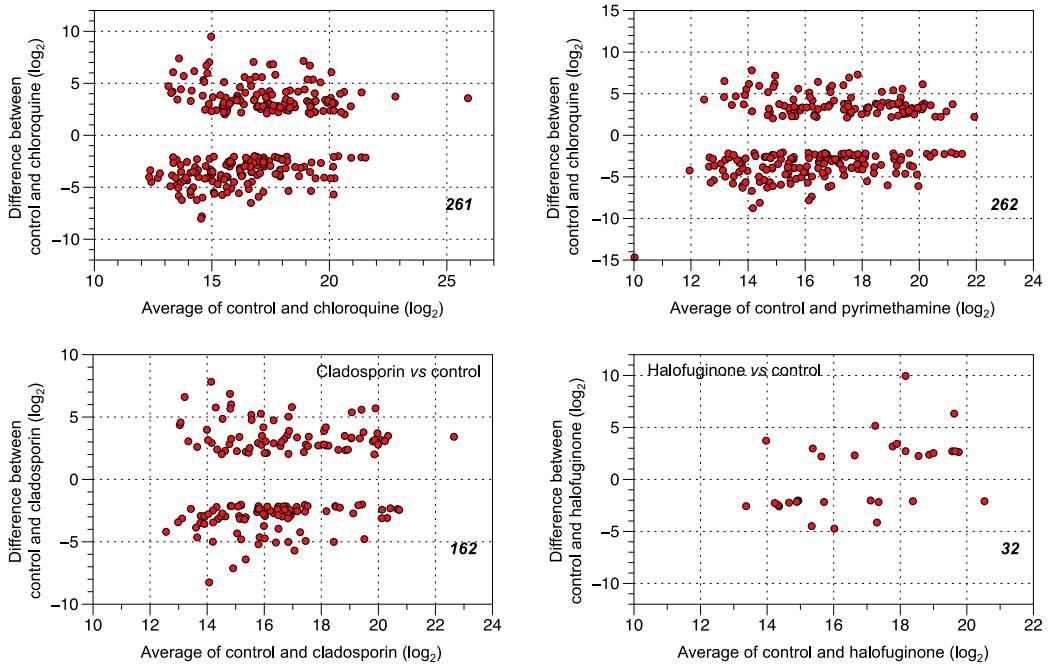

Figure 4.10 Mass features showing significant fold change in their intensity between control and drug treated samples. *The scatter plots show the average of the log_2 intensity values for each metabolites from control and given inhibitor on the x-axis and the difference between the log_2 intensity values between the two on the y-axis. All metabolites shown here are supported by a pValue of at least 0.001 or less.*

From the heatmap, the profile of each metabolite across the 4 different inhibitor treatment can be clearly visualized. It can be observed that most of the metabolites are increasing in abundance, while very few are actually showing a decreasing trend. Although, the identity of these mass features are unknown (as a consequence of the untargeted analysis we have carried out), we can nevertheless speculate that many of these mass feature are likely to be metabolites whose metabolic pathways are under inhibition, either due to primary or secondary effects of the inhibitor's mode of action.

4.3.2.5 Selecting key metabolites as signature molecules representative of each drug treatment.

From the analysis of the untargeted metabolomics data described thus far, we have been looking at the metabolites at the global level. Here, we would like to highlight a few examples metabolites which exhibit drug specific changes in their abundance, which can serve as signature profiles. The individual intensity values for the examples discussed are plotted in [Fig. 4.12]. The first metabolite, is the mass feature 316.8749, which is very highly increased in chloroquine treated samples; ~140 fold increase. The second metabolite is 412.0091 mass feature, which is very highly increased specifically in halofuginone treated sample; ~80 fold increase. The third example metabolite is 431.0255 mass feature, which appears to be increased in all drug treated samples, but to varying degrees; ~700 fold increase in chloroquine treatment, ~220 fold increase in pyrimethamine and cladosporin treatments and only ~7 fold increase in halofuginone treated samples. The fourth metabolite is the 709.4028 mass feature, which is decreased in all drug treated samples, except in case of halofuginone; >2500 fold decrease in chloroquine and pyrimethamine treated samples, ~130 fold decrease in cladosporin treated samples, and no change at all in halofuginone treated samples.

The four mass features which we have highlighted here are shown as examples. There are many other mass features, which can be prioritized based on the global analysis which we have carried out, and used in combination as a signature metabolite profile for tracking inhibitor mode of action. Identification of these metabolites using mass fragment analysis using MS/MS techniques will be necessary for complete understanding of the metabolic perturbations which are imparted by antimalarial compounds on blood stage *P. falciparum* parasites.

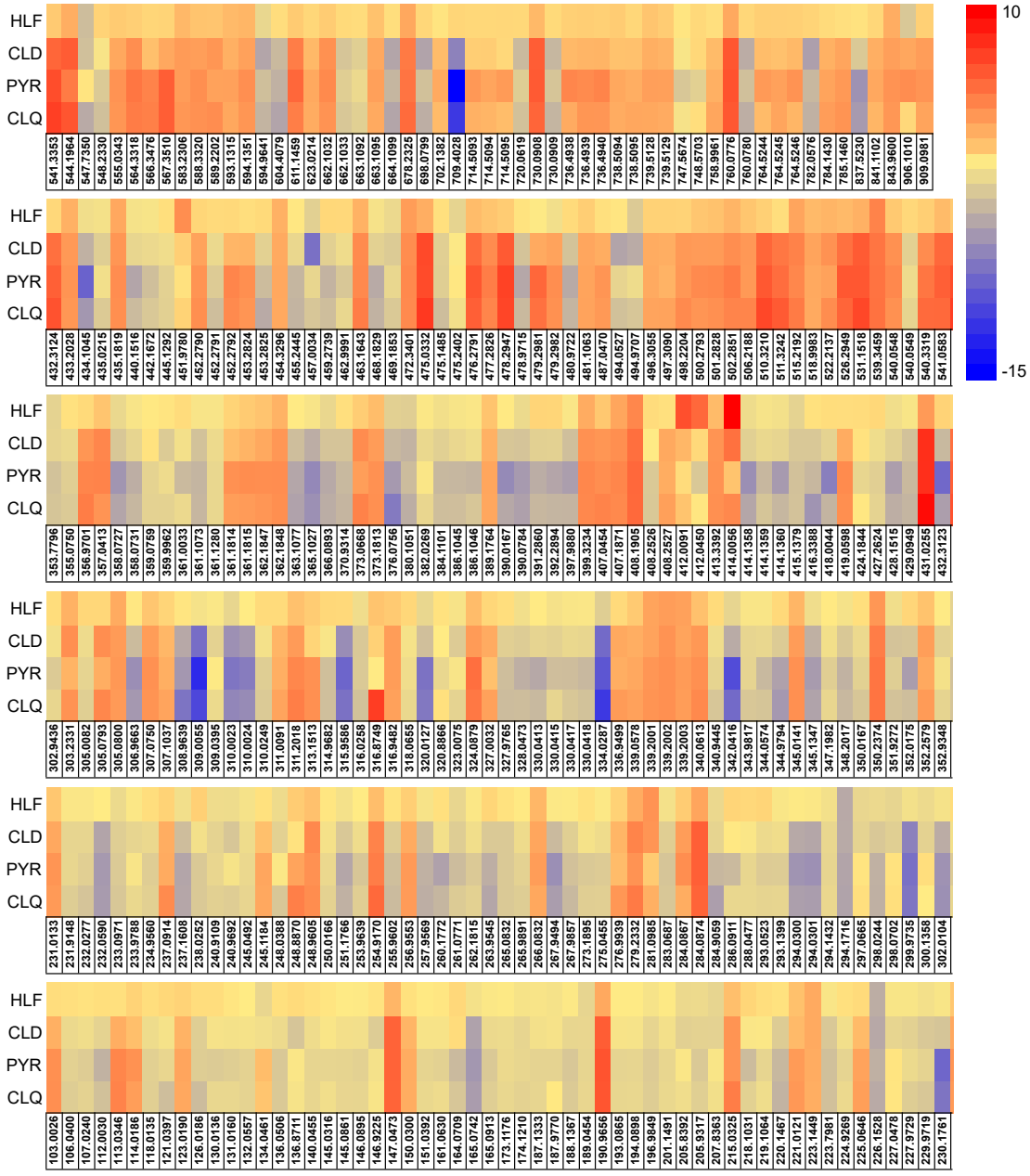

Figure 4.11 Heatmap depicting the difference in log_2 intensity between control and drug treated samples. *The mass feature have been arranged serially in increasing order of median m/z values and the drugs are shown in columns. The color key for the heat map is shown with a range of 10 to -15. The values represent the difference in log_2 intensity values. CLQ, chloroquine; PYR, pyrimethamine; CLD, cladosporin; HLF, halofuginone.*

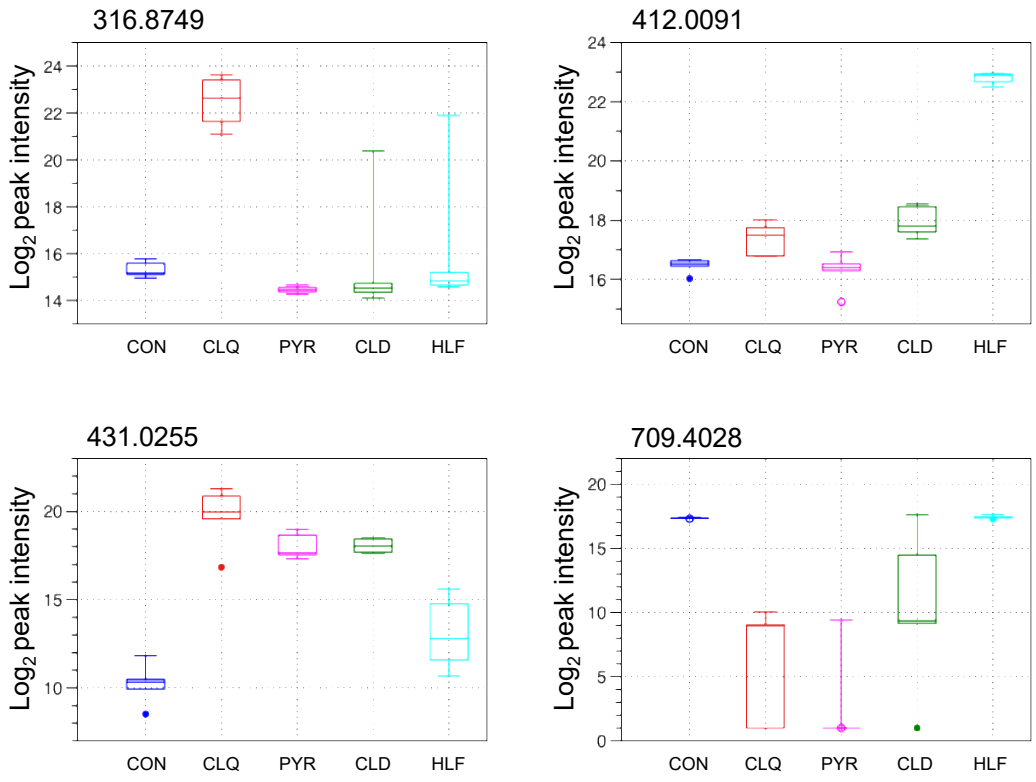

Figure 4.12 Specific examples of mass feature profiles. *The four mass features which are highlighted here are examples that clearly show inhibitor specific profiles. The log_2 transformed peak intensity values were plotted as Wishker plots. CON, control; CLQ, chloroquine; PYR, pyrimethamine; CLD, cladosporin; HLF, halofuginone.*

4.4 Conclusion

In this chapter of the thesis work, untargeted metabolic profiling was carried out to identify drug induced alterations in cellular metabolite levels in erythrocyte stages of *P. falciparum*. Here we have used a limited approach of extracting primarily hydrophilic metabolites and carrying out reverse phase separation using a C18 column before mass spectrometry profiling. Therefore, the changes which we have identified and reported here are only from a subset of metabolites that are found in biological systems. A more expanded approach, using both hydrophilic and hydrophobic extracts, including chemical

processing such as derivatization of metabolites for effective detection, and including multiple analysis platforms, such as LC-MS and GC-MS, will certainly enhance the coverage and provide a more robust and comprehensive drug specific metabolite profile.

In this study, we treated trophozoite stage *P. falciparum* with four different compounds with potent anti-malarial activity; namely, chloroquine, pyrimethamine, cladosporin and halofuginone. While two of these molecules are metabolic inhibitors (chloroquine and pyrimethamine) the other two are indirect inhibitors of protein synthesis in the parasite (acting *via* inhibition of aminoacyl tRNA synthetases). The mechanism of action for these drugs is well established. Chloroquine is known to primarily target heme degradation in the food vacuole of the parasite, although it is not linked to anyone particular protein target. Pyrimethamine is known to inhibit the enzyme dihydrofolate reductase and kill the parasite *via* folate insufficiency. Using targeted approach, it is possible to pick up specific metabolites which are indicative of the inhibitor mode of action, such as the accumulation of pepetides due to improper degradation of hemoglobin in case of chloroquine [Cobbold et al., 2016] and the subsequent depletion of amino acid levels within the parasite. In case of pyrimethamine, the target is the bifunctional dihydrofolate reductase-thymidylate synthase (DHFR-TS) enzyme from *P. falciparum*, which facilitates folate-dependent conversion of dUMP to dTMP. The levels of metabolites which are intermediates in folate biosynthesis, such as *p*-aminobenzoic acid (PABA) and di- or tetrahydrofolate, as well as the downstream products such as the pyrimidine nucleotides, can be studied by mass spectrometry to track the activity of the inhibitor [Allman et al., 2016].

In fact, from the untargeted metabolite profiling carried out in this study, we were able to mine the data for PABA and dUMP, which showed direct impact on levels following pyrimethamine treatment. Although the fold change values for PABA are low,

they are statistically significant and may be with longer period of incubation with the inhibitor, a more pronounced effect will be seen [Fig. 4.13].

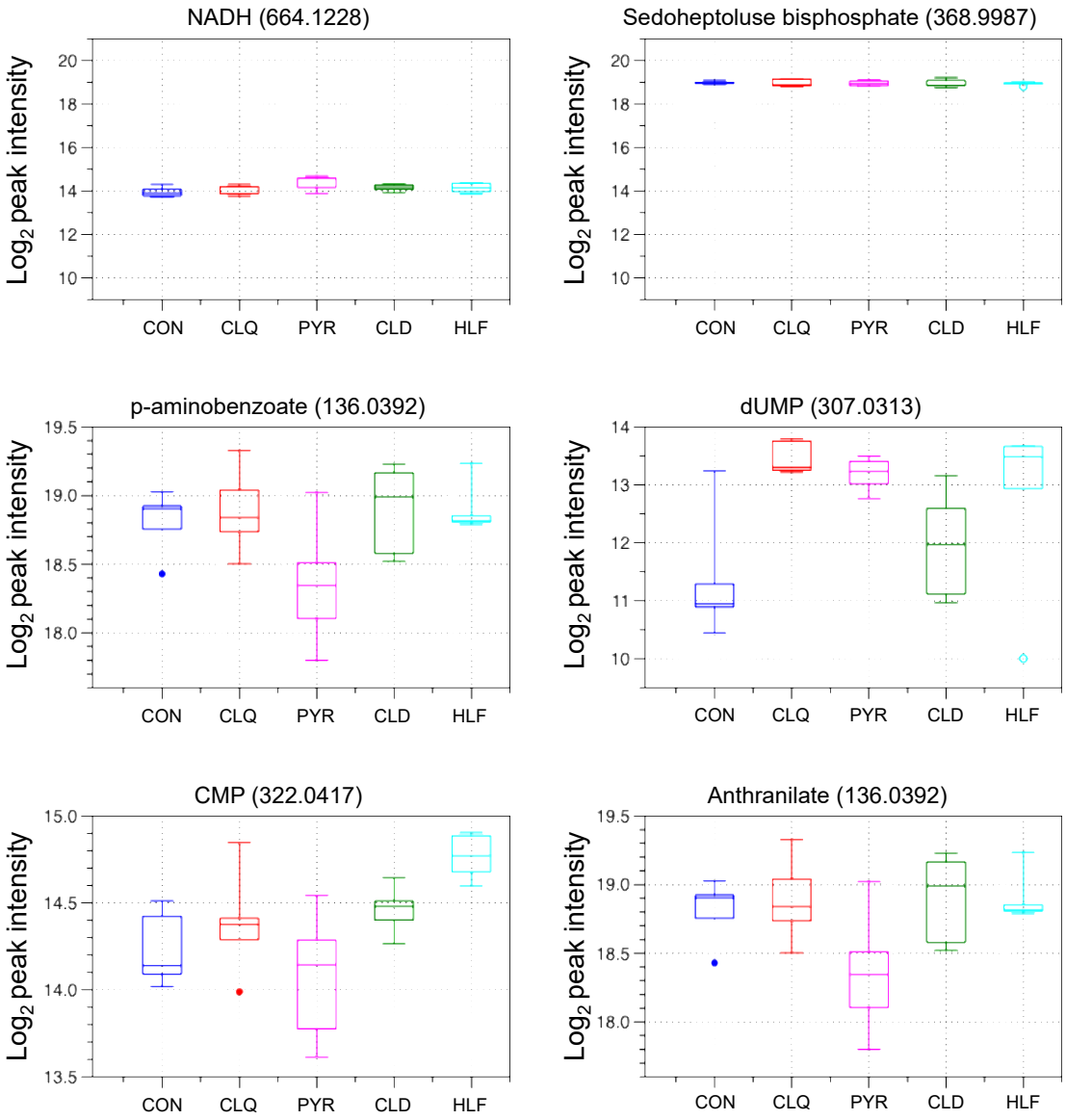

Figure 4.13 Specific examples of metabolites mined from data acquired by untargeted LC-MS profiling. *The peak intensity levels for each metabolite was log_2 transformed and plotted as Wishker plots. The name of the metabolites is shown above the plot along with the media m/z value within brackets. CON, control; CLQ, chloroquine; PYR, pyrimethamine; CLD, cladosporin; HLF, halofuginone.*

The accumulation of dUMP following inhibitor treatment appears not to be specific for pyrimethamine treatment only. Interestingly, we were also able to identify two other metabolites, CMP and anthranilate, which appear to be specifically reduced in *P. falciparum*, following pyrimethamine treatment [Fig. 4.13]. Since these changes can be captured with only 4 h treatment of parasites with inhibitors, these metabolites can serve as very specific reporter for mechanism of action of pyrimethamine or its analogs.

Despite the straight forward use of targeted metabolic profiling to study inhbitor mode of action, this is only possible in cases where there is prior information on the target of the inhibitor. Moreover, the target should have a function, such as enzymatic activity, which can affect the levels of certain metabolites. This is not always the case, and in this study, two of the inhibitors used were targeting protein synthesis in *P. falciparum*. Therefore any metabolite perturbations, which result from inhibitor action will be an indirect consequence and cannot be easily predicted. In this study, we have captured the unique metabolic profile of two novel antimalarial compounds, cladosporin and halofuginone. This finding will pave the way forward for further in-depth analysis on the mode of action of these inhibitors. Identification of exactly what these metabolites are, using MS/MS techniques, will be important to decipher whether these metabolites reflect the inhibitory effect of these antimalarial compounds on primary or secondary targets. Thus, this study establishes the feasibility of using untargeted metabolomics profiling as a tool for studying drug/inhibitor mode of action in *P. falciparum*. Combining this approach with other global perturbation studies using transcriptomics and proteomics will be the path forward in future.

4.5 References

Ahyong V. *et al.* (2016). Identification of Plasmodium falciparum specific translation inhibitors from the MMV Malaria Box using a high throughput in vitro translation screen. Malar J 15:173.

Allman EL. *et al.* (2016). Metabolomic profiling of the Malaria Box reveals antimalarial target pathways. Antimicrob Agents Chemother 60:6635– 6649.

Anke H. (1979). Metabolic products of microorganisms. 184. Onthe mode of action of cladosporin. J Antibiot (Tokyo); 32:952-8.

Baragaña B. *et al.* (2015). A novel multiple-stage antimalarial agent that inhibits protein synthesis. Nature 522:315–320.

Beyoğlu, D. and Idle, J. R. (2013). Metabolomics and its potential in drug development. Biochemical Pharmacology 85, 12–20.

Bowman JD. *et al.* (2014). Antiapicoplast and gametocytocidal screening to identify the mechanisms of action of compounds within the Malaria Box. Antimicrob Agents Chemother 58:811–819.

Casewell MW. Hill RL. (1987). Mupirocin ('pseudomonic acid')–a promising new topical antimicrobial agent. J Antimicrob Chemother 1987; 19:1-5.

Chambers MC. *et al.* (2012). A cross-platform toolkit for mass spectrometry and proteomics. Nat Biotechnol. 30(10):918-20.

Cobbold SA. *et al*. (2016). Metabolic Dysregulation Induced in Plasmodium falciparum by Dihydroartemisinin and Other Front-Line Antimalarial Drugs. J Infect Dis. 15;213(2):276-86.

Combrinck, J.M. *et al*. (2013). Insights into the role of heme in the mechanism of action of antimalarials. ACS Chem. Biol. 8, 133–137.

Cowell AN. *et al*. (2018). Mapping the malaria parasite druggable genome by using in vitro evolution and chemogenomics. Science. 12;359 (6372):191-199.

Creek, DJ. *et al.* (2012a). Metabolomic analysis of trypanosomatid protozoa. Molecular and Biochemical Parasitology 181, 73–84.

Creek DJ. *et al.* (2016). Metabolomic-based screening of the Malaria Box reveals both novel and established mechanisms of action. Antimicrob Agents Chemother 60:6650–6663.

Duffy, S. and Avery, V. M. (2012). Development and optimization of a novel 384-well anti-malarial imaging assay validated for high-throughput screening. American Journal of Tropical Medicine and Hygiene 86, 84–92.

Dunn, WB. *et al.* (2013). Mass appeal: metabolite identification in mass spectrometry-focused untargeted metabolomics. Metabolomics 9, 44–66.

Elkin, M. *et al.* (1999). Inhibition of bladder carcinoma angiogenesis, stromal support, and tumor growth by halofuginone. Cancer Res. 59, 4111–4118.

Flannery EL. *et al.* (2015). Next-generation sequencing of patient samples shows evidence of direct evolution in drug-resistance genes. ACS Infect Dis 1:367–379.

Gamo FJ. *et al.* (2010). Thousands of chemical starting points for antimalarial lead identification. Nature 465:305–310.

Gao, P. *et al.* (2007). Investigation on response of the metabolites in tricarboxylic acid cycle of Escherichia coli and Pseudomonas aeruginosa to antibiotic perturbation by capillary electrophoresis. Journal of Pharmaceutical and Biomedical Analysis 44, 180-187.

Gregson, A. & Plowe, C.V. (2005). Mechanisms of resistance of malaria parasites to antifolates. Pharmacol. Rev. 57, 117–145.

Halevy, O. *et al.* (1996). Inhibition of collagen type I synthesis by skin fibroblasts of graft versus host disease and scleroderma patients: effect of halofuginone. Biochemical Pharmacol. 52, 1057–1063.

Halouska, S. *et al.* (2012). Predicting the in vivo mechanism of action for drug leads using NMR metabolomics. ACS Chemical Biology 7, 166–171.

Hempelmann E. (2007). Hemozoin biocrystallization in Plasmodium falciparum and the antimalarial activity of crystallization inhibitors. Parasitol Research. 100 (4): 671–676.

Hoepfner D. *et al.* (2012). Selective and specific inhibition of the plasmodium falciparum lysyl-tRNA synthetase by the fungal secondary metabolite cladosporin. Cell Host Microbe; 11:654-663.

Istvan ES. *et al.* (2011). Validation of isoleucine utilization targets in Plasmodium falciparum. Proc Natl Acad Sci U S A; 108:1627-32.

Jain, V. *et al.* (2014). Structural and functional analysis of the anti-malarial drug target prolyl-tRNA synthetase. J. Struct. Funct. Genomics 15, 181–190.

Jain, V. *et. al* (2015). Structure of Prolyl-tRNA Synthetase-Halofuginone Complex Provides Basis for Development of Drugs against Malaria and Toxoplasmosis. Structure 23, 819-829.

Kateera, F. *et al.* (2016). Molecular surveillance of Plasmodium falciparum drug resistance markers reveals partial recovery of chloroquine susceptibility but sustained sulfadoxine-pyrimethamine resistance at two sites of different malaria transmission intensities in Rwanda. Acta Trop. 164, 329–336.

Kikuchi, H. *et al.* (2006). Exploration of a new type of antimalarial compounds based on febrifugine. J. Med. Chem. 49, 4698–4706.

Kimura Y. *et al.* (2012). Plant growth activities of aspyran, asperentin, and its analogues produced by the fungus Aspergillus sp. Z Naturforsch C; 67:587-93.

Kuhen KL. e*t al*. (2014). KAF156 is an antimalarial clinical candidate with potential for use in prophylaxis, treatment, and prevention of disease transmission. Antimicrob Agents Chemother 58:5060–5067.

Lehane, AM. *et al*. (2008). A verapamil-sensitive chloroquine-associated H+ leak from the digestive vacuole in chloroquine-resistant malaria parasites. J. Cell Sci. 121, 1624–1632.

Linder, MR. *et al.* (2007). (2R,3S)-(+)- and (2S,3R)-(-)-halofuginone lactate: synthesis, absolute configuration, and activity against Cryptosporidium parvum. Bioorg. Med. Chem. Lett. 17, 4140–4143.

Lu W. *et al*. (2010). Metabolomic analysis via reversed-phase ion-pairing liquid chromatography coupled to a standalone orbitrap mass spectrometer. Anal Chem. 82(8):3212-21.

Metsalu, Tauno and Vilo, Jaak. Clustvis: a web tool for visualizing clustering of multivariate data using Principal Component Analysis and heatmap. Nucleic Acids Research, 43(W1):W566–W570, 2015

McGaha, T. *et al*. (2002). Effect of halofuginone on the development of tight skin (TSK) syndrome. Autoimmunity 35, 277–282.

McNamara CW. *et al*. (2013). Targeting Plasmodium PI (4)K to eliminate malaria. Nature 504: 248-253.

Melamud E, Vastag L, Rabinowitz JD. (2010). Metabolomic analysis and visualization engine for LC-MS data. Anal Chem. 82(23):9818-26.

Miller JD, Sun M, Gilyan A, Roy J, Rand TG. (2010). Inflammation-associated gene transcription and expression in mouse lungs induced by low molecular weight compounds from fungi from the built environment. Chem Biol Interact; 183:113-24.

Nam TG. e*t al*. (2011). A chemical genomic analysis of decoquinate, a Plasmodium falciparum cytochrome b inhibitor. ACS Chem Biol 6:1214–1222.

Olszewski, K.L. and Llinas, M. (2013) Extraction of hydrophilic metabolites from Plasmodium falciparum-infected erythrocytes for metabolomic analysis. Methods Mol. Biol, 923, 259–266.

Osborne MJ. *et al*. (2001). "Backbone dynamics in dihydrofolate reductase complexes: role of loop flexibility in the catalytic mechanism". Biochemistry. 40 (33): 9846–59.

Paiardini A. *et al*. (2015). Screening the Medicines for Malaria Venture "Malaria Box" against the Plasmodium falciparum aminopeptidases, M1, M17 and M18. PLoS One 10:e0115859.

Petersen, I., Eastman, R. & Lanzer, M. (2011). Drug-resistant malaria: molecular mechanism and implications for public health. FEBS Lett. 585, 1551–1562.

Pines, M., and Nagler, A. (1998). Halofuginone: a novel antifibrotic therapy. Gen. Pharmacol. 30, 445–450.

Pines, M., Snyder, D., Yarkoni, S., and Nagler, A. (2003). Halofuginone to treat fibrosis in chronic graft-versus-host disease and scleroderma. Biol. Blood Marrow Transplant. 9, 417–425.

Plouffe D. *et al*. (2008). In silico activity profiling reveals the mechanism of action of antimalarials discovered in a high-throughput screen. Proc Natl Acad Sci U S A; 105:9059-64.

Radfar A. *et al*. (2009); In Vitro Culture of Plasmodium falciparum: Obtention of Synchronous Asexual Erythrocytic Stages. Nature Protocol; 4; 12, 1899-1915.

Rottmann M. *et al*. (2010). Spiroindolones, a potent compound class for the treatment of malaria. Science 329:1175–1180.

Ryley, J.F., and Betts, M.J. (1973). Chemotherapy of chicken coccidiosis. Adv. Pharmacol. Chemother. 11, 221–293.

Ryley, J.F., and Wilson, R.G. (1975). Laboratory studies with some recent anticoccidials. Parasitology 70, 203–222.

Scalbert, A. *et al*. (2009). Mass-spectrometry-based metabolomics: limitations and recommendations for future progress with particular focus on nutrition research. Metabolomics 5, 435–458.

Scott PM, Van Walbeek W, MacLean WM. (1971). Cladosporin, a new antifungal metabolite from Cladosporium cladosporioides. J Antibiot (Tokyo); 24:747-55.

Sharma A, Khan S, Sharma A, Belrhali H, Yogavel M. (2014). Structural basis of malaria parasite lysyl-tRNA synthetase inhibition by cladosporin. J Struct Funct Genomics; 15:63-71.

Sidhu, A.B.S. *et al*. (2006). Decreasing pfmdr1 copy number in Plasmodium falciparum malaria heightens susceptibility to mefloquine, lumefantrine, halofantrine, quinine, and artemisinin. J. Infect. Dis. 194, 528–535.

Spangenberg T. *et al*. (2013). The open access malaria box: a drug discovery catalyst for neglected diseases. PLoS One 8:e62906.

Spillman NJ. *et al*. (2013). Na (_) regulation in the malaria parasite Plasmodium falciparum involves the cation ATPase PfATP4 and is a target of the spiroindolone antimalarials. Cell Host Microbe 13:227–237.

Springer, JP, *et al*. (1981). Plant growth regulatory effects and stereochemistry of cladosporin. J Agric Food Chem; 29:853-5.

Tiwari NK, Reynolds PJ, Calderon AI. (2016). Preliminary LC-MS based screening for inhibitors of Plasmodium falciparum thioredoxin reductase (PfTrxR) among a set of antimalarials from the Malaria Box. Molecules 21:424.

Trager, W., and Jensen, J.B. (2005). Human malaria parasites in continuous culture. J. Parasitol. 91, 484–486.

Van Voorhis WC. *et al*. (2016). Open source drug discovery with the Malaria Box compound collection for neglected diseases and beyond. PLoS Pathog 12:e1005763.

Vasudevan, D.M.; Sreekumari, S.; Vaidyanathan, Kannan (2013). Textbook of Biochemistry for Medical Students. JP Medical Ltd. p. 491. ISBN 9789350905302. OCLC 843532694.

Venkatesan, M. et al. (2014). Polymorphisms in Plasmodium falciparum chloroquine resistance transporter and multidrug resistance 1 genes: parasite risk factors that affect treatment outcomes for P. falciparum malaria after artemether-lumefantrine and artesunate-amodiaquine. Am. J. Trop. Med. Hyg. 91, 833–843.

Wu W. *et al*. (2015). A chemical rescue screen identifies a Plasmodium falciparum apicoplast inhibitor targeting MEP isoprenoid precursor biosynthesis. Antimicrob Agents Chemother 59:356 –364.

Xia J, Wishart DS, (2016). Using MetaboAnalyst 3.0 for UNIT 14.10 Comprehensive Metabolomics Data Analysis; Current Protocols in Bioinformatics 14.10.1-14.10.91.

WHO, List of essential medicines (2017) http://www.who.int/medicines/publications/essentialmedicines/20th_EML2017.pdf?ua=1

Chapter 5

Summary of the thesis and future prospects

Chapter 1: Introduction to *apicomplexan* parasites *Toxoplasm gondii* and *Plasmodium falciparum*, their metabolic capabilities and need for antiparasitic compound discovery

Apicomplexan parasites cause a variety of infectious diseases in humans and animals. The malaria parasite *Plasmodium falciparum*, agent of severe human malaria, and the coccidian parasite *Toxoplasma gondii*, agent of toxoplasmosis, belong to this group of parasites. In the past two decades, scientific advancements have significantly furthered our understanding of various aspects of the biology of these parasites. Availability of genome sequence data, for these and other related parasites, has greatly facilitated this by providing genomic and evolutionary perspective at the molecular level. Moreover, advancements in the various "-omics" technologies, along with the feasibility of genetic manipulation, have opened up unprecedented opportunities to carry out functional studies in these parasites. All of this knowledge is ultimately expected to help in identifying novel anti-parasitic drugs. Metabolic functions are key to parasite survival within the host, and thus, essential pathways and enzymes are potential drug targets. Frontline anti-parasitic drugs such as pyrimethamine and atovaquone are good examples of metabolic inhibitors.

Apicomplexan parasites have dramatically reduced metabolic capability, which appears to be optimally evolved for very specific growth conditions, such as nutrient availability, that can support the successful completion of parasite life cycle. In the first part of my thesis work, I have explored the metabolic plasticity, which allows tachyzoite stage *T. gondii* to cope with alternate nutrient conditions during asexual growth. For this study, I have monitored the growth and replication of tachyzoite stage *T. gondii*, and have carried out biochemical characterization and genetic manipulation to address the objectives. In particular, I have used mass spectrometry based metabolomics extensively

to study parasite metabolism. In the next part of my thesis work, I have studied the metabolic consequences of deficient cytochrome b function, as occurs in parasites that are resistant to the drug atovaquone. In this study, I have used wild type *P. falciparum* and atovaquone resistant parasites carrying *cytb* mutations to find out the metabolic changes which take place when the respiratory chain in the parasite mitochondrion is affected. Perturbation of mitochondrial metabolism was studied using biochemical and LC-MS metabolomics approaches. The last part of my thesis work is focused on tracking the kinetics of drug induced metabolic changes that occur in *P. falciparum*. Untargeted metabolome profiling was carried out in this study to identify early and late metabolic changes that occur following exposure of the parasite to selected drugs. This approach can be useful in studying the mechanism of action for anti-parasitic drugs, and compare the bioactivity of chemically similar molecules. Below I have given a brief description of these studies.

Chapter 2: Genetic and pharmacological studies on nutrient metabolism, and essentiality of hexokinase and phosphoenolpyruvate carboxykinase enzymes in *T. gondii*

Glucose is an important nutrient for *T. gondii* and its availability dictates optimal growth of the parasite. It has been reported previously that glucose is not an essential nutrient for *T. gondii* survival and in its absence glutamine is the major source of carbon and energy for the parasite. This has been shown using mutant parasites lacking the major glucose transporter or the glycolytic enzyme aldolase. Prior work from our laboratory has established that even though the glycolytic enzyme hexokinase is dispensable for growth of tachyzoite stage parasites, it is essential for asexual differentiation of tachyzoites into bradyzoites, and for persisting in host as latent tissue cysts. Growth and metabolic studies

suggested that glutamine supported gluconeogenesis facilitates survival of the hexokinase mutant (Δ*hk*) parasites. As further continuation of these studies, I generated mutant parasites lacking the phosphoenolpyruvate carboxykinase gene (Δ*pepck*) which renders them incapable of gluconeogenesis. Using this mutant, I could demonstrate that glutamine is the sole carbon source, which can sustain parasite growth when they are deprived of glucose or when they lack glycolytic flux. Using isotope resolved metabolomics, I was able to show that, while gluconeogeneis is absent in wt tachyzoites (owing to a very active glycolysis), it is active in Δ*hk* mutant tachyzoites. As expected, in Δ*pepck* mutant tachyzoites there was no detectable gluconeogenic flux when they were deprived of glucose. By performing replication and plaque formation assays, I could demonstrate that Δ*pepck* parasites die when deprived of glucose. However, ATP synthesis, from glycolysis and oxidative phosphorylation was found to be intact in Δ*pepck* parasites. This further shows that the inability of Δ*pepck* parasites to replenish glycolytic intermediates, in the absence if glucose, is the primary reason for their death.

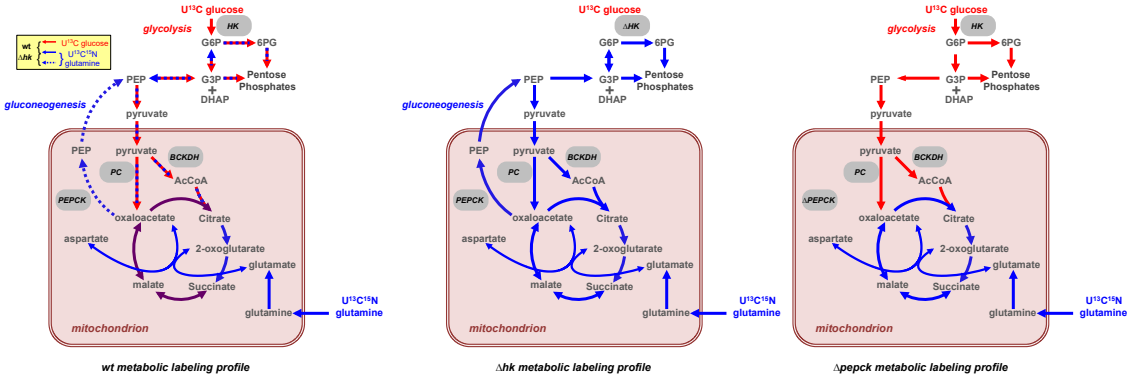

Figure 5.1: Schematic representation of glucose and glutamine metabolism in wt, Δhk and Δpepck T. gondii tachyzoites. *HK, hexokinase; BCKDH, branched chain ketoacid dehydrogenase; PC, pyruvate carboxylase; PEPCK, phosphoenolpyruvate carboxy kinase; G6P, glucose-6-phosphate; 6GP, 6-phosphogluconate; G3P, glyceraldehyde-3-phosphate; DHAP, dihydroxyacetone phosphate; PEP, phosphoenolpyruvate, AcCoA, acetyl CoA.*

Chapter 3: Dissection of mitochondrial metabolism in *cytb* mutants of *P. falciparum* to evaluate ATP synthesis, pyrimidine synthesis, and sensitivity to atovaquone and its analogs

The potent antimalarial compound atovaquone targets the cytochrome b (*cytb*) protein, which is part of the Q-cytochrome c oxidoreductase complex of the mitochondrial respiratory chain. It has been previously shown that when *Pf*CYTb is inhibited by atovaquone, pyrimidine biosynthesis is blocked, since the activity of dihydroorotate dehydrogenase (*DHODH*), which is a key enzyme in this pathway, is coupled to the ubiquinone redox cycle (Q cycle). CYTb activity is essential for maintaining the Q cycle. It has been shown that loss of function mutations in *Pfcytb* confer resistance to atovaquone. Therefore, in atovaquone resistant parasites, the mitochondrial electron transport chain is compromised. In this context, it is surprising that atovaquone resistant parasites continue to synthesize pyrimidine and remain viable. Moreover, in a recent study it was shown that *cytb* mutant parasites cannot complete the sexual cycle within the mosquito host, thereby restricting their transmission.

This finding suggests that *Pf*CYTb is a good anti-malarial target, and potent but less cytotoxic analogues of atovaquone or similar class of inhibitors need to be developed. We have screened molecules based on atovaquone scaffold for their potency against blood stage *P. falciparum* and selected the best hits for mode of action studies. LC-MS metabolomics captures the signature changes in metabolites affected by drug treatment of the parasites. Pyrimidine biosynthesis is affected by atovaquone treatment in *P. falciparum*, leading to the accumulation of N-carbamoyl-L-aspartate and dihydroorotate (DHO), and depletion of UMP and other downstream metabolites. I have carried out LC-MS metabolomics studies to understand how pyrimidine biosynthesis and mitochondrial oxidative metabolism are affected in atovaquone treated *wt* and *cytb* mutant parasites. In

addition, I have also studied the status of mitochondrial ATP synthesis in *wt* and *cytb* mutant *P. falciparum.*

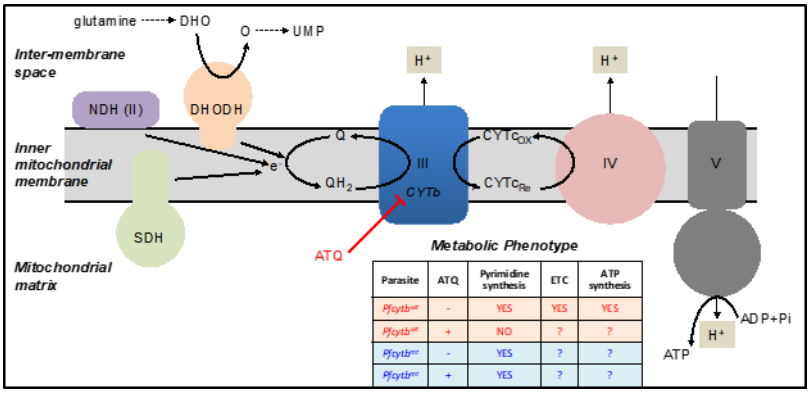

Parasite	ATQ	Pyrimidine synthesis	ETC	ATP synthesis
$Pfcytb^{wt}$	-	YES	YES	YES
$Pfcytb^{wt}$	+	NO	?	?
$Pfcytb^{mt}$	-	YES	?	?
$Pfcytb^{mt}$	+	YES	?	?

Figure 5.2: Perturbation of mitochondrial metabolism by atovaquone and its analogues and metabolic status of atovaquone resistant Pfcytb mutant P. falciparum. *DHO, dihydroorotate; O, orotate; UMP, Uridine monophosphate; DHODH, dihydroorotate dehydrogenase; NDH(II), type II NADH dehydrogenase; SDH, succinate dehydrogenase, e^-, electrons; Q, ubiquinone; QH_2, ubiquinol; III, respiratory chain complex III (ubiquinol cytochrome c oxidoreductase); CYTb, cytochrome b; H^+, protons; $CYTc_{OX}$, oxidized cytochrome c; $CYTc_{RE}$, reduced cytochrome c; IV, respiratory chain complex IV (cytochrome c oxidase); V, respiratory chain complex V (F-type ATP synthase); ADP+Pi, adenosine diphosphate+inorganic phosphate; ATP, adenosine triphosphate; ATQ, atovaquone.*

Chapter 4: LC-MS metabolomics studies to understand drug mechanism of action in *Plasmodium falciparum*

LC-MS metabolomics is fast becoming a method of choice for drug mechanism of action studies. In case of drugs which directly affect a metabolic enzyme or function, the accompanying primary metabolic changes can be easily captured in a targeted manner by this method. However, when drugs affect non-metabolic targets, the accompanying metabolic changes are secondary in nature, and untargeted metabolome analysis can capture these changes. Either way, drug specific metabolite perturbations can provide a

signature profile that can be informative in classifying drugs according to their mechanism of action. This approach is especially useful when trying to identify off-target effects of drugs or for carrying out initial mechanism of action studies on novel inhibitors. This approach has been used recently to characterize the mode of action of selected compounds with potent antimalarial activity from the Malaria Box collection. As described above, I have used targeted metabolomics to characterize the metabolic changes occurring in atovaquone treated or *cytb* mutant parasites. In this part of my thesis work, untargeted metabolomics analysis was used to identify signature changes in *P. falciparum* metabolites when the parasites are treated with potent anti-malarial compounds. The two compounds that were used in these studies are the fungal and plant natural products, cladosporine and halofuginone, which are known to target *P. falciparum* protein synthesis by inhibiting the lysyl- and prolyl-tRNA synthetase enzymes respectively. The metabolic perturbations induced by these molecules were compared to standard antimalarial drugs such as chloroquine, atovaquone, and pyrimethamine. Although drug specific metabolic changes were identified, a majority of the changes, especially in samples with longer drug treatment times, were found to be common to the different drug treatments. The exception was halofuginone, which induced a markedly different change in metabolite profile when compared to cladosporine. This suggests that even though both of these molecules target tRNA synthetases in *P. falciparum*, their secondary effects on the parasite can be very different. This finding will impact studies on the antimalarial effect of analogs for cladosporine and halofuginone, and help in dissecting precise mode of action and drug resistance phenotypes.

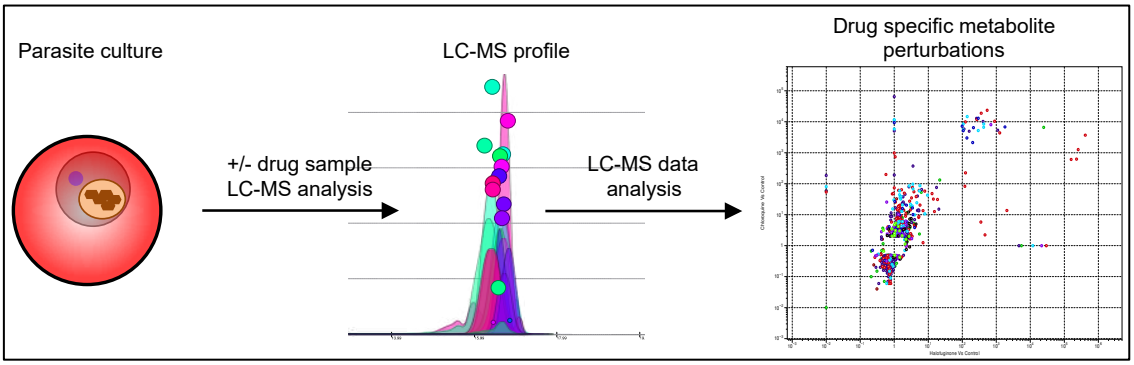

Figure 5.3: Workflow summary for profiling drug induced alterations in metabolite levels in P. falciparum using untargeted LC-MS analysis.

Overall summary of thesis

The overall focus of this thesis work was to carry out details studies on select metabolic functions in both *P. falciparum* and *T. gondii*, with the view of understanding fundamental aspects of metabolic adaptation in the parasite (as discussed under Chapter-2 studies) and to identify and study essential metabolic functions as targets for antiparasitic interventions (as discussed under Chapter-3 studies). I have used mass spectrometry as a tool to study parasite metabolism. Using this technique I have also explored the possibility of interrogating the mode of action of drugs and the metabolic response they induce in parasites (as discussed under Chapter-4 studies).

Thank you